Elisabeth Gruber, Milan Ončák, Roland Wester (Eds.)

XXVth Symposium on Atomic, Cluster and Surface Physics 2026 (SASP 2026)

February 1 – 6, 2026
Obergurgl, Austria

Contributions

XXVth Symposium on Atomic, Cluster and Surface Physics 2026 (SASP 2026)

February 1 – 6, 2026
Obergurgl, Austria

Organizing Committee:
Institut für Ionenphysik und Angewandte Physik,
Universität Innsbruck

Elisabeth Gruber, Milan Ončák, Roland Wester
Chitra Perotti, Irmgard Staud

Preface

The international Symposium on Atomic, Cluster and Surface Physics, SASP, is a continuing biennial series of conferences, founded in 1978 by members of the Institute of Atomphysik, now Institute of Ion Physics and Applied Physics of the University of Innsbruck, Austria. SASP symposia aim to promote the growth of scientific knowledge and effective exchange of information among scientists in the field of atomic, molecular, cluster and surface physics, stressing both fundamental concepts and applications across these areas of interdisciplinary science.

Since the beginning, the SASP format has been similar to that of a Gordon Conference, with invited lectures, hot topic oral presentations, posters and ample time for discussions.

SASP traditionally takes place in Austria every second time, and is held in another Alpine country in between. So far, the SASP conferences took place in the following locations:

1978 Zirog, Italy
1980 Maria Alm, Austria
1982 Maria Alm, Austria
1984 Maria Alm, Austria
1986 Obertraun, Austria
1988 La Plagne, France
1990 Obertraun, Austria
1992 Pampeago, Italy
1994 Maria Alm, Austria
1996 Engelberg, Switzerland
1998 Going, Austria
2000 Folgaria, Italy
2002 Going, Austria
2004 La Thuile, Italy 2006
2006 Obergurgl, Austria
2008 Les Diablerets, Switzerland
2010 Obergurgl, Austria
2012 Alpe d´Huez, France
2014 Obergurgl, Austria
2016 Davos, Switzerland
2018 Obergurgl, Austria
2020 St. Moritz, Switzerland
2022 Obergurgl, Austria
2024 Andalo, Italy

SASP Erwin Schrödinger Gold Medal 2026

The “SASP Award for Outstanding Scientific Achievements,” in the form of the Erwin Schrödinger Gold Medal designed by Zdenek Herman, was initiated in 1992 by the SASP International Scientific Committee. This award is granted during the biennial SASP meeting to one or two scientists chosen among those who have strong connections to the themes and activities of SASP.

The recipient of the SASP Award 2026: will be announced at SASP 2026. Stay tuned.

At previous SASP meetings, the Schrödinger Gold Medal was awarded to:

1992 – **David Smith**, Birmingham, UK
1994 – **Zdenek Herman**, Praha, Czech Republic
1996 – **Werner Lindinger** and **Tilmann Märk**, Innsbruck, Austria
1998 – **Eldon Ferguson**, Boulder, USA and **Chava Lifshitz**, Jerusalem, Israel
2000 – **Jean H. Futrell**, Richland, USA
2002 – **Eugen Illenberger**, Berlin, Germany
2004 – **Anna Giardini**, Roma, Italy
2006 – **Davide Bassi**, Trento, Italy and **Martin Quack**, Zürich, Switzerland
2008 – **Helmut Schwarz**, Berlin, Germany
2010 – **Kurt Becker**, New York, USA
2012 – **Dieter Gerlich**, Chemnitz, Germany and **John Maier**, Basel, Switzerland
2014 – **Stephen D. Price**, London, United Kingdom
2016 – **Roberto Marquardt**, Strasbourg, France and **Paul Scheier**, Innsbruck, Austria
2018 – **Tom Rizzo**, Lausanne, Switzerland
2020 – **Frédérik Merkt**, Zürich, Switzerland

2022 – **Gereon Niedner-Schatteburg**, Kaiserslautern, Germany
2024 - **Jana Roithova** Nijmegen, The Netherlands and **Karl-Heinz Ernst**, Dübendorf, Switzerland

Program

	Sunday Feb.1	Monday Feb. 2	Tuesday Feb. 3	Wednesday Feb. 4	Thursday Feb. 5	Friday Feb. 6	
09:00-09:35		Wang	Richardson	Beyer	Osterwalder	Fouquet	09:00-09:35
09:35-10:10		Bieske	Asvany	Lushchikova	Ascenzi	Pohl	09:35-10:00
10:10-10:35		Minissale	Pal	Schmidt	Coffee	Zhi	10:00-10:25
10:35-11:05		Coffee	Coffee	Coffee	SASP AWARD	Coffee	10:25-10:55
11:05-11:40		Joblin	Pluharova	Matyus	Beck	Farnikova	10:55-11:20
11:40-12:05		Foitzik	Kocisek	Aigner	Tosi	Schöpfer	11:20-11:25
12:05-16:00		Lunch + Break	Lunch + Break	Lunch + Break	Lunch + Break	Closing Lunch	11:45-12:00
16:00-16:30	Registration	Coffee	Coffee	Coffee	Coffee		
16:30-17:05		Balucani	Perez-Rios	Bastian	Shagam		
17:05-17:30		Thissen	Farnik	Lindkvist	Stohner		
17:30-17:55		Horka-Zelenkova	Kocabkova	Lengyel	Keppler		
18:30-20:00	Dinner	Dinner	Dinner	Dinner	Conference Dinner		
20:00-20:10	Welcome	1st Poster session (Group A)	Social Activity	2nd Poster session (Group B)			
20:10-20:45	Stapelfeldt						
20:45-21:10	Toker						

invited talk (30 + 5 min)
hot topic talk (20 +5 min)

Contents

Invited Talks

Real time observation of the diffusion-limited formation of an ion-molecule complex

Henrik Stapelfeldt
Department of Chemistry, Aarhus University, Denmark

Time-resolved studies of bond making between two molecules or atoms are notoriously difficult due to the challenge of measuring when the two reactants meet. This is determined by diffusion – a process that is typically not controllable on ultrafast time scales. Previous works used a weakly-bonded precursor complex of the two reactants to eliminate diffusion or introduced one of the reactants in a dense environment of reactants to minimize diffusion or allow it to be simulated by models.

I will present recent real-time measurements of the bimolecular reaction where a Li^+ ion diffuses towards a benzene dimer and forms a Li^+Bz_2, a textbook cation-π-system inside a liquid helium nanodroplet [1]. After formation at the droplet surface, Li^+ solvates [2-3], then diffuses ballistically with a velocity of 43 m/s and finally binds to Bz_2 near the droplet center to form Li^+Bz_2.
The experimental results are compared to and rationalized by ring-polymer molecular dynamics simulations. Our work points to real-time imaging of stereodynamics, i.e. how the molecular orientation changes as the ion approaches.

References

[1] J. K. Christensen et al., *Nature Comm*. (in print).
[2] S. H. Albrechtsen et al., *Nature* **623**, 319 (2023).
[3] J. K. Christensen et al., *Phys. Chem. Chem. Phys.*, **27**, 24184 (2025).

Boron Nanoclusters

Lai-Sheng Wang
Department of Chemistry, Brown University, Providence, RI 02912

The study of carbon clusters led to the discoveries of fullerenes, carbon nanotubes, and graphene. Are there other elements that can form similar nanostructures? Motivated by this question, we have been investigating the size-dependent structures and chemical bonding of boron nanoclusters using photoelectron spectroscopy in combination with computational chemistry [1, 2].

We have found that bare boron clusters possess planar structures [3], in contrast to that of bulk boron, which is dominated by three-dimensional polyhedral building blocks. The discovery of planar boron clusters laid the foundation for 2D boron nanomaterials [4]. In particular, the observation of the planar B_{36} cluster with a central hexagonal vacancy provided the first experimental evidence that single-atom boron-sheets with hexagonal vacancies (borophene) were viable (Fig. 1) [5]. Borophene has been synthesized and characterized on inert substrates, forming a new class of synthetic 2D materials [6].

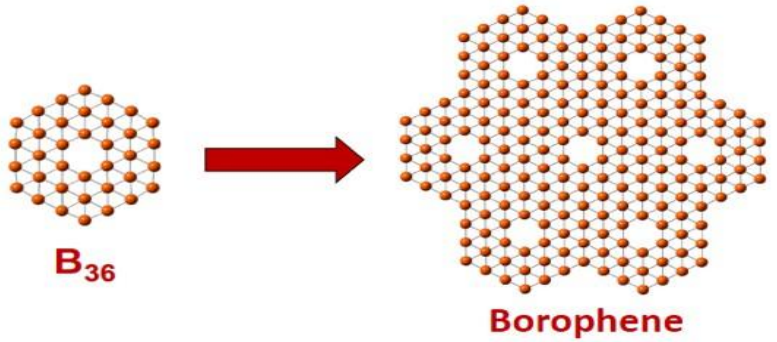

Fig. 1. From planar boron clusters to borophenes.

The B_{40} cluster was first found to be an all-boron fullerene [7], which possesses D_{2d} symmetry with a cage diameter slightly smaller than that of C_{60}. In this talk, I review our progresses and focus on recent advances in our investigation of large boron clusters, including 2D-3D transitions, the appearance of bulk-like boron features [8], and other novel boron nanostructures.

References

[1] L. S. Wang et al., *Int. Rev. Phys. Chem*. **35**, 69-142 (2016).

[2] T. Jian et al., *Chem. Soc. Rev*. **48**, 3550-3591 (2019).

[3] A. P. Sergeeva et al., *Acc. Chem. Res*. **47**, 1349-1358 (2014).

[4] W. L. Li et al., Wang. *Nat. Rev. Chem*. **1**, 0071 (2017).

[5] Z. A. Piazza et al., *Nat. Commun*. **5**, 3113 (2014).

[6] Y. V. Kaneti et al., *Chem. Rev.* **122**, 1000−1051 (2022).

[7] H. J. Zhai et al., *Nat. Chem*. **6**, 727 (2014).

[8] Q. Chen et al., *Proc. Natl. Acad. Sci*. (USA) **122**, e2510702122 (2025).

The weird world of carbon clusters – infrared and electronic spectra of chains, rings and fullerenes

Chang Liu, Patrick Watkins, Samuel Marlton, Evan Bieske
School of Chemistry, University of Melbourne, 3010, Australia

Small carbon clusters play important roles in a variety of contexts, and are present in flames and discharges, and in interstellar space. Although buckminsterfullerene (C_{60}) is well characterized, less is known about the properties and behaviour of smaller carbon clusters, which tend to progressively adopt structures as chains, rings, bi-rings, and fullerenes.[1] As shown in Figure 1, carbon clusters are part of an extended hydrocarbon landscape, that includes partially hydrogenated clusters and molecules and polycyclic aromatic hydrocarbons (PAHs). PAHs can be progressively dehydrogenated when energised by light or collisions to eventually produce bare carbon clusters, including cyclocarbons.[2,3]

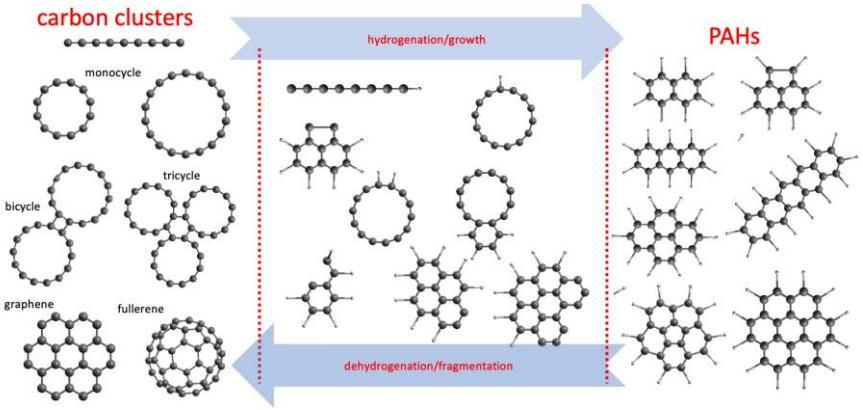

Figure 1: Bare carbon clusters, partially hydrogenated carbon clusters, and polycyclic aromatic hydrocarbons (PAHs).

To learn more about carbon clusters we have measured electronic and infrared spectra for clusters of different sizes and isomeric structures. To avoid isomeric ambiguities, we have adopted a strategy whereby the target isomer (linear, ring, bi-ring, or fullerene) is preselected using tandem ion-mobility and mass spectrometer stages, prior to spectroscopic interrogation with beams of tunable light in a cryogenically cooled ion trap.[4]

Prominent electronic transitions of charged cyclocarbons (cations and anions) are found to occur in the visible and near-IR spectral regions, with a progressive, regular shift of the main bands to longer wavelength with increasing ring size.[5] The C_{4n}^{+} rings possess extraordinarily sharp, intense IR transitions that are at least 50 times stronger than transitions of the corresponding bi-ring and fullerene isomers, and which are associated with a single vibrational mode that propels charge back and forth across the ring.[6] The intense vibrational transitions may serve as a signature for the presence of carbon rings in remote or hostile environments and may also provide a means for energised rings to dissipate energy through IR emission.

References

[1] G. von Helden, M-T. Hsu, P. Kemper, M. Bowers, *J. Chem. Phys.* **95**, 3835-3837 (1991)

[2] C. Lifshitz, T. Peres, I. Agranat, *Int. J. Mass. Spectrom. Ion Proc.* **93,** 149-163 (1989)

[3] H. Hrodmarsson, J. Bouwman, A. Tielens, H. Linnartz, *Int. J. Mass Spectrom.* **476,** 116834 (2022)

[4] J. Buntine, *et al. Rev. Sci. Instrum.* **93,** 043201 (2022)

[5] S. Marlton, *et al. J. Phys. Chem.* **127,** 1168–1178 (2023)

[6] C. Liu, P. Watkins, P. Taylor, E. Bieske, *J. Phys. Chem. Lett.*,**16,** 12989–12996 (2025)

$C_{11}H_9^+$ as a Key Intermediate in PAH Growth in Astrophysical Environments

Christine Joblin, Ana I. Lozano, Anthony Bonnamy
Institut de Recherche en Astrophysique et Planétologie (IRAP), Université de Toulouse – CNRS, France

Aude Simon
Laboratoire de Chimie et Physique Quantiques (LCPQ) /Institut FeRMI, Université de Toulouse – CNRS, France

Pavol Jusko
Max Planck Institute for Extraterrestrial Physics (MPE), Garching, Germany

Jérôme Bernard
Institut Lumière Matière (iLM), Université Lyon1 - CNRS, France

Introduction

The recent detection of abundant aromatic hydrocarbons in cold dark clouds has revived the possibility that these complex organic molecules can form and grow at low temperatures. Most of the species identified so far are cyano-substituted PAHs, whose large dipole moments greatly facilitate their detection by radio astronomy. To date, PAHs as large as cyano-coronene ($C_{24}H_{11}CN$) have been reported, with column densities approximately twice that of the smaller cyano-naphthalene ($C_{10}H_7CN$) [1,2]. Several of the detected molecules contain pentagonal rings, such as indene and cyano-acenaphthylene [3,4].

The formation pathways are thought to involve gas-phase chemistry and likely include efficient ion–molecule reactions and subsequent ion-electron recombination. In parallel, PAH —including methylated PAHs—are found to be abundant in primitive bodies of the Solar System such as carbonaceous chondrite meteorites and the Ryugu asteroid [5-8].

Understanding the chemical processes leading to the formation of these species is therefore essential to trace the evolution of PAHs from cold interstellar clouds to the primitive solar nebula [9].

Experimental approach

The physical conditions prevailing in interstellar clouds are extreme, characterized by very low temperatures and densities. Studying the formation and survival of PAHs in such environments therefore requires access to long timescales over which radiative cooling processes—particularly slow infrared emission—can operate.
Several experimental setups dedicated, or largely dedicated, to laboratory astrophysics address these challenges. These include the PIRENEA cryogenic FT-ICR setup [10] and electrostatic storage rings (ESRs) such as Mini-Ring and the cryogenic DESIREE facility. As will be illustrated here, PIRENEA offers multiplex capabilities that enable the investigation of both chemical reactivity and photostability within the same experiment. In contrast, ESRs are particularly well suited for studying cooling dynamics and charge-recombination processes [11-14]. Experiments performed in ESRs have demonstrated that recurrent fluorescence can play a significant role in the radiative stabilization of large molecular ions.

Results: the isomers of $C_{11}H_9^+$

The −H cations of methylated PAHs are of particular astrophysical interest because of their enhanced stability relative to their parent cations[10]. Here, we report on the photophysics and reactivity of $C_{11}H_9^+$, the -H cation of methyl-naphthalene (MeNp). This species has been detected by *in situ* mass spectrometry in Titan's ionosphere [15] and is expected to exist in several isomeric forms [16,17]. Using the PIRENEA setup, we combined action spectroscopy, photofragmentation kinetics, and ion–molecule reaction studies. We identified three long-lived isomers of $C_{11}H_9^+$: 1-naphthylmethylium (1-NpCH_2^+), 2-naphthylmethylium (2-NpCH_2^+), and benzyltropylium (BzTr^+) [18].
In a subsequent study, we demonstrated that $C_{11}H_9^+$ is the exclusive fragmentation channel of di$MeNp^+$. This provides the opportunity to investigate the reactivity of $C_{11}H_9^+$ with several diMeNp isomers. On

this basis, we assign the reaction products $C_{12}H_{11}^+$ and $C_{13}H_{13}^+$ to reactions involving 1- and 2-$NpCH_2^+$, respectively, while confirming that $BzTr^+$ is essentially unreactive [19].

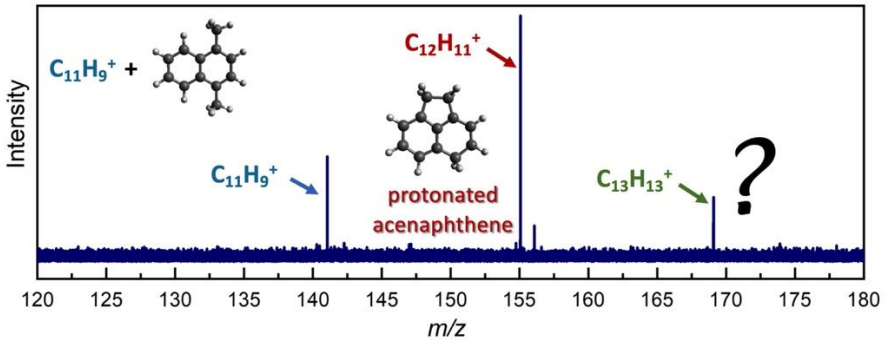

Further irradiation of the reaction products with a Xe lamp allowed us to propose structures for both the primary products and their fragments. Acenaphthene-like species were identified as key intermediates, with the acenaphthylene radical cation ($C_{12}H_8^+$) emerging as the final and most stable fragment. These results are rationalized by a chain-growth mechanism followed by ring closure [19]. Given the recent detection of cyano-acenaphthylene in the TMC-1 cold cloud, our findings provide insight into plausible formation pathways for this species in space.

Perspectives

The PIRENEA setup will enable the investigation of potential PAH growth pathways under astrophysically relevant conditions [20]. These studies should be complemented by experiments using ESRs, which are particularly well suited to probing relaxation dynamics and the survival of these species following UV photon absorption. Initial experiments performed at the Mini-Ring on $C_{11}H_9^+$ have revealed a complex behaviour, possibly associated with the interplay between radiative cooling via recurrent fluorescence and isomerization, a process that is rarely accounted for in such studies [21]. The next-generation instrument Polar Mini-Ring, which will be interfaced with the VUV DESIRS beamline at SOLEIL, will provide

improved control over the internal energy of the ions and is therefore expected to help disentangle these competing processes [22].

Acknowledgements

This work was supported by the Agence Nationale de la Recherche (ANR 21-CE30- 0010, SynPAHcool), the recurrent funding for the Nanograin platform at IRAP, and the Thematic Action “Physique et Chimie du Milieu Interstellaire” (PCMI) of the INSU Programme National “Astro”.

References

[1] B. A McGuire et al., *Science* **371**, 1265 (2021)
[2] G. Wenzel et al., *Astrophys. J. Letter* **984**, L36 (2025)
[3] J. Cernicharo et al., *Astron. Astrophys.* **649**, L15 (2021)
[4] J. Cernicharo et al., *Astron. Astrophys.* **690**, L13 (2024)
[5] J. E. Elsila et al., *Geoch. Cosm. Act.* **69**, 1349 (2005)
[6] G. Danger et al., *Planet. Sci. J.* **1** (3), id55 (2020)
[7] J. C. Aponte et al., *Earth Planets Space* **75**, 28 (2023)
[8] H. Sabbah et al., *Natural Sciences* **4**, id. e20240010 (2024)
[9] S. S. Zeichner et al., *Science* **382**, 1411 (2023)
[10] A. Marciniak et al., *Astron. Astrophys.* **652**, A42 (2021)
[11] S. Martin et al., *Phys. Rev. A* **92**, 053425 (2015)
[12] M. H. Stockett et al., *Nat. Comm.* **14**, 395 (2023)
[13] M. H. Stockett et al., *ACS Earth Space Chem.* **9**, 382 (2025)
[14] J. N. Bull et al., *Phys. Rev. Let.* **134**, 228002 (2025)
[15] F. Crary et al., *Planet. Space Sci.* **57**, 1847 (2009)
[16] I. Gotkis et al., *Org. Mass Spectrom.* **28**, 372 (1993)
[17] A. Nagy et al., *J. Am. Chem. Soc*. **133**, 19796 (2011)
[18] A. I. Lozano et al., *ACS Earth Space Chem.* **9**, 2017 (2025)
[19] A. I. Lozano et al., subm.
[20] P. Jusko et al., in prep.
[21] J. W. L. Lee et al., *J. Chem. Phys.* **158**, 174305 (2023)
[22] https://anr.fr/Project-ANR-21-CE30-0010

Reactive collisions of atomic oxygen and aromatic compounds in crossed-beam experiments

Nadia Balucani
Dipartimento di Chimica, Biologia e Biotecnologie, Università degli Studi di Perugia, 06123 Perugia, Italy

In our laboratory, we have started a systematic investigation of the reactions involving oxygen atoms and aromatic compounds under single collision conditions using the crossed molecular beam technique with mass spectrometric detection.

The first systems we have looked at are $O(^3P)$ + benzene [1], $O(^3P)$ + pyridine [2], and $O(^3P)$ + toluene [3]. More recently, we have investigated the reactions on $O(^3P)$ + ethylbenzene, $O(^3P)$ + thiophene, $O(^3P)$ + phenol, and $O(^3P)$ + naphthalene while we plan to investigate the reactions with styrene, anisole, and other functionalized aromatics.

From a fundamental point of view, these studies aim to derive the structure dependency of the reactivity of aromatics. However, a detailed understanding of these reactive systems has practical implications ranging from biomass gasification processes to the design of novel space-technology aromatic polymers.

As in the case of the $O(^3P)$ reactions with unsaturated organic compounds, the investigated reactions are strongly affected by intersystem crossing (ISC) to the underlying singlet potential energy surface associated with a significant alteration of the reaction mechanism and product branching fractions. ISC can occur in the entrance channel, as observed for the O + pyridine reaction [2], or at a later stage.

In all cases, upon ISC, either ring-contraction or ring-opening (in the case of O + thiophene) mechanisms with CO elimination were

observed to be significant or dominant (in the case of the reaction with pyridine and thiophene).
Electronic structure calculations of the reactive potential energy surfaces are pivotal for the interpretation of the crossed-beam experiments [1-3]. In preparation of the experiments, we have also anticipated the theoretical simulations (using density functional theory with the ωB97X-D functional) for O(3P) + aniline, phenol, 1,3-diphenylpropane, diphenyl ether, propylbenzene, formanilide, and benzonitrile along the adiabatic triplet PES [4]. The competition between ortho and ipso was assessed [4].

I acknowledge financial support under the National Recovery and Resilience Plan (NRRP), Mission 4, Component 2, Investment 1.1, Call for tender No. 104 published on 02.02.2022 by the Italian Ministry of University and Research (MUR), funded by the European Union – NextGenerationEU– Project Title 20227W5CLJ Biomass gasification for hydrogen production (Bio4H2) – CUP J53D23001970006 - Grant Assignment Decree No. 961 adopted on 30.06.2023 by the Italian Ministry of Ministry of University and Research (MUR).

References

[1] G. Vanuzzo et al., *J. Phys. Chem. A*, **125**, 8434 (2021).
[2] P. Recio et al., *Nature Chemistry* **14**, 1405 (2022).
[3] N. Balucani et al., *Faraday Disc*. **251**, 523 (2024).
[4] D. Campisi et al., *Chem. Phys. Lett*. **885**, 142592 (2026)

Coulomb crystal studies of the reactions of NH_3/ND_3 with $Ar^{\bullet+}$ and $NH_3^{\bullet+}$

Paul Regan, Lucy Morris, Vincent Richardson, Jake A Diprose, Kyriaki Vourka, Maksymilian J Roman, Kane Stevenson, Rahul K Pandey, Rahab Gardner, and Brianna R Heazlewood
Department of Physics, University of Liverpool, Oliver Lodge Laboratory, Oxford Street, Liverpool, UK

Timothy P Softley
School of Chemistry, University of Birmingham, Edgbaston, B15 2TT, UK

Introduction

Ion-molecule reactions are of significant value to astrochemistry due to a combination of charge-dipole/induced dipole interactions and the coordination between charge and functional groups that leads to rates that are typically far higher than for comparative neutral-neutral reactions [1]. There is therefore a significant need for experimental data recorded under representative conditions, both as input data for astrochemical models and test data to validate the capture theory models that are widely used in the absence of relevant experimental measurements [2].

One experimental method that has shown significant promise in the study of astrochemical ion-molecule reactions involves Coulomb crystals, which enable a wide range of atomic and molecular ions to be maintained at low (< 1K) kinetic temperatures [3]. Here, we present results for the reactions of $Ar^{\bullet+}$ and $NH_3^{\bullet+}$ with rotationally cold NH_3/ND_3 using a pair of Coulomb crystal instruments, through which we explore effects of internal energy on reactivity at low kinetic temperatures.

Methods

Coulomb crystals are strongly coupled non-neutral plasmas of laser-cooled ions with 3D lattice-like structures. In this work, we have used

$^{40}Ca^+$ ions, with Ca atoms being non-resonantly ionized at the centre of a linear Paul trap using a 355 nm Nd:YAG laser. The Ca^+ ions are then laser-cooled using a combination of 397 and 866 nm diodes. When sufficient kinetic energy is removed from the ions such that the trapping fields are in equilibrium with the Coulombic repulsion between the ions, a phase change is observed to give the pseudo-crystalline structure.

Reactant ions are introduced into the crystal using appropriate REMPI schemes, with elastic collisions between the laser-cooled Ca^+ ions and the reactant ions sympathetically cooling the reactant ions to < 1 K. The progress of the reaction following the admission of neutral reactants can then be monitored either through imaging the central slice of the crystal or through time-of-flight (ToF) mass spectrometry, with an example of the central slice images from a previous study [4] given in Figure 1.

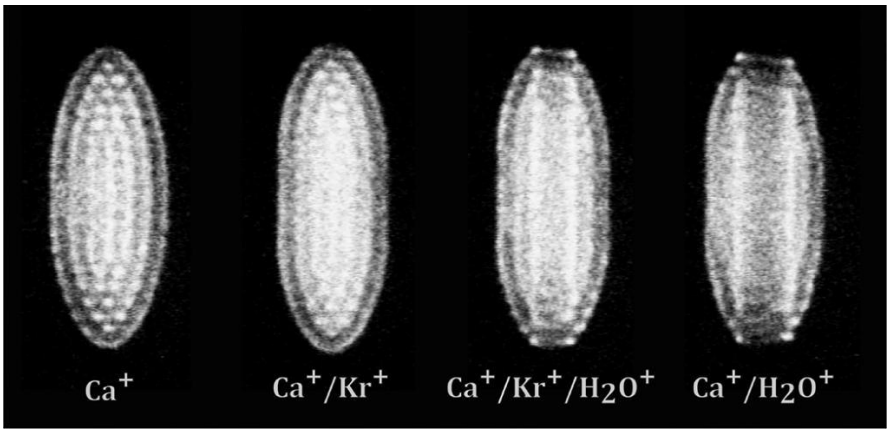

Figure 1. Experimental images of the central slice of Coulomb crystals containing different combinations of Ca^+, $Kr^{\bullet+}$ and $H_2O^{\bullet+}$ [4]. The positions of different ions in the crystal are determined by their relative *mass-tocharge* (*m/z*) ratios, with lighter ions closer to the trap axis.

Building upon previous studies using effusive sources of NH_3 and ND_3 with rare gas ions, which noted a distinct inverse kinetic isotope

effect [5, 6], in this work we have looked to explore the impact of the internal energy of the neutral reactant using a supersonic expansion.

Results

We present results for the reaction of $Ar^{\bullet+}$ with NH_3 and ND_3, in addition to the reactions of $NH_3^{\bullet+}$ with NH_3 and $ND_3^{\bullet+}$ with ND_3. These results are compared with state-selective capture theory calculations, with rotational populations of the neutral obtained through REMPI spectroscopy. This enables an exploration of the impact of both the neutral internal energy of the neutral and isotopic substitution on reactivity.

References

[1] M. Larsson, W. D. Geppert, and G. Nyman, *Rep. Prog. Phys.* **75**, 066901 (2012)

[2] A. Tsikritea, J. A. Diprose, T. P. Softley, and B. R. Heazlewood, *J. Chem. Phys.* **157**, 060901 (2022)

[3] B. R. Heazlewood, *Mol. Phys.* **117**, 1934 (2019)

[4] A. Tsikritea, J. A. Diprose, J. Loreau, and B. R. Heazlewood, *ACS Phys. Chem. Au* **2**, 199 (2022)

[5] L. S. Petralia, A. Tsikritea, J. Loreau, T. P. Softley, and B. R. Heazlewood, *Nature Commun.* **11**, 173 (2020)

[6] A. Tsikritea, K. Park, P. Bertier, J. Loreau, T. P. Softley, and B. R. Heazlewood, *Chem. Sci.* **12**, 10005 (2021)

Revealing high-resolution spectra of hydrocarbon cations with leak-out spectroscopy

Oskar Asvany, Philipp Schmid, Weslley Silva, Thomas Salomon, Sven Thorwirth and Stephan Schlemmer
Physikalisches Institut, Universität zu Köln, 50937 Köln, Germany

Introduction

Molecular ions are key intermediates driving the chemistry of the interstellar medium through ion–molecule reactions. An example reaction network for the family of hydrocarbon cations is given in the Figure below (taken from [1]). Although some of these species have been known for decades in the interstellar medium - CH^+ being the first molecular ion ever detected [2] - in recent years, some more of these ions have been observed, the most spectacular one being the detection of CH_3^+ with the James Webb Space Telescope (JWST) toward the UV-irradiated protoplanetary disk d203-506 in the Orion bar [3]. However, high-resolution laboratory data for many other hydrocarbon cations are still lacking, making them elusive to both astronomers and experimentalists. With the advent of leak-out spectroscopy (LOS) [4], high-resolution rovibrational spectra of many bare ions, long missing, can now be rapidly recorded with unprecedented signal-to-noise ratios. In addition, applying a rotational-rovibrational double resonance version of LOS [5], also pure rotational spectra can be recorded for these species, laying the basis for their potential detection in space. This talk reviews the detection

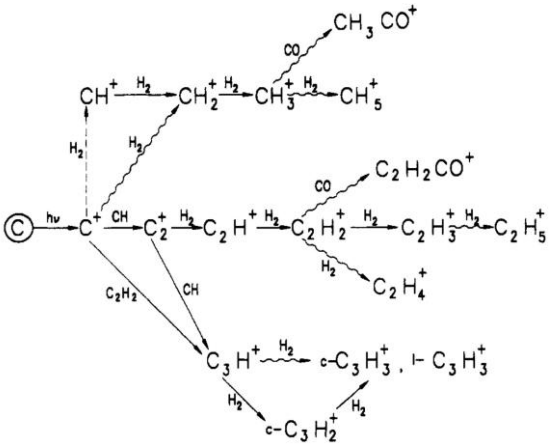

history of these species and presents recent laboratory results for some astrophysically relevant hydrocarbon cations, including H_2CCCH^+, C_2H^+ and CH_3^+.

Experimental setup and Leak-Out Spectroscopy (LOS)

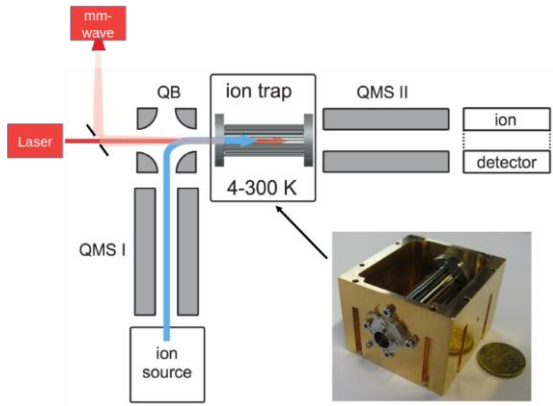

The experimental setups in Cologne [6] typically comprise a storage ion source, a first quadrupole mass selector (QMS I), an electrostatic quadrupole bender (QB), the 22-pole ion trap mounted on a 4K (or 10K) coldhead, the second quadrupole mass selector (QMS II), and finally a Daly-type ion detector. An IR laser and a mm-wave beam can be combined and introduced into the vacuum system via a diamond window. With this, one can perform rovibrational as well as rotational spectroscopy of cold molecular ions stored in the 22-pole trap. The method of choice here is LOS [4] which is based on the collision-induced transfer of vibrational energy into kinetic energy. This is illustrated below for the C_3H^+ cation. Upon resonant absorption of a

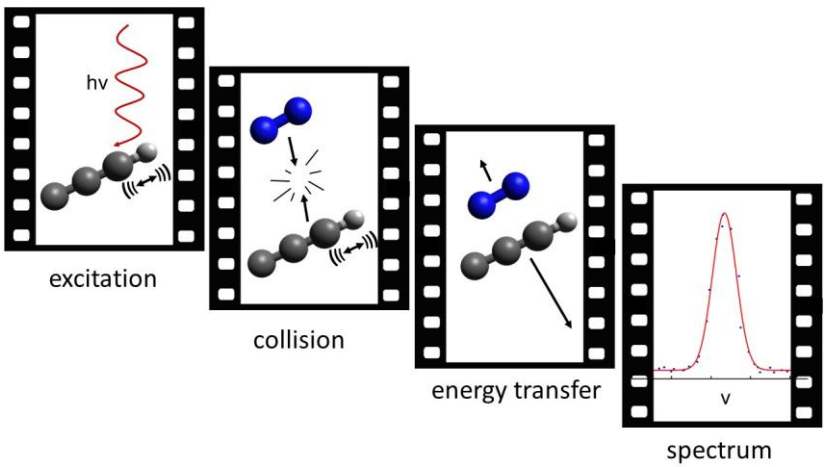

laser photon, the molecular ion is lifted into a vibrationally excited state. If this excited ion collides with a neutral non-reactive particle (N_2 in the Figure below), a part of the vibrational energy may be released into kinetic energy of both collision partners. The ion is thus considerably accelerated, and can “leak out” from the trap and be directed towards the ion detector (right hand side in the experimental setup). By counting these escaping ions as a function of the wavenumber of the exciting laser, a rovibrational spectrum can be recorded. This scheme can straightforwardly be extended to record pure rotational transitions by applying the well-known double resonance approach [5].

Results

We always start our investigations by recording high-resolution spectra of a few selected rovibrational modes of the target cation, typically C-H or C-C stretches in the 3 µm or 5 µm region, respectively. Once these modes are assigned and analyzed, pure rotational transitions can be well predicted and subsequently measured via the mentioned double-resonance approach. The rotational spectra can then be compared to astronomical observations. One such successful example is that of H_2CCCH^+ [7]. The adjacent Figures show the recorded rovibrational spectrum (top) and a single rotational line (bottom). In total, fourteen rotational lines were measured and finally allowed the identification of H_2CCCH^+ in the cold cloud TMC-1. Its cyclic isomer c-$C_3H_3^+$, on the other hand, has no rotational spectrum, and

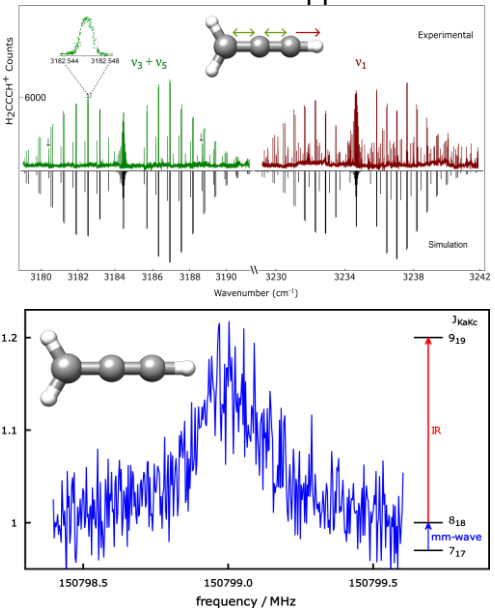

attempts to detect deuterated c-$C_3H_2D^+$ via its rotational transitions failed due to the low column density of c-$C_3H_2D^+$ in TMC-1 [8]. Other interesting molecules which will be touched in this talk are CH_3^+, for which we measured the bending vibrations at 7 µm in high resolution, thus confirming the recent JWST detection [3], as well as the open-shell triatomic molecule C_2H^+ ($^3\Pi$).

Outlook

Despite all these advancements, still many ions in the presented ion reaction network remain elusive. In particular, in the reaction chain $C^+ \rightarrow CH^+ \rightarrow CH_2^+ \rightarrow CH_3^+ \rightarrow CH_5^+$, only C^+ [9] and CH^+ [2,3] have been known for a long time, and CH_3^+ has been detected only recently [3]. Thus CH_2^+ and CH_5^+ remain completely unobserved. In particular, it has been pointed out [10] that it is puzzling why CH_3^+ is so prominent in the JWST data of the protoplanetary disk d203-506, but not its precursor CH_2^+. Reasons might be the swift reaction of CH_2^+ to CH_3^+, or the dilution of its emission signal due to a multitude of transitions caused by a low-lying electronic state. But also spectroscopic data about the bending vibration of CH_2^+ at 10 µm are missing, which we hope to target with LOS soon. Similarly, it is important to point out that the $^2P_{3/2} \leftarrow {}^2P_{1/2}$ fine structure transition of the C^+ atomic ion at 1.9 THz, the transition by which it is detected in space and which is one of the most important cooling lines in the interstellar medium, is not well characterized in the laboratory, in particular for its isotope $^{13}C^+$ [11]. We would therefore like to extend the LOS principle to atomic species, starting with C^+. First experiments for the $^2P_{3/2} \leftarrow {}^2P_{1/2}$ transition of $^{12}C^+$ failed, being rooted in a lack of excitation power (transition is dipole forbidden) and not in the LOS principle itself, as theoretical calculations reveal the relaxation of the $^2P_{3/2}$ level in a collision to be quite effective [12]. Improved test experiments on C^+ using LOS might therefore be carried out in the future with electronic excitation, e.g. the $^4P_{1/2} \leftarrow {}^2P_{1/2}$ transition at about 232 nm, where more excitation power is commercially available. A double resonance experiment might then finally lead to the $^2P_{3/2} \leftarrow {}^2P_{1/2}$ fine structure transition at 1.9 THz, as needed by astronomers.

References

[1] Gerlich and Horning, *Chem. Rev.* **92**, 1509 (1992)
[2] Douglas and Herzberg, *Astrophys. J.* **94**, 381 (1941)
[3] Berne et al, *Nature* **621**, 56 (2023)
[4] Schmid et al., *J. Phys. Chem. A* **126**, 8111 (2022)
[5] Asvany et al., *PCCP* **25**, 19740 (2023)
[6] Asvany et al., *Appl. Phys. B* **114**, 203 (2014)
[7] Silva et al., *Astron. Astrophys* **676**, L1 (2023)
[8] Gupta et al., *Faraday Discuss.* **245**, 298 (2023)
[9] Russell et al., *Astrophys. J*. **240**, L99, (1980)
[10] Zannese et al., *Astron. Astrophys.* **696**, A99 (2025)
[11] Cooksy et al., *Astrophys. J.* **305**, L89, (1986)
[12] Lique et al., *J. Chem. Phys.* **138**, 204314 (2013)

Molecular modeling of collisions and uptake of volatile organic compounds with hydrated nitric acid clusters

Eva Pluhařová, Karolína Fárníková, Andriy Pysanenko, Michal Fárník
J. Heyrovský Institute of Physical Chemistry, v.v.i., Czech Academy of Sciences, Dolejškova 2155/3, 18223 Prague 8, Czech Republic

Yihui Yan, Jozef Lengyel
Lehrstuhl für Physikalische Chemie, TUM School of Natural Sciences,Technische Universität München, Lichtenbergstraße 4, 85748 Garching, Germany

The Earth's atmosphere is complex in terms of chemical composition as well as types of phases. One of the key components of the atmosphere are aerosols that are suspensions of solid or liquid particles in the air. They function as heterogeneous catalyst and influence various processes, such as the greenhouse effect. In polluted areas, they have been found to severely impact human health [1].

Aerosol particles emerge and then evolve via so-called new particle formation (NPF), which is a process, where through nucleation and condensation of gaseous components, molecular clusters form. Despite the previous extensive studies of aerosol particles and the NPF in particular, the details at molecular level are still unknown.

Molecular dynamics simulations and molecular beam experiment [2, 3] are useful tools to investigate early stages of NPF with atomistic resolution. As model volatile organic compounds we have chosen alcohol molecules with various alkyl chain lengths and branching [4], aldehydes and carboxylic acids. We simulated their collisions with hydrated nitric acid clusters and compare obtained uptake cross-sections with experimental data.

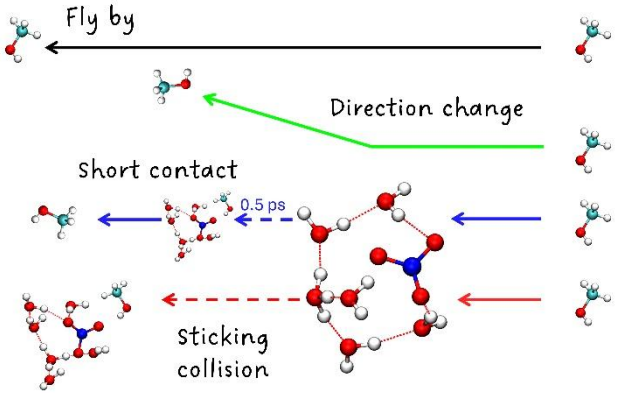

Figure1. Processes taking place upon the encounter of the organic molecule and the water cluster as observed in molecular dynamics simulations: fly-by, direction change, short contact and sticking collision.

Figure 1 depicts various processes that we observed in the simulations: fly by, direction change, short contact and sticking collision. Evaporation of water molecule(s) after the collision might happen too. The calculated relative pick-up cross sections for the series of alcohol molecules with small hydrated nitric acid clusters were in exceptional agreement with experimental data. This allowed us to rationalize the effect of size and bulkiness on the uptake efficiency. Next, carboxylic acids are picked-up more efficiently than aldehydes. Overall, our combination of simulations and experiment provides new insight into the early stages of the formation of aerosol particles.

References

[1] M. Fárník, *J. Phys. Chem. Lett.* **14**, 287 - 294 (2023).
[2] A. Pysanenko, J. Lengyel, M. Fárník, *J. Chem. Phys*. **148**, 154301 (2018).
[3] J. Lengyel, A. Pysanenko, K. Fárníková, E. Pluhařová, M. Fárník, *J. Phys. Chem. Lett*. **11**, 2101 – 2105 (2020).
[4] K. Fárníková, E. Pluhařová, A. Pysanenko, M. Fárník, Y. Yan, J. Lengyel, *Faraday Discuss.* **251**, 296 – 312 (2024).

The role of coordination complexes on the stability of protonated argon clusters

Jesús Pérez-Ríos

Department of Physics and Astronomy, Stony Brook University, Stony Brook, NY 11794, USA

The stability of rare-gas clusters can be described by a sphere packing model. However, when adding a charged impurity, the set of magic numbers grows significantly. Therefore, charged impurities seem to drastically affect the structural stability of rare-gas clusters. One primary example of this behavior has been observed in protonated argon clusters, which exhibit a large set of magic numbers: 7, 13, 19, 23, 26, 29, 32, 34, 46, 49, and 55 [1]. However, only 7, 13, and 19 have been explained. In this talk, I will present our joint experiment-theory approach to study the stability of protonated argon clusters. We use a combination of quantum Monte Carlo techniques, fed by a realistic $[Ar\text{-}H\text{-}Ar]^+$-Ar interaction potential that accounts for the proton's coordination number of 2. Only with this potential can one explain the set of magic numbers and even identify a transition from many-body to few-body physics effects on the structure of the clusters. Our work indicates that a proper description of ion coordination properties is essential to explain the stability of doped clusters containing ion impurities [2]. Hence, it may have profound implications for studies of ion solvation dynamics and cold molecular science.

References

[1] M. Gatchell, P. Martini, L. Kranabetter, B. Rasul, and P. Scheier, *Phys. Rev. A* **98**, 022519 (2019)
[2] S. Chowdhury, M. J. Montes de Oca-Estévez, F. Foitzik, E. Gruber, P. Scheier, P. Villarreal, R. Prosmiti, T. González-Lezana, and J. Pérez-Ríos, arXiv:2601.00591 (2026)

Competing dissociation and ionization in superexcited states of molecular hydrogen

D. Ochoa, D. Knapp, S. Sharma and M. Beyer
Department of Physics and Astronomy, VU Amsterdam, The Netherlands

Molecular hydrogen remains a benchmark system for studying the spectra and dynamics of superexcited Rydberg states with multichannel quantum-defect theory (MQDT). Here, we provide benchmark, product-resolved data to test and constrain MQDT implementations for the competing dissociation and ionization pathways of superexcited H_2.

Quantifying the branching between neutral fragments, ions, and ion pairs is relevant for understanding H_2 formation pathways via H_2^+ in the early universe and for developing schemes toward controlled production of antimatter H_2^-.

We excite the ungerade superexcited manifold of H_2 by resonant three-photon absorption using a (1+2′) REMPI scheme and follow the subsequent post-excitation dynamics into a coupled reaction network. The accessible channels include (i) direct ionization and autoionization to $H_2^+ + e^-$, (ii) ion-pair formation to $H^+ + H^-$, and (iii) neutral dissociation to $H(n\ell) + H(n'\ell')$. Time-of-flight spectra reveal competition between ionization and dissociation continua, while velocity-map imaging of H^+ fragments provides kinetic-energy-release spectra and anisotropy parameters. Together, these observables separate overlapping contributions, constrain the accessed dissociation limits, and probe the partial-wave composition of the outgoing fragments, providing stringent tests for dynamical models.

In addition, we observe photodissociation of H_2^+ formed by both autoionization and direct photoionization. This secondary step produces distinct kinetic-energy-release signatures and must be

accounted for when assigning product channels and extracting branching information.

If time permits, I will also discuss a new experiment aimed at state-selective production and trap injection of H_2^+ as a route toward precision measurements on this fundamental molecular ion.

Effect of doping on electronic and geometric structure of metal clusters

Miho Hirakawa, Yuna Aonuma, Yuta Suzuki, Ukyo Kawamura, Takuya Horio and Akira Terasaki
Department of Chemistry, Faculty of Science, Kyushu University, Japan

Olga V. Lushchikova, Deepak Pradeep, Piero Ferrari and Joost M. Bakker
Condensed Matter Physics, HFML-FELIX, The Netherlands

Metal clusters have emerged as promising building blocks for applications in catalysis, medicine, and functional nanomaterials due to their size-dependent electronic structure and high chemical activity.[1] While isolated atoms are described by discrete energy levels and bulk metals by continuous band structures, metal clusters occupy an intermediate regime. Their electronic structure can often be rationalized using the Jellium model, in which delocalized valence electrons fill superatomic orbitals.[2] For clusters doped with a single heteroatom, this concept can be extended by the two-step Jellium model, where the dopant locally perturbs the otherwise homogeneous potential of the metal host and modifies the occupation and ordering of the superatomic states.[3] Doping therefore provides a powerful strategy to fine-tune cluster properties, as the dopant inevitably influences both the electronic structure and the geometric arrangement of the cluster, even at the single-atom level.

Doped cationic silver clusters offer an effective platform for testing the two-step Jellium model. We investigate these systems using UV–VIS photodissociation spectroscopy of trapped Ag_nX^+ clusters, complemented by TD-DFT calculations, building on earlier studies of pristine Ag_n^+ clusters [4]. A direct comparison between Ag_nSc^+ and Ag_nAl^+ clusters with identical numbers of silver atoms and total valence electrons reveals pronounced differences in encapsulation

behavior (Figure 1): fewer silver atoms are required to enclose Sc, and Sc-doped clusters adopt higher-symmetry structures. Despite their equal electron count, the two systems also exhibit distinct electronic structures (Figure 2). While Ag_nSc^+ clusters closely follow the predictions of the two-step Jellium model, Ag_nAl^+ clusters show clear deviations from this behavior. This difference is attributed to the distinct origin and localization of the dopant valence electrons, indicating that local orbital interactions play a more dominant role than global electrostatic effects.

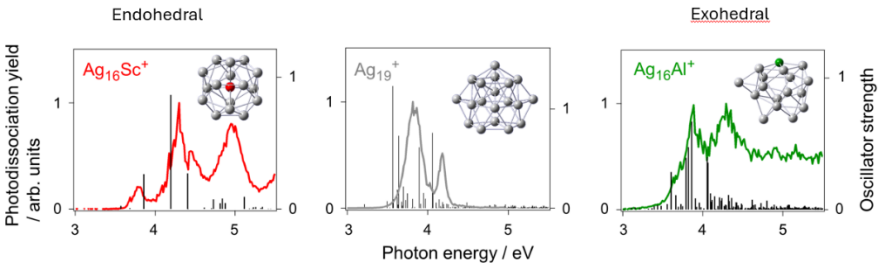

Figure 1: Photodissociation spectra of isoelectronic Ag_{19}^+ and Sc- and Al-doped Ag_{16}^+ clusters, compared with TD-DFT calculations. Despite all having 18 valence electrons, the clusters exhibit distinct electronic and geometric structures. At this size, Sc is positioned exohedrally and adopts a T_d symmetry, whereas Al is located on the surface of the silver cluster with only C_1 symmetry.

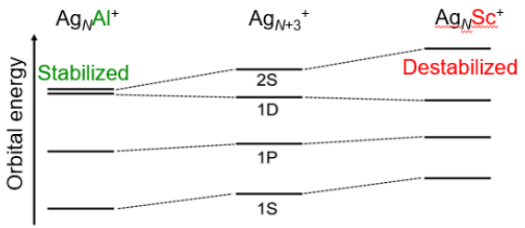

Figure 2: Electronic structure of 18-electron systems, showing that Al doping leads to stabilization of the 2S superatomic orbital, whereas Sc doping destabilizes it.

To extend these insights, we systematically study silver clusters doped with the transition metals V, Mn, Co, and Ni. By varying both the dopant element and the number of silver atoms, we disentangle the effects of valence electron count and cluster size on the electronic structure. This approach allows us to assess how dopant valence electrons are incorporated into the cluster, ranging from strong delocalization over the silver framework to more localized electronic character, depending on dopant identity and cluster size. Similar to Sc-doped systems, all investigated transition metal dopants are found to follow the two-step Jellium model, further emphasizing the universal influence of the dopant on cluster properties.

While UV–VIS spectroscopy is highly sensitive to changes in electronic structure, it is less responsive to subtle geometric variations. To directly probe dopant-induced structural changes, we employ infrared multiphoton dissociation spectroscopy of Ar-tagged doped transition metal clusters in the low-frequency region below 300 cm^{-1} [4], using the FELICE free electron laser at the HFML-FELIX facility [5]. The clusters are produced in a laser ablation source, tagged with Ar, and analyzed by time-of-flight mass spectrometry after IR irradiation. The resulting vibrational spectra, combined with DFT calculations, provide direct insight into dopant-induced geometric rearrangements.

Together, these electronic and vibrational spectroscopic studies provide a comprehensive picture of how dopants modulate the geometric and electronic structure of metal clusters, advancing the fundamental understanding of structure–property relationships relevant to catalysis and nanotechnology.

References

[1] P. Jena and Q. Sun, *Chem. Rev.*, **118**, 11 (2018).
[2] W.D. Knight *et al*., *Phys. Rev. Lett.*, **52**, 24 (1984).
[3] E. Janssens *et al*., *Curr. Opin. Solid. State. Mater. Sci.*, **8**, 3-4 (2004).
[4] S. Kawamura *et al*., *J. Phys. Chem. A*, **127**, 29 (2003).

[5] A. Fielicke *et al*., *Phys. Rev. Lett., **93*** (2004).
[5] J. M. Bakker *et al*., *J. Chem. Phys.*, **132** (2010).

The abc of triplet helium dimer: a computational study

Edit Mátyus
MTA-ELTE "Momentum" Molecular Quantum electro-Dynamics Research Group, Institute of Chemistry, Eötvös Loránd University, Pázmány Péter sétány 1/A, Budapest, H-1117, Hungary

The ground electronic state of the helium dimer, He_2 X $^1\Sigma_g^+$, has been extensively studied by Jeziorski and co-workers. It is a very weakly bound system, bound by dispersion forces, and its potential energy curve supports a single (ro)vibrational state.

The present work focuses on the electronically excited states of the helium dimer, which possess a highly complex rovibronic energy-level structure with intriguing magnetic properties, and have recently attracted experimental interest for generating cold molecules and precision spectroscopy.

We computed the potential energy curves (PECs) of the a $^3\Sigma_u^+$, b $^3\Pi_g$, and c $^3\Sigma_g^+$ electronic states, converged to a few ppm ($1{:}10^6$) precision, using variationally optimised floating explicitly correlated Gaussian functions (fECGs). The Born-Oppenheimer (BO) PECs were appended with diagonal BO, regularised relativistic, and quantum electrodynamical (QED) corrections.

The non-adiabatic coupling, as well as relativistic (spinspin, spin-orbit) couplings, appended with QED corrections for the anomalous magnetic moment of the electron, were also computed with the fECG wave functions. Furthermore, we have included (a less accurate) representation of the B $^1\Pi_g$ and C $^1\Sigma_g^+$ electronic states for the relativistic couplings with the b and c states.

Non-adiabatic vibrational and rotational mass corrections were computed to model non-adiabatic effects arising from distant electronic states.

The coupled rovibrational and rovibronic equations are solved using the discrete variable representation. The X $^2\Sigma_g^+$ ground state of the He_2^+ cation and all bound rovibrational energies with

relativistic, QED, and non-adiabatic corrections are also recomputed, resulting in an estimated few ppb (1:10^9) accuracy.

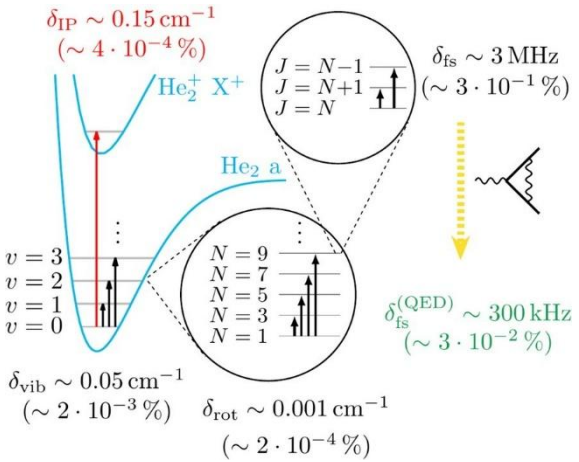

Figure 1: Schematic representation of the computed processes for a $^3\Sigma_u^+$ He_2. Similar computations have been performed for the coupled b $^3\Pi_g$-c $^3\Sigma_g^+$ electronic subspace.

All in all, the ionisation, electronic, vibrational, rotational, and finestructure splitting energy intervals of the lowest-energy triplet helium dimer states were obtained with unprecedented accuracy, spanning a total of nine orders of magnitude of the energy scale and being accurate to at least five or six digits at all scales of motions. The computed results aim to help guide and interpret ongoing and future experimental work on this simple open-shell dimer.

References

[1] B. Rácsai, P. Jeszenszki, Á. Margócsy, E. Mátyus, *J. Chem. Phys*. 163, 081102 (2025) arXiv
[2] Á. Margócsy, B. Rácsai, P. Jeszenszki, E. Mátyus, under review (2025). arXiv
[3] P. Jeszenszki, P. Hollósy, Á. Margócsy, E. Mátyus, *ACS Phys. Chem. Au* (2025). arXiv
[4] E. Mátyus, Á. Margócsy, *Mol. Phys.* under review (2025). arXiv

Ion-trap driven charge control and fluorescence studies in a single NP gas phase experiment

Bastian Björn, Kleopatra Papagrigoriou, Sophia C. Leippe
Universität Leipzig

Isolating single nanoparticles (NPs) in the gas phase prevents inhomogeneous broadening and support interactions, enabling the analysis of intrinsic NP properties. A cryogenically cooled, temperature controllable ion trap allows for single NP mass spectrometry [1], UV/Vis action spectroscopy [2], and temperature-programmed desorption protocols. Here, we present recent developments that enable reversible charge state control of positively charged SiO_2 NPs [3] as well as fluorescence thermometry [4] and lifetime measurements of trapped CdSe/CdS core-shell quantum dots.

Positively charged SiO_2 NPs of 100 nm diameter were charged or discharged using a nearby cold cathode gauge in combination with different buffer gas species, pressures and waveforms of the trap potentials. Charging rate measurements [3] provide insight into the dominant mechanisms and their dependence on the nature of the buffer gas. We show that RF-induced ion acceleration in the trap is essential to reach high NP charge states.

Wavelength dispersed fluorescence measurements with QDs enable spectroscopy-based NP temperature determination over a broad temperature range (50 K – 300 K), paving the way for temperature-controlled experiments. Subsequently, fluorescence lifetimes of core-shell NPs with different shell thicknesses were recorded using time-correlated single photon counting.

References

[1] T.K. Esser, B. Hoffmann, S.L. Anderson, K.R. Asmis, Rev. Sci. Instrum. 90, 125110 (2019).
[2] B. Hoffmann, S.C. Leippe, K.R. Asmis, Molecular Physics 122, e2210454 (2024).

[3] S.C. Leippe, K. Papagrigoriou, C. Behrendt, B. Bastian, submitted (2025).
[4] S.C. Leippe, F. Johst, B. Hoffmann, S. Krohn, K. Papagrigoriou, K.R. Asmis, A. Mews, B. Bastian, Phys. Chem. C 128, 50 (2024).

Towards the imaging of dynamics at liquid-liquid interfaces

Niels van der Burg, Mi Zhou, Lei Xu, Adriana Caraciolo, Andreas Osterwalder
Institute for Chemistry and Chemical Engineering, Ecole Polytechnique Fédérale de Lausanne, Switzerland

Based on the demonstration [1] that the liquids from two impinging jets in the formation of a liquid flat-jet do not mix by turbulences we are developing a technique to study physical and chemical dynamics at the interface between two liquids.
The photo above [1] shows the series of leaf-shaped liquid structures formed in an imping-jet arrangement; here the two initial jets contained different reactants for a chemiluminescence reaction, and the gradual increase of luminescence intensity in the first leaf reflects the kinetics of this process, since the liquids only mix through diffusion of reactants from one liquid layer to the other.
Building on these results we are working toward a robust implementation of such a technique, and the present talk gives a status review of these efforts.

References

[1] Schewe et al., JACS **144**, 7790 (2022)

Astrochemical ions beyond the Second Period of the Periodic Table

Matteo Michielan, Daniela Ascenzi, Paolo Tosi
Dipartimento di Fisica, Universitá di Trento, Trento, Italy

Roland Thissen, Christian Alcaraz, Nicolas Solem, Claire Romanzin
Institut de Chimie Physique (ICP) & Paris Saclay Univ., Centre National de la Recherche Scientifique, Paris-Orsay, France.

Luca Mancini, Fernando Pirani, Nadia Balucani, Dimitrios Skouteris
Dipartimento di Chimica, Biologia e Biotecnologie, Universita degli Studi di Perugia, Perugia, Italy

Marzio Rosi
Dipartimento di Ingegneria Civile e Ambientale, Universita degli Studi di Perugia, Perugia, Italy.

Cecilia Ceccarelli
Institut de Planétologie et d'Astrophysique de Grenoble (IPAG), Universite Grenoble Alpes, Grenoble, France.

Introduction

The inventory of molecules detected in various regions of the interstellar medium (ISM) is rapidly expanding, both in number and in chemical complexity. Thanks to the enhanced sensitivity, spatial resolution and broadband capabilities of new-generation ground- and space-based telescopes, it is now possible to detect molecules present at very low abundances, including species containing elements heavier than the most abundant second-row ones C, H, O, and N (see https://cdms.astro.uni-koeln.de/ for an updated list of molecules detected in our Galaxy and beyond).

Species containing the biogenic elements phosphorus (P) [1] and sulfur (S) [2, 3] are of particular interest, as their incorporation into

organic molecules can provide insights into the formation of prebiotic species, i.e. the simple building blocks that may ultimately lead to the synthesis of the first proto-biological nutrients, such as biopolymers including DNA, RNA, and phospholipids [4].

In contrast, silicon (Si) is a key element in the formation of interstellar dust, where it is primarily present in the form of oxides and carbides [5]. The subsequent coalescence of the dust grains leads to the formation of planets during the early stages of solar system evolution. Interstellar dust also plays a crucial catalytic role in the growth of icy mantles and in driving subsequent heterogeneous interstellar chemistry. In addition, gas-phase Si-bearing species serve as tracers of shocked regions in protostellar environments.

Given the lower ionization energies of Si (8.15 eV) and P (10.36 eV) compared to their second-period counterparts (carbon and nitrogen), both elements can be readily converted into singly charged cations. Consequently, formation pathways involving ion–molecule reactions should be considered for Si- and P-containing species in astrochemical models.

Results

We report on experimental (via the guided ion beam technique) and theoretical investigations of reactions involving Si^+ and P^+ ions with simple molecules. In the case of Si^+, we propose an alternative ionic pathway leading to the formation of SiS, focussing on the reaction of silicon cations with H_2S, which has not previously been considered in astrochemical models. Experiments are supported by electronic structure calculations of the PES, RRKM calculations and a stereodynamical model, which together are used to derive branching ratios and temperature dependent rate constants over the 10-300 K range [6].

Preliminary experimental results will be presented on the reactivity of Si^+ ions with amines and nitriles, leading to the formation of species containing Si–N and Si–C bonds. Comparisons with

analogous reactions involving C^+ will be discussed to highlight similarities and differences in the reactivity of second- and third-row atomic ions. This is a relevant point for the community involved in astrochemical modelling: in the absence of any kinetic data, the chemistry of species containing heavier elements is often inferred on the basis of chemical analogies with second row elements. However, such analogies may break up and lead to erroneous conclusions, as in the $HCO^+/HSiO^+$ case: while the most stable isomer of protonated CO is HCO^+, when C is replaced by Si, the most stable species is $SiOH^+$ [7]

As for the reaction of P^+ ions, we will present experimental and theoretical results on the reactivity with D_2O. Given the ubiquitous presence of water in the ISM, this reaction can contribute to the formation of PO radicals and ions, both detected in the ISM [8, 9]

Acknowledgements
Work supported by MUR PRIN 2020 n. 2020AFB3FX & NRRP MUR 2022JC2Y93

References
[1] F. Fontani, *Frontiers in Astronomy and Space Sciences* **11**, 1451127 (2024)
[2] T. H. G. Vidal and V. Wakelam, *MNRAS* **474**, 5575 (2018)
[3] F. Fontani, E. Roueff, L. Colzi, and P. Caselli, *Astronomy & Astrophysics* **680**, A58 (2023)
[4] L.M. Ziurys, *Ann. Rev. Phys. Chem.* **75**, 307 (2024)
[5] N. Job, and K. Thirumoorthy, *ACS Earth and Space Chemistry* **8**, 467 (2024)
[6] M. Michielan, L. Mancini, D. Ascenzi, et al. *Astronomy & Astrophysics* **698**, A205 (2025)
[7] L. Tinacci, S.Ferrada-Chamorro, C. Ceccarelli, et al. *Ap. J. Suppl. Ser.* **266**, 38 (2023)
[8] V. M. Rivilla, J.G. De La Concepción, I. Jiménez-Serra, et al. *Front. Astron. Space Sci.* **9**, 829288 (2022)
[9] S. Scibelli, A. Megías, I. Jiménez-Serra, et al. *Ap.J. Lett.* **985**, L25 (2025)

Probing catalytic activity and quantum interference effects in state-to-state methane/surface scattering

Christopher Reilly, Patrick Floss, Rainer D. Beck
École Polytechnique Fédérale de Lausanne, Lausanne, Switzerland

Daniel J. Auerbach
Max Planck Institute for Multidisciplinary Sciences, Göttingen, Germany

We present state-to-state methane scattering experiments from different solid surfaces obtained in a new, dedicated UHV state-to-state molecule/surface scattering apparatus [1] that combines the preparation of a surface incident molecular beam in a specific initial rovibrationally excited state with angle- and quantum-state-resolved detection of the scattered species. Our detection technique uses a cryogenic bolometer in combination with infrared laser tagging and is applicable to any molecule with an infrared active vibrational mode and a rotationally resolved infrared spectrum.

Comparison of the relative yield for vibrationally elastic and inelastic scattering of methane from Ni(111), NiO/Ni(111), Au(111), and graphene covered Ni(111), reveals a propensity for surface induced vibrational redistribution (SIVR) which scales with catalytic activity of the target surface as characterized by the barrier height for the methane dissociation [2]. The experimental observation of SIVR can be rationalized by quantum mechanical inelastic scattering calculations by the group of Bret Jackson [3] which show the quantum state distribution of the scattered molecules contains valuable information on the potential energy surface of the reactive molecule/surface system.

For methane scattering from the inert Au(111) surface, we are able to detect, for the first time to our knowledge, the conservation of

wavefunction reflection parity in molecule-surface scattering [4] which is a uniquely quantum mechanical effect. By preparing molecules in a $J = 0$ rotational state, we prepare a state of pure (odd) reflection parity, and when probing the scattering molecules we find an almost total absence of population in rovibrational states of the opposite parity due to destructive interference.

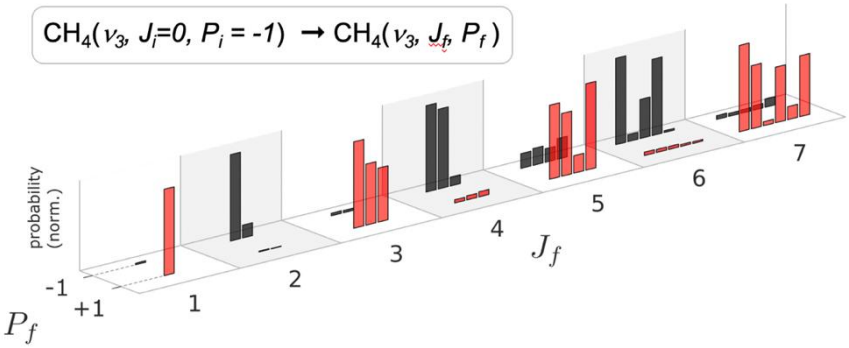

Fig. 1: Rovibrational level populations [4], grouped by rotational quantum number J_f and inversion parity P_f, for scattering of vibrationally excited CH_4 (n_3, $J_i = 0$) from a room temperature Au(111) surface. We observe a distinct, high-contrast interference pattern for the preferred reflection parity channel with the rotational quantum number J_f.

References

[1] C. Reilly et al., J. Chem. Phys. **158**, 214202, (2023).
[2] P. Floss et al., Frontiers in Chemistry **11**, 88, (2023).
[3] J. Werdecker, et al., Phys. Rev. Res. **2**, 43251, (2020).
[4] C. Reilly et al., Science **387**, 962–967 (2025).

Searching for parity violation in trapped chiral molecular ions

Yuval Shagam
Faculty of Chemistry, Solid State Institute & Helen Diller Quantum Center, Technion–Israel Institute of Technology, Haifa, Israel

Experimentally comparing left- and right-handed enantiomers is a powerful way to isolate parity-violating (PV) forces due to the unique asymmetry of chiral molecules (Fig. 1). Usually such searches are designed to be sensitive to the Standard Model nuclear weak force, which is predicted to break the degeneracy between enantiomers. However, in principle the platform is sensitive to any PV effect including new forces, making chiral molecules an intriguing platform to search for more clues to solve the observed incompleteness of the Standard Model [4].

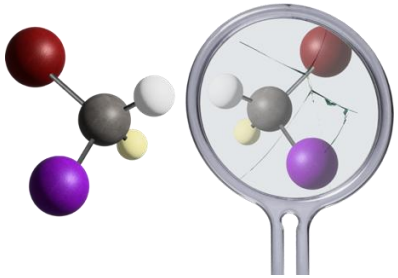

Figure 1: Mirror symmetry breaking between enantiomers

We are developing a chiral molecular ion version of the search for PV in molecules leveraging ion trapping to access long coherence times. Our isotopically chiral candidate molecule, $CHDBrI^+$ is predicted to exhibit a relatively large PV shift of a few Hz between the two enantiomers for the C-H bend vibrational transition at ~10um [1,2]. Notably, the transition's computed natural linewidth is narrower than the predicted shift making it particularly promising for the search. Additionally, our candidate species has been synthesized and is available for spectroscopic studies in the lab.

Precision spectroscopy of such complex polyatomic molecular ions requires both cold generation and state-selective detection. With respect to the former, we aim to prepare cold $CHDBrI^+$ through state-selective ionization [1]. We will present our preliminary results of the ionization of neutral CH_2BrI with VUV photons, which avoids dissociative tendencies. Shifting the VUV light near the ionization threshold we will use Rydberg states, which provide an avenue for selective preparation of $CHDBrI^+$. Such Rydberg states have been observed in CH_2BrI and CH_2ClI [5,6] indicating that vibrational selectivity will be achievable. We will discuss our progress toward experimental implementation of this novel method for loading cold polyatomic into the ion trap.

Our approach to probe the PV signature uses a mixed handedness ensemble of trapped chiral molecular ions in order to suppress technical noise in the measurement. To this end, we have proposed a variant of vibrational Ramsey spectroscopy which is combined with enantiomer separation through three-wave mixing [3], which we will discuss.

Finally, all these experiments require state-selective detection techniques to measure the internal state populations of chiral molecular ions. Our plan is to use resonant state-selective photo-dissociation of molecules as well as direct velocity map imaging (VMI) of the photofragments in single photon dissociation [1,3]. We will present our implementation of an RF ion trap that is integrated with a VMI detector and present preliminary results showing a single-shot resolution below 10 m/s, limited only by the imaged spot size of a single ion.

Importantly, we will also show that chiral molecule radicals such as $CHDBrI^+$ can provide insights in the search for new inter-nuclear forces that violate parity symmetry.

References

[1] A. Landau et al., *J. Chem. Phys.* **159**, 114307 (2023)

[2] Eduardus et al., *Chem. Comm.* **59**, 14579 (2023)
[3] I. Erez et al., *Phys. Rev. X* **13**, 041025 (2023)
[4] C. Baruch et al., *Phys. Rev. Research* **6**, 043115 (2024)
[5] M. Lee et al., *Angew. Chem Int Ed* **44**, 2929 (2005)
[6] M. Lee et al., *J. Chem. Phys.* **123** 024310 (2005)

Molecular diffusion on surfaces: insights from neutron scattering

Peter Fouquet
Institut Laue-Langevin, Grenoble, France

If we want to develop an accurate understanding of surface diffusion of molecules, we need to investigate diffusion processes on molecular or atomic length scales, which requires experimental and calculational methods that deliver sub-nanometer spatial resolution at nanosecond time scale. One of the few spectroscopy techniques that fulfil these characteristics is quasi-elastic neutron scattering. Although, neutron scattering does not naturally provide the required surface sensitivity, we will show that a wide range of 2D materials exist, where a high specific surface area favours the use of neutron scattering.

Our research started with rather small and structurally simple molecules on carbon substrates, such as the aromatic molecule benzene adsorbed on the basal plane surface of graphite [1]. The research led us to a surprisingly simple model: The 2D viscosity could be explained by a model of colliding cogwheels that glide with little resistance over the surface [2].

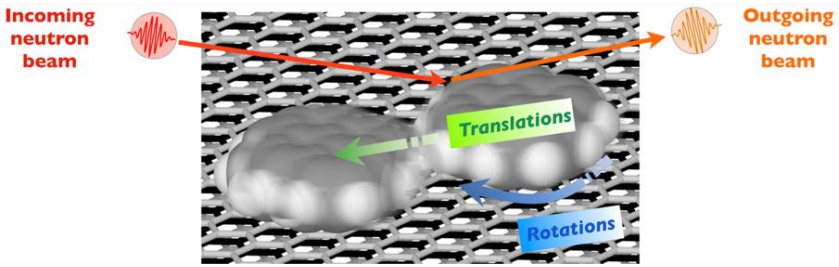

To develop our models further we expanded to investigations of larger aromatic molecules on the one hand [3] and to molecules with stronger surface interactions on the other hand. Recently we have

turned to the study of hydrogen in a perspective to explore the potential of 2D materials for hydrogen storage and catalysis [4].

References

[1] H. Hedgeland et al., Nature Phys. **5**, 561 (2009); E. Bahn et al., Phys. Chem. Chem. Phys. **16**, 22116 (2014).
[2] I. Calvo-Almazan, E. Bahn et al., Carbon 79, 183 (2014).
[3] I. Calvo-Almazan, et al., J. Phys. Chem. Lett. 7, 5285 (2016).
[4] E. Bahn et al., Carbon 98, 572 (2016) ; V. Kuznetsov et al. PCCP **23**, 7961-7973, (2021) ; V. Kuznetsov et al., J. Phys. Chem. C **126**, 21667 (2022).

Hot Topic Talks

Peptide bond formation within amino acid clusters in the gas phase

Yoni Toker
Physics Department and Institute for Nanotechnology and Advanced Materials, Bar-Ilan University, Israel

Inter-cluster bond formation (ICBF) refers to the possibility of forming covalent bonds between neighboring molecules within molecular clusters. This process provides a pathway to the abiotic formation of large and complex biomolecules in the interstellar medium as well as in primordial earth. In recent years our group has been studying the particular case of peptide bond formation (PBF) within amino acid (AA) clusters. We have found that absorption of light in the vacuum ultra violet (VUV) spectral region can induce PBF in all protonated dimers of AA's we have studies so far, even though thermal excitation only causes the dimers to break-up. We have differences in the propensity towards PBF between different AAs. In the case of mixed amino acid dimers we observe specificity in the peptide that is formed, and in some cases we observe a strong chiral preference – PBF is formed more abundantly in the homo-chiral case.

References

[1] Ori Licht et al., *Ang. Chem. Int. Ed*. **62** (2023)

Toward Solving the Sulfur Depletion Enigma: VUV Spectroscopy and Electron Processing of SO_2 and CS_2 Ices

M. Minissale[1], S. Ioppolo[2], E. Salomon[3], Z. Kanuchova[4], A. Cassidy[2], F. Fantuzzi[5], C. Paula De Souza[5], A. Wilson[2]
[1]Laboratory PIIM, CNRS
[2]Center for Interstellar Catalysis and Department of Physics and Astronomy, Aarhus University, Denmark
[3]PIIM Laboratory, Aix-Marseille University, CNRS
[4]Astronomical Institute of Slovak Academy of Sciences, 059 60 Tatranská Lomnica, Slovakia
[5]University of Kent

Sulfur is expected to play a key role in astrochemical environments, yet its chemistry in dense interstellar regions remains poorly understood, leading to the long-standing “sulfur depletion enigma.” Observations show that while sulfur is abundant in diffuse and photon-dominated regions, it is depleted by orders of magnitude in dense molecular clouds, suggesting that it may be sequestered in or transformed within icy grain mantles. Laboratory processing of astrophysical ices—via photolysis, radiolysis, thermal activation, or neutral-neutral chemistry—offers a potential explanation by driving desorption and the formation of refractory sulfur-bearing compounds. To clarify these processes, we performed a systematic study of the VUV (120–340 nm) photoabsorption properties of sulfur ices SO_2 and CS_2 (pure and mixed with H_2O and CO) grown at 10 K on MgF_2 substrates, including their evolution under 1 keV electron irradiation. Experiments were performed at the AV-UV beamline at Astrid2 Synchrotron facility (Aarhus, Denmark) using a UHV apparatus equipped with TPD–mass spectrometry, enabling correlation between spectral evolution and chemical changes in the processed ices. This work provides a comprehensive dataset of pristine and electron-processed sulfur-ice spectra to support future astronomical detections. In parallel, our work involves the fundamental study of the spectral features through computational simulation of the electronic absorption spectra using advanced

computational tools and a cluster approach to approximate solid phase effects, providing complementary microscopic insight into experimentally observed properties.

Oligomerization of acetylene upon ionization inside helium nanodroplets: Formation of benzene

Florian Foitzik[1], Vincent Richardson[2], Gabriel Schöpfer[1], Milan Ončák[1], Lisa Ganner[1], and Elisabeth Gruber[1]
[1] *Institute for Ion Physics and Applied Physics, University of Innsbruck, Austria*
[2] *Department of Physics, University of Liverpool, Liverpool, United Kingdom*

Ion-molecule reactions, often characterized by very low or vanishing activation barriers, play a fundamental role in the formation of complex organic molecules in space. One key molecular precursor of larger aromatic molecules is acetylene due to its unique stability and reactivity upon ionization. This molecule is one of the most promising candidates for bottom-up processes, which lead to the formation of polycyclic aromatic hydrocarbons [1]. Nevertheless, despite extensive efforts [2], a viable formation pathway for even the simplest aromatic building block, benzene, under astrophysical conditions has not yet been confirmed. In fact, one promising pathway, starting with the protonation of acetylene, was cast into doubt recently [3].

In this contribution, we report the formation of the benzene radical cation, formed by the sequential addition of two neutral acetylene molecules to the acetylene cation. The reaction was observed inside helium nanodroplets at cryogenic temperatures. The product is unambiguously characterized as benzene through helium tagging spectroscopy in the UV/vis spectral region and by the investigation of its solvation characteristic in neutral acetylene.

References

[1] Pentsak et al., *ACS Earth Space Chem.* **8**, 798–856 (2024)
[2] Geppert et al., *Chem. Rev.* **113**, 8872–905 (2013)
[3] Kocheril et al., *Nat. Astron.* **9**, 685-691 (2025)

Ion Molecule Chemistry studied with the CERISES instrument; new results on anion chemistry, cluster chemistry and energy transfers in collisions

R. Thissen, N. Solem, C. Romanzin, C. Alcaraz,
ICP, UMR8000 CNRS-Univ. Paris-Saclay, Orsay, France

E.L. Zins, I. Derbali, O. Aroule, L. Albouy
MONARIS, UMR 8233 Sorbonne University, Paris, France

K. Nagy, Á. Révész, K. Vékey, L. Drahos
HUN-REN Research Centre for Natural Sciences, Institute of Organic Chemistry, H-1117 Budapest, Magyar tudósok krt. 2

Introduction

New results on the reactivity of ions obtained with the CERISES setup [1] will be presented. The instrument has been designed to produce cations by photoionization by use of VUV light from synchrotron radiation (DESIRS beamline at the synchrotron SOLEIL [2]). In this way, internal energy dependent reactivity of cations has been explored throughout the years, with specific interest in the cation chemistry related to astrochemistry and ionospheric chemistry.

The guided beam architecture of the instrument allows for control of the collision energy, while the photoionization by VUV allows for energy dependent (and in some conditions, state-selected) measurements of the absolute cross sections and branching ratios of ion molecule reactions.

During the last years, new applications of the set-up were explored and will be presented in this communication. Anion chemistry, clusters and microhydrated clusters chemistry, and the microphysical description of the collision induced dissociation will illustrate new opportunities resulting from the recent developments.

Anion Chemistry, Nitriles reactivity related to Astrochemistry and new production method based on photons [3]

The anion-molecule reactivity of CN^- and C_3N^-, produced by dissociative electron attachment of the respective bromide precursors, with four oxygenated molecules has been investigated. The four targets are formic acid, acetic acid, acetaldehyde, and methanol. Exothermic and endothermic proton transfer has been observed as the main reaction channel, with differences in cross-section between the two anions. Oxidation of the anions is also observed, forming OCN^- and OC_3N^-, for both anions and limited to the targets with endothermic proton transfer for CN^-.

Very recently, we have explored the ability to induce an intense production of CN^- by colliding BrCN with argon atoms photoexcited or photoionized close to the valence shell ionization. This methods proofs to be efficient and produces intense signal of molecular anion signal.

Clusters and microhydrated clusters chemistry, proton affinity in acid base reactions involving Acetic acid and methylamine [4]

Acetamide, a small organic compound containing a peptide bond, was observed in the interstellar medium, but reaction pathways leading to the formation of this prebiotic molecule remain uncertain. We investigated [4] the possible formation of a peptide-like bond from the reaction between acetic acid (CH_3-COOH) and methylamine (CH_3-NH_2) that were identified in the interstellar medium. Acetic acid was photoionized, and the reactivity of $CH_3COOH^{+\bullet}$ as well as $COOH^+$ (produced from either acetic acid or formic acid) ions with neutral CH_3NH_2 was studied. With no surprise, charge transfer, proton transfer, and concomitant dissociation processes were found to largely dominate the reactivity. However, a C(O)–N bond formation process between the two reactants was also evidenced, with a weak cross section reaction.

The study was continued recently using a supersonic expansion in Ar to induce the formation of either pure or microhydrated clusters of proton bound acetic acid (up to 9 acetic acid and up to 3 water were produced by photoionization). Their reactivity with methylamine was studied, demonstrating an intense and exothermic proton transfer mechanism, leading to the systematic evaporation of either acetic acid or water, in a very systematic manner.

Microphysical description of the collision induced dissociation of butylbenzene, following collision with rare gases.

Collision induced dissociation (CID) is a very common methodology used in analytical chemistry to bring information on the structure of ionic species. The principle is to induce fragmentation of selected ions in the gas phase. The selected ions (typically molecular ions or protonated molecules) are accelerated to given kinetic energy and then allowed to collide with neutral molecules (often helium, nitrogen or argon). In the collision, some of the kinetic energy is converted into internal energy which eventually results in the fragmentation of the molecular ion into smaller fragments which are analyzed by tandem mass spectrometry.

Beyond the mere observation of specific fragments, the collision-energy dependent recording of the fragmentation signal is used by specialized groups to derive Bond Dissociation Energy (BDE), obtained from calculations, which is precious thermodynamic information, difficult to derive from other methods. This method relies on theoretical models, RRKM calculations and the evaluation of the energy transfer, from kinetic to internal energy, occurring in the collision process.

Surprisingly, the latter information concerning the amount of energy transferred is still poorly described.

The butylbenzene radical cation is a benchmark system that has already been well characterized. It exhibits two fragmentation channels corresponding to the loss of C_3H_7 or C_3H_6, which can be produced through simple bond fission or retro-ene rearrangement,

respectively. The C_3H_6 loss is favoured at low internal energy (m/z 92), while the C_3H_7 loss channel becomes dominant at high energy (m/z 91) and involves competition between a rearrangement route leading to tropylium ion and a simple bond fission fragmentation route leading to the benzylium ion. The relative abundance of the two ionic channels is very sensitive to the internal energy of the parent ion and can be used as a thermometer of internal energy.

We have recorded absolute CID cross sections of the butylbenzene radical cation after collision with 4 neutral targets (Xe, Ar, N_2 and Kr). The set of results were confronted to results of RRKM calculations to derive an absolute and energy specific estimate of the energy partitioning in the collision with the targets, aiming at a detailed description of the effects of relative mass, polarizability and transfer of energy to the neutral target.

References

[1] B. Cunha de Miranda, C. Romanzin, S. Chefdeville, V. Vuitton, J. Žabka, M. Polášek, and C. Alcaraz, J. Phys. Chem. A **119**, 6082 (2015).
[2] L. Nahon et al., J. Synchrotron Radiat. **19**, 508 (2012).
[3] N. Solem, C. Romanzin, R. Thissen, ACS Earth and Space Chemistry, **9/3** (2025)
[4] I. Derbali, R. Thissen, C. Alcaraz, C. Romanzin, EL Zins, J Phys Chem A, **125(46)** (2021)

High-power laser-plasma chemistry of methanol vapor

Veronika Horka-Zelenkova[1], Josef Krasa[1], Martina Toufarova[1], Jakub Cikhardt[2,3], Pooja Devi[1], Shubham Agarwal[1], Norbert Kanaloš[1], Roman Dudžák[1,3], Tomáš Burian[1], Michal Krupka[1,3], Sushil Singh[1,2,3], and Libor Juha[1]

Institute of Physics of the Czech Academy of Sciences, Prague, Czech Republic[1];

Technical University in Prague, Faculty of Electrical Engineering, Prague, Czech Republic[2];

Institute of Plasma Physics of the Czech Academy of Sciences, Prague, Czech Republic[3]

Introduction

This research focuses on the study of chemical processes initiated by a laser plasma in molecular gases. The plasma is generated by focusing a NIR beam delivered by high-power iodine photodissociation laser system PALS (Prague Asterix Laser System) [1]. The primary mechanism is Laser-Induced Dielectric Breakdown (LIDB), which creates a short-lived, energetic plasma fireball known as a laser spark. Large laser sparks are scientifically significant as they provide the opportunity to observe chemical reactions under extreme conditions that cannot typically be achieved in a conventional laboratory environment. They serve as laboratory models of high-energy-density phenomena occurring in the atmospheres of planets and moons and in interstellar matter.

In our experiment, we focus on studies of methanol (CH_3OH) and its deuterated isotopologues. Methanol is one of the most abundant and widespread organic molecules in the interstellar medium, detected from dense molecular clouds and protostars to comets [2]. Its rich chemistry makes it a key precursor to more complex organic molecules, including precursors of prebiotic molecules like aldehydes and amino acids [3,4]. Deuterated methanol isotopologues serve as a powerful diagnostic tool for tracing the chemical evolution through the stages of star and planet formation

[6,7]. The mono-deuterated forms CH_2DOH and CH_3OD are common from prestellar cores to hot cores, and even more highly deuterated forms, such as CHD_2OH and CD_3OH, have also been detected [8].
The advantages of utilizing large laser sparks, such as those generated at the PALS facility, over compact lasers with high repetition rates stem from their characteristics: high energy content and shorter duration of pulses providing higher intensities over larger areas. Therefore, they can produce much larger plasma volumes, generating a greater quantity of products. Essentially, it allows for a realistic laboratory simulation of a single event with high energy density. Using a single laser pulse eliminates the influence of the plasma on products formed during previous pulses.
The primary objective was to simulate the behaviour of methanol (CH_3OH) molecules in the interstellar medium when they are exposed to high-energy-density events, such as a high-speed impact or an EUV/x-ray/gamma burst. The laser spark generated in methanol vapor CH_3OH (and its isotopologues - CH_3OD, CD_3OH and CD_3OD) simulates initiation under such extreme astrophysical environments.

Experimental

The experiments employed the high-power iodine photodissociation laser system PALS operating in the near infrared spectral region (1315.2 nm). The laser delivers pulses with a duration of 350 ps and a maximum pulse energy up to 1000 J. The experimental setup involved focusing a 15 cm diameter laser beam, using a 30 cm focal length lens, into the centre of a glass cuvette containing methanol vapor (for more details see Figure 1). The cell is equipped with a Murytal flange that allows operation under atmospheric pressures [9]. In the methanol vapour experiment the pressure for all samples inside the cuvette was held at 100 Torr. In this experiment, a single pulse energy ranged from 124-144 J. Each sample was irradiated with 4 shots at a repetition rate of one shot per 30 minutes. The chemicals were obtained in the highest available purity (99.5 - 99.9 %). When the laser pulse strikes the gas sample, it generates a hot plasma that emits short- and long-wavelength radiation,

launches shock and thermal waves, and produces a dense hot mixture of highly reactive atoms, ions, and radicals. These processes together define the complex physical and chemical environment within the plasma generated by the laser–methanol-vapor interaction. The products formed in reactions initiated by LIDB of methanol and its isotopologues were analyzed ex situ by Fourier-Transform Infrared (FTIR) spectroscopy. The analysis of the decomposition products was performed with a Nicolet iS50 FTIR spectrometer using a home-made cell equipped with ZnSe windows. Simultaneously, we detected products using gas chromatography with a mass spectrometer detector (GC-MS).

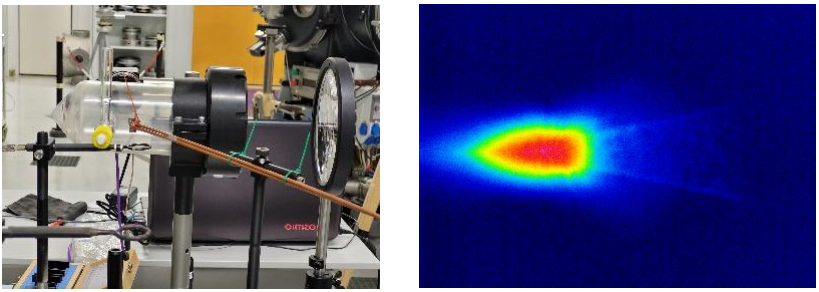

Figure 1: The photograph on the left presents an experimental setup with a lens focusing the laser beam in the middle of a glass cell; the right image shows a laser spark (diameter 40 mm) created in methanol vapor.

2. Analysis

The FTIR technique is a perfect tool for analyzing methanol products and their isotopologues, particularly for the distinction between deuterated and non-deuterated products. A very sensitive GC-MS technique allowed us to detect also minor products that cannot be indicated by FTIR spectroscopy. The main products identified by FTIR in the reaction glass cell are summarized in the Table below.

CH_3OH	-	C_2H_2	-	CH_4	-	-	-	-	H_2O
CH_3OD	C_2HD	C_2H_2	-	CH_4	-	-	-	D_2O	-
CD_3OH	C_2HD	-	C_2D_2	-	CH_2D_2	CD_3H	CD_4	-	H_2O

CD_3OD	-	-	C_2D_2	-	-	-	CD_4	D_2O	-

In addition, all studied isotopologues gave common products CO and CO_2. The GC-MS technique further reveals minor products as ethane, propyne, 1-buten-3-yne, 1,3-butadiyne, and formaldehyde, together with their corresponding deuterated isotopologues.

Discussions and Outlook

Typical main products of methanol photolysis include H_2 and HCHO [10,11], while C_2H_2 is generally absent or appears only in trace amounts. This does not align with our results, in which acetylene and its deuterated isotopologues are the dominant products. Production of C_2H_2 has been reported under highly energetic conditions produced by multiphoton photolysis, where it arises from the secondary reaction of C_2H_4 [5]. In our relatively different experiment, C_2H_4 is not identified and thus the formation of C_2H_2 likely proceeds through alternative pathways involving recombination or rearrangement of highly fragmented hydrocarbon radicals. As a next step, we aim to clarify the reaction mechanisms leading to C_2H_2 formation, as well as those responsible for the other products observed across all studied molecules.

References

[1] K. Jungwirth et al., *Phys. Plasmas* **8**, 2495 (2001).
[2] V. Richardson et al., *Phys. Chem. Chem. Phys.* **24,** 22437 (2022).
[3] S. L. Nickerson et al., *Astrophys. J. Lett.* **989**, L51 (2025).
[4] C. J. Bennett, S.-H. Chen, B.-J. Sun, A. H. H. Chang, R. I. Kaiser, *Astrophys. J.* **660**, 1588 (2007).
[5] S. E. Bialkowski and W. A. Guillory, *J. Chem. Phys.* **67**, 2061 (1977).
[6] J. L. Neill, N. R. Crockett, E. A. Bergin, J. C. Pearson, L.-H. Xu, *Astrophys. J.* **777**, 85 (2013).
[7] Y. Okoda, Y. Oya, N. Sakai, Y. Watanabe, A. López-Sepulcre, T. Oyama, S. Zeng, S. Yamamoto, *Astrophys. J.* **970**, 28 (2024).
[8] M. N. Drozdovskaya, L. H. Coudert, J. K. Jørgensen, S. Manigand, *A&A* **659**, A69 (2022).

[9] V. Horká-Zelenková, J. Krása, M. Toufarová, J. Cikhardt, P. Devi, *et al.*, *High Power Laser Science and Engineering* **13**, e77 (2025).
[10] R. P. Porter and W. A. Noyes Jr., *J. Amer. Chem. Soc.* **81**, 2307 (1959).
[11] R. J. Buenker, G. Olbrich, H.-P. Schuchmann, B. L. Schürmann, and C. von Sonntag, *J. Amer. Chem. Soc.* **106**, 4362 (1984).

Beating Tunnel Vision: Probing scattered products Near-Surface using Velocity-Map Imaging

Nitish Pal, Paul D. Lane, Matthew L. Costen, and Kenneth G. McKendrick and Stuart J. Greaves
Heriot-Watt University, Edinburgh, UK

We demonstrate a new methodology for probing scattered products near a surface using velocity-map imaging (NS-VMI). Building on our previous design, this upgraded instrument enables direct imaging of the scattering plane and provides a wider angular acceptance for scattered products. It allows us to investigate the reaction dynamics of atoms, molecules, and radicals following collisions with a surface, yielding quantum-state-dependent angular and speed distributions that offer insight into energy-transfer pathways relevant to atmospheric, marine, and heterogeneous catalytic processes.

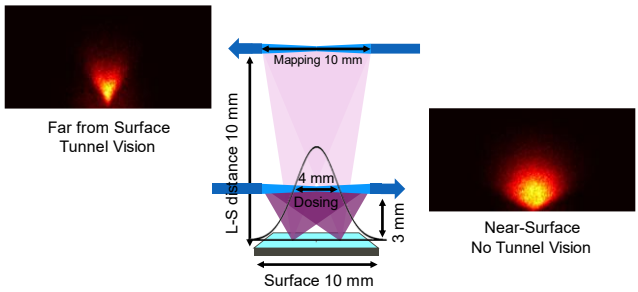

Figure 1: The schematic describes the ionization of the scattered products at two laser-surface (L-S) distances. The top left shows the raw ion image of NO acquired at L-S distance of 10 mm and right bottom shows raw ion image at L-S distance of 3 mm where the in-going molecular is directed normal to the surface.

Using a molecular beam of nitric oxide (NO) colliding with highly oriented pyrolytic graphite (HOPG) as a model system, we demonstrate the performance of near-surface VMI (NS-VMI). Fig. 1

shows raw ion images of scattered NO for laser–surface (L–S) distances of 10 mm (top left) and 3 mm (bottom right), where the molecular beam is directed normal to the surface. By positioning the surface close to the ionization laser within the VMI electrodes, Fig. 1 illustrates the increased angular acceptance for the scattered products. This approach overcomes the “tunnel vision” limitation, a term describing the restricted angular acceptance that occurs when measurements are taken too far from the gas–surface interaction region. A comparison of speed distributions summed over all angles for L-S distances of 10, 5 and 3 mm shows that the speed resolution remains sufficient even at an L–S distance of 3 mm to resolve key scattering features. This capability enables detailed examination of translation–rotation energy exchange as a function of the quantum states of the scattered products.

We observe a clear correlation between speed and scattering angle. Fig. 2 presents speed–angle flux maps converted from the raw ion densities of scattered NO at an L-S distance of 3 mm, where the molecular beam is directed normal to the surface (top panel) and at 45° with respect to the surface normal (bottom panel). Angular distribution plots for three speed ranges 0-500, 500-1000, and 1000-1500 ms^{-1} extracted from these maps reveal progressively narrower angular distributions, consistent with predominantly specular scattering from an atomically flat surface such as HOPG.

In this work, we discuss these and other quantum-state-dependent results in detail and show that the NS-VMI provides insights previously inaccessible due to geometric constraints in earlier experimental approaches used to measure angular distributions.

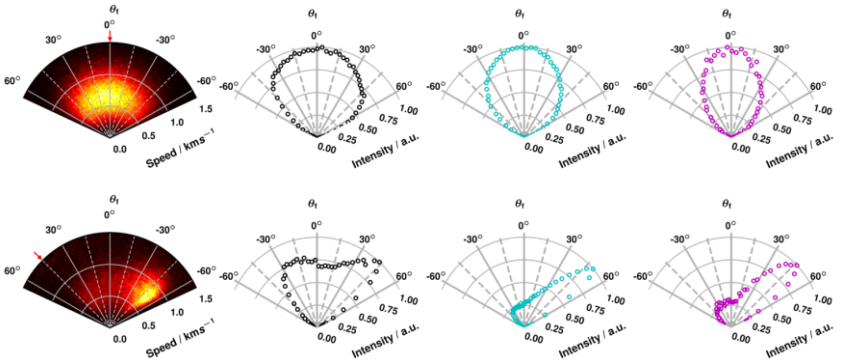

Figure 2 Density-flux-corrected intensity map of NO^+ ions for j = 33.5 from Q_1 transition recorded at L-S distance of 3 mm with ingoing molecular beam of NO (1% mix in Helium) impinging normal to surface and at 45 degrees with respect to surface normal is presented in first column (red arrow shows direction of ingoing beam). The angular distribution for three speed range 0-500, 500-1000, and 1000-1500 m/s extracted from the flux map is presented in 2nd, 3rd and 4th column, respectively.

References

[1] Hadden et al., *Rev. Sci. Inst.* **87**, 106104 (2016)

Ring-opening electron attachment in azoles and beyond

Jaroslav Kočišek, Michal Fárník, Juraj Fedor
J. Heyrovský Institute of Physical Chemistry of the CAS, 41118 Prague, Czech Republic

Ring-opening electron attachment is an important means of isomerization induced by low-energy electrons. The isomerization is enabled by the initial energy gain of the molecule by electron attachment and the preference of the linear form of the anion over the cyclic form thermodynamically favoured in the neutral state. While the ring-opening is common in dissociative electron attachment, during molecular fragmentation, there are only a few examples in non-dissociative electron attachment, where the parent anion stabilizes, including, for example, octafluorooxolane [1,2] or benzene [3].

In the present contribution, we overview our results of electron attachment mass spectrometry experiments with molecules and molecular clusters isolated in a vacuum of the molecules with predicted ring-opening reactivity. These include tri- and tetrazoles (e.g. 4,5) as well as more complex benzothiophene derivatives.

We acknowledge the support of the joint project of the Czech Science Foundation (25-16240L) and Austrian Science Fund (10.55776/PIN4290924) and the Ministry of Education, Youth and Sports of the Czech Republic project "AMULET" co-funded by the European Union (CZ.02.01.01/00/[0]22_008/0004558).

References

[1] T. Sommerfeld and M.C. Davis, J. Chem. Phys. 149 (2018)
[2] J. Kočišek, R. Janečková, J. Fedor, J. Chem. Phys. 148 (2018)
[3] A. Pysanenko, *J. Chem. Phys.* 157, (2022)
[4] T. F.M. Luxford, J. Fedor, J. Kočišek, J. Chem. Phys. 154 (2021)
[5] S. Pataraprasitpon, et al., J. Am. Chem. Soc. 147, 16 (2025)

Electron attachment to Na-doped water clusters

Barbara Kocábková, Jozef Ďurana, Andrij Pysanenko, Viktoriya Poterya, Juraj Fedor, and Michal Fárník
J. Heyrovský Institute of Physical Chemistry, Czech Academy of Sciences, Dolejškova 2155/3, 182 23 Prague, Czech Republic; michal.farnik@jh-inst.cas.cz

Introduction

Sodium in water represents a fundamentally interesting system. In the bulk water, adding Na results in an energetic reaction releasing molecular hydrogen H_2, while solvated Na^+ and OH^- ions are generated, and NaOH crystals are formed when all water is vaporized. On the other hand, collision of an isolated Na atom with a single H_2O molecule does not lead to any reaction [1].

In water clusters, the outcome of the Na–H_2O interaction depends on the degree of doping. A single Na atom does not lead to any chemical reaction, and Na^+ and solvated electron e_{aq}^- form in the cluster. Low-energy photons (≥ 3.2 eV) can remove the electron and ionize the doped clusters without any significant fragmentation. Thus, sodium doping was used as a fragmentation-free ionization method to obtain the corresponding neutral cluster size distributions [2,3]. Although, the method has some limitations [4-7].

Doping a water cluster with more Na atoms leads to reactions that have been investigated by experiments and theory in detail [8-12]., and the following picture emerged: in the first step, $Na^+ \cdot e_{aq}^-$ is formed, which interacts with sodium dimer Na_2 leading to the ion pair $Na^+ \cdot Na^-$ generation. The Na^- anion attracts a proton from water yielding the sodium hydride NaH, and the remaining OH^- recombines with Na^+ forming NaOH. The sodium hydride reacts spontaneously with a water molecule producing the second NaOH and H_2, which evaporates from the cluster.

What happens when an extra electron is added to the Na-doped water clusters? Since the system already contains the solvated electron e_{aq}^-, can the extra electron attachment form an interesting dielectron state, which was proposed theoretically?

Experiment

We have performed experiments with Na-doped water clusters on our cluster beam (CLUB) apparatus described elsewhere [13-14]. The water clusters generated by supersonic expansion of pure water vapor through a conical 90 µm nozzle are doped by Na atoms in a temperature controlled oven. The Nam(H_2O)n clusters fly about 0.7 ms through several differentially pumped vacuum chambers, providing time for the above-described reactions. Then the clusters are ionized and their mass spectra recorded with a perpendicularly mounted reflectron time-of-flight mass spectrometer (RTOF).

We have measured the positive ion mass spectra using 193 nm (6.4 eV) photoionization (PI) compared to 9 eV electron impact ionization (EI). In the negative ion mode, we have recorded the spectra after low energy (≤ 2.5 eV) electron attachment (EA). All spectra are measured with the same neutral beam allowing comparison of different ionic fragments from the same neutral clusters.

Results and Discussion

The positive ion spectra after PI and EI exhibit mainly $(H_2O)_nNa^+$, and $(H_2O)_n(NaOH)_kNa^+$, k = 2 and 4, series. They confirm the aboveoutlined reactions. An interesting feature, not observed in the previous experiments with a lower mass resolution, is the presence of strong peaks corresponding to metastable evaporation of molecules from the clusters in the RTOF field-free-region on a timescale of 10-30 µs. Recently, we have investigated the metastable evaporation of pure water clusters [15]. The contribution of the reaction to the stability of the clusters will be discussed.

The negative ion spectra of Na-doped water clusters, Fig. 1, have not been measured yet. We will discuss the observed anion series and their assignment. The metastable evaporation is detected in the

negative spectra too and will be compared to that in the positive ion spectra and discussed.

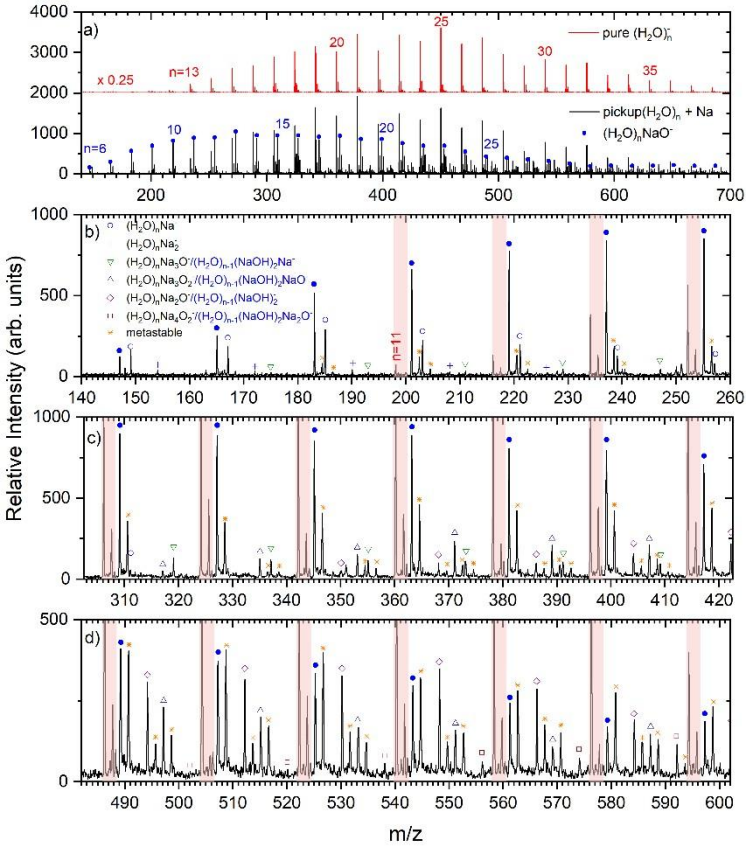

Fig. 1: Negative ion mass spectrum measured at 2 eV electron energy: a) The red line shows the spectrum of pure water clusters; numbers indicate the $(H_2O)_n^-$ cluster size n. The black line shows the spectrum after the Na uptake. The main $(H_2O)_nNaO^-$ series is labelled with blue circles and n. Detailed sections of the spectra are shown in panel b)–d) with series indicated by different symbols (see legend). Orange stars label the peaks corresponding to metastable decay of cluster ions.

References

[1] R. Düren, U. Lackschewitz, S. Milošević, and H.-J. Waldapfel, *Chem. Phys.* **140**, 199 (1990)
[2] C. Bobbert, S. Schütte, C. Steinbach, and U. Buck, *Eur. Phys. J. D* **19**, 183 (2002)
[3] B. L. Yoder, J. H. Litman, P. W. Forysinski, J. L. Corbett, and R. Signorell, *J. Phys. Chem. Lett.* **2**, 2623 (2011)
[4] J. Lengyel, A. Pysanenko, J. Kočišek, V. Poterya, C. Pradzynski, T. Zeuch, P. Slavíček, and M. Fárník, *J. Phys. Chem. Lett.* **3**, 3096 (2012)
[5] J. Lengyel, A. Pysanenko, P. Rubovič, and M. Fárník, *Eur. Phys. J. D* **69**, 269 (2015)
[6] D. Šmídová, J. Lengyel, A. Pysanenko, J. Med, P. Slavíček, and M. Fárník, *J. Phys. Chem. Lett.* **6**, 2865 (2015)
[7] D. Šmídová, J. Lengyel, J. Kočišek, A. Pysanenko, and M. Fárník, *Int. J. Mass Spectrom.* **421**, 144 (2017)
[8] C. P. Schulz, R. Haugstätter, H. U. Tittes, and I. V. Hertel, *Phys. Rev. Lett.* **57**, 1703 (1986)
[9] C. P. Schulz, R. Haugstätter, H. U. Tittes, and I. V. Hertel, *Z.*
Phys. D **10**, 279 (1988)
[10] U. Buck and C. Steinbach, *J. Phys. Chem. A* **102**, 7333 (1998).
[11] C. Steinbach and U. Buck, *Phys. Chem. Chem. Phys.* **7**, 986 (2005).
[12] C. Mundy, J. Hutter, and M. Parrinello, *J. Am. Chem. Soc.* **122**, 4837 (2000)
[13] M. Fárník and J. Lengyel, *Mass Spec Rev.* **37**, 630 (2018)
[14] [14] M. Fárník, J. Fedor, J. Kočišek, J. Lengyel, E. Pluhařová, V. Poterya, and A. Pysanenko, *Phys. Chem. Chem. Phys.* **23**,3195 (2021)
[15] V. Poterya, A. Pysanenko, M. Fárník, J. Fedor, and K. Hansen, *J. Phys. Chem. A* **128**, 8679 (2024)

Electron Attachment to Formic Acid Clusters Doped with Sodium

Barbora Kocábková*, Jozef Ďurana*, Andrij Pysanenko, Viktoriya Poterya, Eva Pluhařová, Michal Fárník
J. Heyrovský Institute of Physical Chemistry v.v.i.,
Czech Academy of Sciences,
Dolejškova 3, 182 23 Prague, Czech Republic;

Introduction

Sea spray aerosols (SSA) are the most abundant aerosols in the Earth's atmosphere. Also, they are very variable and complicated systems usually consisting of water, sea salts, and various organic materials coming from marine biome [1] and their composition and properties change over time. [2] As such, they are in the focus of aerosol scientists for quite some time.

For studying SSA, simplified model systems are used. Hydrated NaCl clusters can serve as a base [3] and can be doped with different organic molecules to simulate the biogenic influence. Organic molecules can also provide chromophores, which is usefull in the photoaging studies of SSA. [4] To generate charged salt clusters, electrospray ionisation of a salt solution is predominantly used [5], [6]. With our experimental setup, we adopted a different approach – a pickup of sodium atoms on neutral acid clusters.

For this experiment, we chose formic acid. As the simplest carboxylic acid, it serves as a model molecule for polar organic environment. It is atmospherically interesting molecule, as it is very abundant [7]. We probed pure and hydrated FA clusters with electron ionization and electron attachment in our previous work [8]. Sodium doped FA clusters were studied by photoionization both pure [9] and hydrated [10]. To the best of our knowledge, no works on electron attachment to mixed sodium acid-sodium formate clusters are published yet.

Experiment

The experiment was done on the CLUB apparatus described in [11]. Cluster beam was created by continuous supersonic expansion of FA with helium as a buffer gas through a conical nozzle. The beam then passed through a heated pick-up cell filled with evaporated sodium metal (application of this method described in [12]). The doped cluster beam was then ionized by electron attachment, and the anions were probed with a reflectron time-of-flight mass spectrometer.

All calculations were done with Gaussian 16 package on the M062X/aug-cc-pvdz level of theory.

Results

After electron attachment, the mass spectrum contains predominantly pure FA clusters (**Fig. 1a**). However, detailed look on the spectra (**Fig. 1b**) shows three cluster series containing sodium: intact $[FA_n \cdot Na]^-$ clusters with sodium atom, clusters without one hydrogen $[(FA-H)_n \cdot Na]^-$, and without two hydrogens $[(FA-2H)_n \cdot Na]^-$. Calculations suggest possible rearrangement of the clusters (example in **Fig. 2**). The structures of these small systems are explored, and formation mechanisms are discussed.

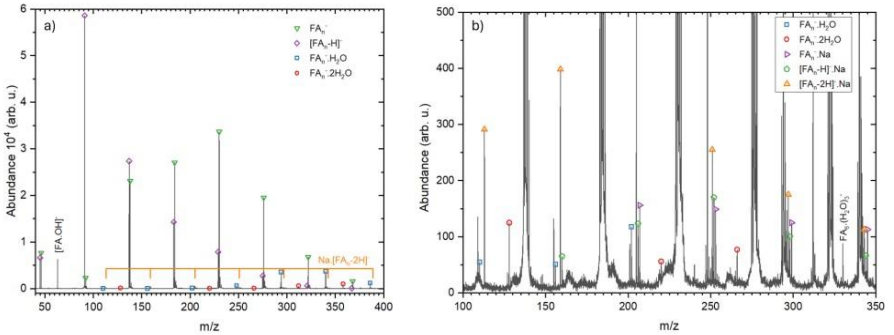

Fig**. 1**

a) Overview of the negative mass spectrum of Na doped FA clusters,

b) detail of the same spectrum with marked doped peaks

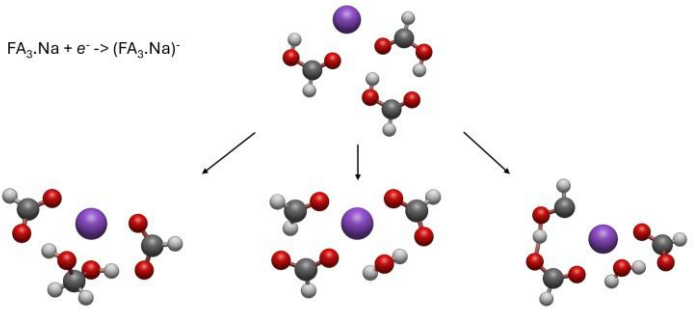

Fig. 2 Three possible structures of FA trimer doped with sodium after electron attachment.

References

[1] M. Kanakidou et al. *Atmos. Chem. Phys.* **5**, (2005)
[2] B. Su et al., *Atm. Env.* **290**, (2022)
[3] J. C. Hartmann *Phys. Chem. Chem. Phys*. **26**, (2024)
[4] N. K. Bersenkowitsch et al., *Phys. Chem. Chem. Phys*. **20**, (2018)
[5] S. M. Kruse et al. *Anal. Chem.* **96**, 31 (2024)
[6] J. Hartmann et al. *Phys. Chem. Chem. Phys.* **26**, (2024)
[7] D. B. Millet, *Atmos. Chem. Phys.* **15** (2015)
[8] K. Li, Chem. *Phys. Chem.* **25**, 10 (2024)
[9] A. Bende et al., *Chem. Phys. Chem.* **19**, 20 (2018) [10] A. Bende et al. *Chem. Phys. Chem*. **23**, 5 (2022)
[11] M. Fárník et al., *Phys. Chem. Chem. Phys.* **23** (2021)
[12] J. Lengyel et al., *Eur. Phys. J. D* **69**, 269 (2015)

How rotation shapes the decay of diatomic carbon anions

V. C. Schmidt[1,2], R. Čurík[3], M. Ončák[2], K. Blaum[1], S. George[1], J. Göck[1], M. Grieser[1], F. Grussie[1], R. von Hahn[1], C. Krantz[1], H. Kreckel[1], O. Novotný[1], K. Spruck[1], A. Wolf[1]
[1]Max-Planck-Institut für Kernphysik, Heidelberg, Germany
[2]Institut für Ionenphysik und Angewandte Physik, Leopold-Franzens-Universität, Innsbruck, Austria
[3]J. Heyrovský Institute of Physical Chemistry, Prague, Czech Republic

Molecules that are internally highly excited play an important role in a range of fields from atmospheric to plasma physics. Modelling such environments requires a detailed understanding of the molecules' behaviour at very strong excitations. However, this is a non-trivial task due to the high density of excited states as well as the variety of competing decay mechanisms available. The diatomic carbon anion C_2^- presents an excellent benchmark to understand the interplay of different decay channels at high internal excitation. The system is arguably the most extensively studied molecular anion in history. Yet, its decay behaviour at high internal excitation has long remained a riddle. When produced in a hot ion source, a subset of the resulting anions spontaneously eject their excess electron with a very narrow lifetime span of about 3 ms. While this autodetachment phenomenon has been known since the 1990s, the responsible anionic excited states and their decay mechanism have long remained elusive. Based on our measurements of autodecay of highly excited C_2^- at the Cryogenic Storage Ring (CSR) facility in Heidelberg, we carried out detailed calculations of the excited states and their decay behaviour [1,2]. Here, we were able to uncover the profound effect rotational excitation has on the system's electronic landscape, causing a reshuffling of the electronic states. This in turn alters the available decay channels at high excitations. The most severe example of this effect is visible in the lowest-lying electronic quartet state, $a^4\Sigma_u^+$. Here, a newly discovered autodetachment

mechanism, rotationally assisted autodetachment, explains the feature measured at different ion storage facilities throughout the world over the last three decades.

References

[1] V. C. Schmidt et al., *Phys. Rev. Lett.* **133**, 183001 (2024)
[2] V. C. Schmidt et al., *Phys. Rev. A* **110**, 042828 (2024)

Variational Autoencoder: A Generative Neural Network for Path Integral Monte Carlo Sampling

Zarah Aigner, Michael Hütter, Milan Ončák
Department of Ion Physics and Applied Physics, Universität Innsbruck

To model nuclear quantum effects, Path Integral Monte Carlo (PIMC) simulations can be used as an exact stochastic framework. A main difficulty represents the efficient sampling of imaginary-time configurations, as slow convergence and large statistical variance can significantly affect the accuracy of computed observables.
We propose a Variational Autoencoder (VAE), a generative approach that enhances sampling efficiency by reproducing and generating imaginary-time configurations consistent with PIMC statistics. The VAE maps high-dimensional imaginary-time configurations onto a lowdimensional latent space, capturing the underlying statistical structure of the PIMC ensemble.
The VAE enables fast resampling, thereby reducing the reliance on extensive Monte Carlo propagation. The generative approach, in contrast to conventional sequential sampling, enables parallel generation of independent configurations and can integrate symmetry-aware architectures to ensure translational and rotational invariance.
We show that VAE-based sampling can approximate the structural and thermodynamic properties obtained from reference PIMC simulations, while reducing sampling overhead in existing frameworks [1]. These results highlight generative models as a promising accelerator for quantum statistical simulations of molecular systems.

References

[1] M. Hütter, M. Ončák, *J. Chem. Theory Comput.* 2025, 21, 4397.

Small changes to the GFP chromophore significantly impact intrinsic fluorescence

Thomas Toft Lindkvist, Iden Djavani-Tabrizi, Lars H Andersen, Steen Brøndsted Nielsen
Department of Physics and Astronomy, Aarhus University, Denmark

New fluorescent proteins with tailored properties such as higher fluorescence quantum yield and red-tuned emission often build upon the green fluorescent protein (GFP). In a bottom-up approach, we explore how the native GFP microenvironment shapes fluorescence and furthermore, how small modifications to the chromophore can significantly alter the chromophore's photophysical properties.

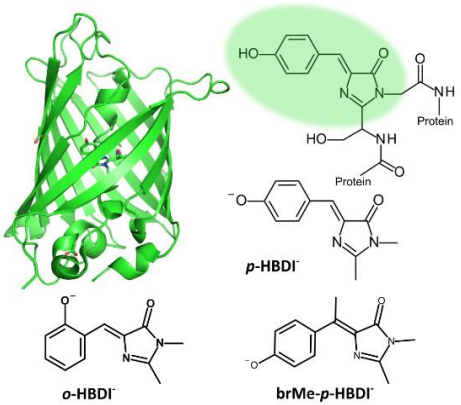

Figure 1: The GFP chromophore model and derivatives studied here.

The *p*-HBDI anion, often used to model the GFP chromophore (Figure 1), was first studied in the gas phase by our group in 2001 [1]. The action absorption spectrum revealed an absorption maximum closely matching that of the protein. However, intrinsic fluorescence is lost at room temperature as photoexcited bare anions undergo ultrafast internal conversion via torsional motion. At cryogenic temperatures, the fluorescence can be restored as protein steric hinderance is mimicked by reduced thermal motion [2].

We have studied *p*-HBDI$^-$ and two derivatives (Figure 1): the brMe-*p*-HBDI anion [3], methylated on the central bridge, and the *o*-HBDI anion [4], where the phenolate oxygen is moved to the *ortho* position. We performed cryogenic action and fluorescence spectroscopy with two homebuilt instruments located in Aarhus (Figure 2), the SAPHIRA ion storage ring and the LUNA2 fluorescence mass spectrometer. These experiments together with quantum chemical calculations reveal significant shifts in the spectroscopy as well as substantially altered photophysics. In brMe-*p*-HBDI, methylation promotes excited-state twisting and quenches fluorescence, while the *ortho*-HBDI experiences enhanced excited-state stabilization and redshifted emission.

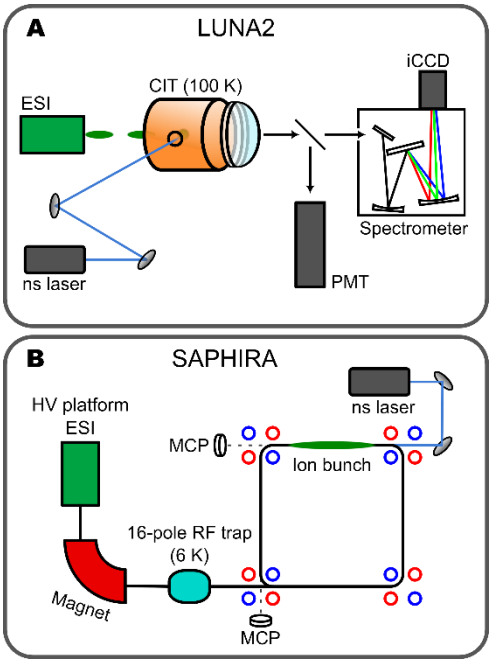

Figure 2: Schematic of the two homebuilt instruments used here. Reprinted from Ref. [4].

References

[1] S Brøndsted Nielsen, A Lapierre, JU Andersen, UV Pedersen, S Tomita, LH Andersen. *Phys Rev Lett* **87**, 228102 (2001).
[2] TT Lindkvist, I Djavani-Tabrizi, LH Andersen, S Brøndsted Nielsen. *Phys Rev Lett* **134**, 093001 (2025).
[3] TT Lindkvist, C Sillesen, N Klinkby, HH Jensen, LH Andersen, S Brøndsted Nielsen. *J Phys Chem A* **129**, 4245-4251 (2025).
[4] TT Lindkvist, AP Rasmussen, N Klinkby, LH Andersen, S Brøndsted Nielsen. *J Phys Chem Lett*, In Press.

Synergistic effects in ammonia uptake by mixed sodium sulfate-bisulfate cluster cations

Kevin Li, Jozef Lengyel
School of Natural Sciences, Technische Universität München, Lichtenbergstr. 4, 85748 Garching, Germany jozef.lengyel@tum.de

Gabriel Schöpfer, Milan Ončák
Institut für Ionenphysik und Angewandte Physik, Universität Innsbruck, Technikerstr. 25/3, 6020 Innsbruck, Austria

Understanding the earliest stages of atmospheric new particle formation requires direct measurements of subnanometer molecular clusters, yet such studies remain experimentally challenging. To address this size regime, we developed a cryogenic ion trap mass spectrometer designed for kinetic studies of mass-selected cluster ions. The instrument consists of an electrospray ionization source, a quadrupole mass filter, a ring electrode ion trap for kinetic experiments, and a time-of-flight mass spectrometer. Operating the ring electrode ion trap at multicollisional conditions of about 2 Pa ensures isothermal conditions during the nucleation process.
In this study, we demonstrate the capability of the instrument for kinetic measurements by investigating ammonia uptake on mass-selected sodium sulfate-bisulfate cluster ions. We show that studies of mixed multicomponent clusters can reveal synergistic effects in new particle formation, where the presence of different components in a cluster jointly enhances the sticking efficiency. In mixed sodium sulfate-bisulfate clusters, bisulfate units determine the number of ammonia molecules taken up, while sulfate units seem to control the nucleation rate. As shown in Figure 1, the kinetic measurements further reveal that steady-state conditions can be established between reactant and product clusters, which indicates the presence of both growth and evaporation channels. Such behavior is characteristic of new particle formation below the critical cluster size. These measurements introduce a new ion trap-based approach for

the aerosol community, suitable for studying the nucleation pathways of subnanometer particles relevant to atmospheric ion-induced nucleation.

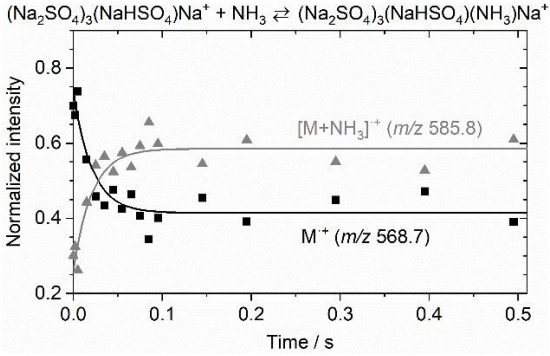

Figure 1: Kinetic analysis of the uptake of ammonia onto $[Na_2(SO_4)]_3 \cdot NaHSO_4 \cdot Na^+$ cluster ions at room temperature.

Towards a circular economy based on CO_2, H_2O, and N_2

Luca Matteo Martini, Paolo Tosi
Department of Physics, University of Trento, Italy

The current energy supply and chemical feedstocks depend primarily on fossil resources, which significantly contribute to anthropogenic greenhouse gas emissions. The goal of a sustainable energy and materials system is to shift to a circular economy, in which emissions are minimized and critical materials are reused. With this vision, we can explore replacing fossil resources with chemicals obtained from abundant molecules such as CO_2, H_2O, and N_2, while also using low-carbon energy sources [1].
Significant issues with renewable energy include variability and temporal and spatial mismatches between energy production and demand. To solve these problems, energy storage is required across various time scales. Power-to-X encompasses a range of technologies that convert electricity into chemical energy carriers and valuable industrial feedstocks. Examples of these technologies include water electrolysis and methanol synthesis.
Plasma discharges are an effective tool for activating strongly bonded molecules, such as CH_4, CO_2, and N_2, and for initiating chemical reactions without requiring thermal energy. Plasmas create a unique non-equilibrium environment in which electrons are significantly hotter than the bulk gas, enabling effective bond breaking. A well-known natural example is the lightning-induced production of NO, O_3, and OH during thunderstorms [2]. Potential advantages of discharges include the direct use of electricity to generate plasma, low inertia that accommodates fluctuations in renewable energy, and synergy between plasma and catalysis. Finally, plasma technologies do not require critical materials. This is especially important considering the European economic security strategy. The reduction of CO_2 to CO and O_2 is highly significant in the Carbon Capture and Utilization (CCU) strategy, as CO is a crucial feedstock for the production of synthetic hydrocarbons.

In plasma, three mechanisms can lead to dissociation: electron-impact dissociation, vibrational-induced dissociation, and thermal dissociation. As these mechanisms exhibit varying efficiencies, selecting the optimal discharge parameters to harness the desired mechanism is desirable but often challenging. We have recently made progress in understanding the CO_2 activation by adopting a novel approach to studying these discharges. Rather than treating the plasma reactor as a black box—simply correlating discharge parameters with product yield—we aimed to understand what is happening inside the plasma. This shift required non-invasive diagnostics capable of capturing the real-time dynamics of CO_2 dissociation within the plasma. Using time-resolved Optical Emission Spectroscopy (OES), we estimated the gas temperature and electron density and retrieved information on plasma-chemical kinetics in a nanosecond discharge [3]. However, this technique detects the radiation emitted by excited states, which does not readily provide information about molecules in their ground state. To address this issue, a complementary approach is to use active laser spectroscopy, such as laser-induced fluorescence. The spontaneous emission (i.e., the fluorescence) from the laser-excited state of a suitable probe molecule can reveal insights into gas composition. This is because the light-emitting state can be selectively depopulated by collisions with background particles.
As a result, changes in the fluorescence spectrum can be linked to specific collisional partners [4]. The success of this methodology hinges on understanding collisional energy transfer processes that modify the fluorescence spectrum [5]. With this technique, which we call collisional energy-transfer laser-induced fluorescence (CET-LIF), we successfully monitored the transformation of CO_2 into CO and either O or O_2, beginning just 40 nanoseconds after the discharge [6]. It is important to note that traditional analytical techniques, such as chromatography, typically operate on time scales of seconds to minutes, making them unsuitable for local and real-time measurements. Measuring the time dependence of the CO_2 conversion revealed a surprising non-monotonic behavior, with a peak occurring a few microseconds after the discharge pulse rather than during it. This finding challenges a long-held assumption by ruling out electron collisions as the direct cause of dissociation.

While everything starts with electron-impact excitation, molecular dissociation occurs over longer time scales and is therefore driven by energy-transfer processes that continue after the discharge.
Ongoing theoretical work suggests that electron collisions populate excited vibrational and electronic states. The rapid quenching of these states results in significant gas heating, up to thousands of degrees.
It turns out that thermal chemistry plays a crucial role in the dissociation process, with the reaction $CO_2 + CO_2 \rightarrow CO_2 + CO + O$ being the primary contributor [7]. Interestingly, electron-induced heating occurs locally in both space and time. This process does not require thermal energy input, reducing losses and enhancing energy efficiency.

References

[1] G.A. Olah et al., *J. Am. Chem. Soc.* **133**, 33 (2011)
[2] W.H. Brune et al*. Science* **372**, 6543 (2021)
[3] M. Ceppelli et al. *Plasma Sources Sci. Technol*. **30**, 115010 (2021)
[4] L.M. Martini et al. *Plasma Phys. Control. Fusion* **60**, 014016 (2018)
[5] M. Ceppelli et al. *Plasma Sources Sci. Technol*. **29**, 065019 (2020)
[6] C. Montesano et al. *J. Phys. Chem. C* **127**, 10045 (2023)
[7] V. Guerra et al. *78 Annual Gaseous Electronics Conference 2025,* Seoul, Republic of Korea.

Synthesis, enantio-separation and absolute configuration of small chiral molecules involving isotopes

Michele Perrino and Jürgen Stohner*
Zürich University of Applied Science (ZHAW), Institute of Chemistry and Biotechnology (ICBT), Campus Reidbach RT 309.3, Einsiedlerstrasse 31, CH-8820 Wädenswil, Switzerland,

Chiral molecules are of central importance in many areas of physics, chemistry and biology [1]. These are important target molecules for fundamental investigations of chiroptical properties in general as well as of attempts to measure parity violating effects in molecular spectroscopy [2-5]. A relatively new analytical tool is vibrational circular dichroism (VCD) which probes the different responses of enantiomeric molecules to circularly polarized infrared radiation and is used to determine the absolute configuration.
The FDA (food and drug administration) requests the absolute configuration at each chiral center for pharmaceutical drug approval [6]. Quite a number of deuterium substituted drugs are on the market:

"Selective incorporation of deuterium into known molecules has the potential, on a case-by-case basis, to provide better pharmacokinetic or metabolic properties, thereby enhancing their clinical safety, tolerability or efficacy. Our approach typically starts with approved drugs that may be improved with deuterium substitution. Our technology provides the opportunity to develop products that may compete with the non-deuterated drug in existing markets or to leverage the known activity of approved drugs to expand into new indications." [7]

This triggers also new instrumental developments to determine the absolute configuration at each chiral center more efficiently [8].

Our research is largely focused on the synthesis of small chiral molecules (C_1- and C_2-compounds) in enantio-pure or enantio-enriched form which have been used recently to investigate chiral photon electron detachment [9] and photoelectron circular dichroism

of chemical reactions [10]. Since asymmetric synthesis schemes are very complicated to develop and difficult to adapt to modified target compounds, we rather focus on gas-chromatographic separation of enantiomers although it is far from being trivial when larger quantities need to be separated. GC-separation on an analytical scale (a few microgram) is possible by using commercially available chiral stationary phases. The search for column material which facilitates preparative separation for larger quantities is rather difficult. We report here in general on our most recent achievements in this respect and focus particularly on deuterated small chiral molecules.

Our automatic fraction collector which we devised allows us to collect our target molecules almost 24/7. Key are liquid nitrogen traps with a continuous level regulation and a software tool to program three automated valves for collecting both enantiomers as well as a “waste”, the latter caused by overlapping chromatograms and can contain impurities. We are able to collect a few hundred mg per week, a considerable acceleration of the collection process [10,11].

Our target molecules are also not commercially available and thus require an efficient (high yield and purity) synthetic route. Such synthesis schemes have been developed for halogenated chiral acetic acids, which serve as precursors to chiral methane. We can obtain H- and D-isotopomers of the chiral halomethanes [12] and oxiranes. CHBrClF, for example, has been used to demonstrate the capability of gas-phase Coulomb explosion imaging (CEI) for the direct determination of the absolute configuration of molecules in the gas phase [13, 14]. COLTRIMS would be a method of choice for the direct determination of the absolute configuration of isotopically chiral compounds. We will report our recent results on the synthesis of some of our target molecules mentioned as well as on the determination of the absolute configuration.

We thank past members of the Physical Chemistry research group which contributed also to some of our results described above, namely P. Kappeler, J. A. Thoma, J. Durrer, L. Müller, and W. H. Fischer. Financial support from the Swiss National Science

Foundation (SNF, grant no. 200021_207787 and BRIDGE grant number 40B2-0_218759) are gratefully acknowledged.

References

[1] E. Babaev, D. Kharzeev, M. Larsson, A. Molochkov, and V. Zhaunerchyk, editors. Chiral Matter - *Proceedings of the Nobel Symposium 167*. Lidingö/Stockholm (2021). World Scientific Publishing Company, Singapore, 2023.
[2] M. Quack, *Angew. Chem. Int. Ed.* **41**, 4618 (2002)
[3] M. Quack and J. Stohner, *Chimia* **59**, 530 (2005)
[4] M. Quack, J. Stohner, and M. Willeke, *Annu. Rev. Phys. Chem*. **59**, 741 (2008)
[5] R. Berger and J. Stohner, *WIREs Comput. Mol. Sci.* **9**, e1396, 1 (2019)
[6] L. Böselt, D. Sidler,T. Kittelmann, J. Stohner, D. Zindel, T. Wagner and S. Riniker, *J. Chem. Information and Modelling* **59**, 1826 (2019)
[7] Concert Pharmaceutical, Inc, Annual Report 2016/7, US Securities and Exchange Commisssion, Washington DC, from EDGAR Online Inc.
[8] Mohamad Zarif Mohd Zubir, Nurul Fajry Maulida, Yoshihiro Abe, Yuta Nakamura, Mariam Abdelrasoul, Tohru Taniguchi, and Kenji Monde. *Org. Biomol. Chem.*, 20:1067–1072, 2022.
[9] C. Lux, M. Wollenhaupt, C. Sarpe, T. Baumert, *ChemPhysChem* **16**, 115 (2015)
[10] V. Svoboda, N. Bhargava Ram, R. Rajeev, M. Ochsner, B. Spenger, D. Zindel, J. Stohner and H. J. Wörner, *Science Advances* **8**, abq2811, 1 (2022)
[11] M. Perrino, B. Spenger, S. Manov, M. Meister, S. Näf, M. Eckl, L. Rüegg, J. Stohner, to be submitted.
[12] M. R. Mazenauer, S. Manov, V. M. Galati, P. Kappeler, J. Stohner, *RSC Advances* **7**, 55434 (2017)
[13] M. Pitzer, M. Kunitski, A. S. Johnson, T. Jahnke, H. Sann, F. Sturm, L. Ph. H. Schmidt, H. Schmidt-Böcking, R. Dörner, J.

Stohner, J. Kiedrowski, M. Reggelin, S. Marquardt, A. Schiesser, R. Berger and M. S. Schöffler, *Science* **341**, 1096 (2013)
[14] M. Pitzer, G. Kastirke, M. Kunitski, T. Jahnke, T. Bauer, C. Goihl, F. Trinter, C. Schober, K. Henrichs, J. Becht, S. Zeller, H. Gassert, M. Waitz, A. Kuhlins, H. Sann, F. Sturm, F. Wiegandt, R. Wallauer, L. Ph. H. Schmidt, A.S. Johnson, M. Mazenauer, B. Spenger, S. Marquardt, S. Marquardt, H. Schmidt-Böcking, J. Stohner, R. Dörner, M. Schöffler, R. Berger, *ChemPhysChem* **17**, 2465 (2017)

Isotopic chirality and high-resolution spectroscopy of the deuterated oxiranes

Karen Keppler, Sieghard Albert, Carine Manca Tanner, Georg Seyfang, Gunther Wichmann, Martin Quack
ETH Zürich, CH-8093 Zürich, Switzerland

Alexandra Brandenberger, Michele Perrino, Jürgen Stohner
ZHAW, CH-8820 Wädenswil, Switzerland

Introduction

The singly and doubly deuterated oxiranes c-C_2H_3DO, c-$C_2H_2D_2O$ are of interest in relation to the concept of isotopic chirality, which introduces a new isotope effect arising from the parity violating weak nuclear force [1−3]. In addition, these molecules are of particular interest for a detection of chirality and deuterium fractionation in the interstellar medium (ISM). The parent oxirane, c-C_2H_4O, was detected in the star-forming region Sagittarius B2 already in 1997 [4]. We had therefore started some time ago a project with the aim of detecting the isotopically chiral oxiranes in relation to the observation of extraterrestrial homochirality as a signature of life [5, 6]. In this context we reported the analysis of GHz and THz spectra of the isotopically chiral molecule monodeuterooxirane [7], predicting its likely observation in the ISM. On this basis Müller, et al. [8] recently reported the detection of c-C_2H_3DO and the tentative detection of the achiral species 2,2-dideuterooxirane [9] in IRAS 16293-2422 B.

We have previously also reported new results on the analysis of GHz and THz spectrum of the achiral cis- and the chiral trans-cCHD-CHDO [10], and have provided a first high resolution analysis of the infrared spectra of the two c-C_2H_3DO fundamentals at 896.025 cm^{-1} and 837.36 cm^{-1} [11]. Here we report new measurements (room temperature, Doppler-limited resolution) of the infrared spectrum of improved, newly synthesized samples of *c*C_2H_3DO, making possible

the extension of our analysis towards the two lowest frequency fundamentals, as well as further stronger fundamentals, combination and overtone bands throughout the mid- to near-infrared range.

Experimental

The infrared spectrum of a newly prepared sample of *c*-C_2H_3DO was measured using the Bruker IFS 125 HR ETH SLS 2009 Prototype FTIR Spectrometer, allowing for the world highest best possible resolution of 0.00053 cm^{-1} (16 MHz) based at a synchrotron light source [6,12]. Our other measurements of *c*-C_2H_3DO and of the achiral *cis*- and the chiral *trans*-*c*-2,3-dideutero-oxirane *c*CHDCHDO were performed using the IFS 125 HR Zurich prototype (ZP 2001) spectrometer, with a resolution of 0.0015 cm^{-1}. Depending on the measurement region, a globar source, a KBr (CaF_2) beamsplitter and a liquid-nitrogen-cooled MCT (InSb) detector were used for a series of measurements using an 18 cm glass cell or a White-type cell with optical path lengths up to 10 m (see [12] and references cited therein)

Analysis of the Results and Discussion

The line positions were assigned with the help of Loomis-Wood programs and a rovibrational analysis using the Watson A-reduced effective Hamiltonian in the I^r representation, including up to sextic centrifugal distortion constants using the WANG program (see [12, 13] and references therein). We have obtained effective molecular parameters for several bands of both *c*-C_2H_3DO and *c*-CHDCHDO species. Of particular interest has been the analysis of the weak ν_{15} and ν_{14} fundamental bands in *c*-C_2H_3DO, centered near 702 and 817 cm^{-1}. The inclusion in the analysis of these weak bands, which were analyzed following our most recent measurement 2025 campaign for the first time, has made possible a better determination of the molecular parameters of *c*-C_2H_3DO, as these weak bands have been the missing pieces of the tetrad of the four lowest interacting vibrational levels of *c*-C_2H_3DO. The weak fundamental ν_{15} (CHD rocking mode) band is shown in Figure 1: the strong feature near

667 cm^{-1} is v_2 of CO_2, used as a wavenumber calibration standard [14].

We compare our results with ab initio calculations performed at the MP2 level with an aug-cc-pVTZ basis set, as described in more detail elsewhere [7], and with calculations by Puzzarini, et al. [15].

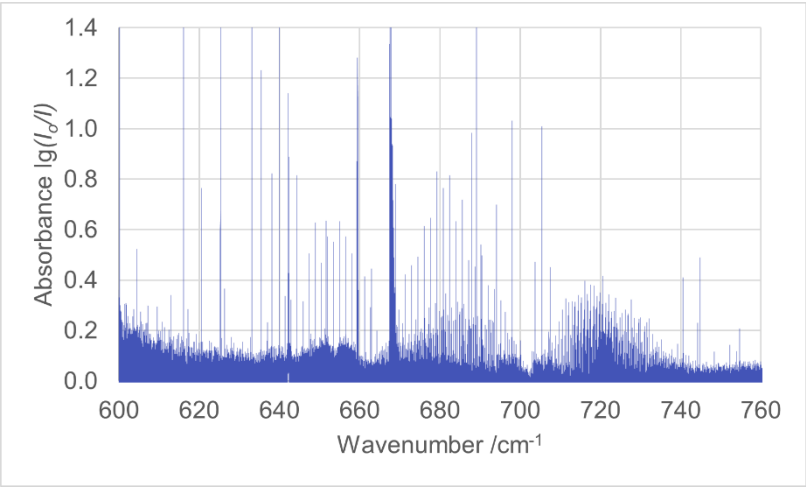

Figure 1: FTIR spectrum, v_{15} of *c*-C_2H_3DO near 700 cm^{-1} (v_2 of CO_2 at 667 cm^{-1}). Res.=0.0012 cm^{-1}, l = 4.8m, P = 0.45 mbar, T = 296K.

Acknowledgements

We thank Guy Matmon for his help with the most recent measurements. We also thank Philippe Lerch, Volker Schurig, Oliver Trapp, Eduard Miloglyadov, Jacqueline Strassmann, Fabian Hobi, Daniel Zindel, Guido Grassi, Reto Ulrich and Leon Becht for their help with earlier work in our project. We are deeply grateful to Frédéric Merkt for his continuous support. Our work is financially supported by ETH Zürich (LPC, IMPS), the Swiss National Science Foundation (Bridge), an ERC Advanced Grant, COST MOLIM and

COSY of the EU, and the Fundamental Research Funds for Chinese Central Universities.

References

[1] M. Quack, Angew. Chem., 101, 588 (1989); Angew. Chem. Int. Ed. 28, 571 (1989).
[2] R. Berger, G. Laubender, M. Quack, A. Sieben, J. Stohner, M. Willeke, Angew. Chem. Int. Ed., 44, 3623 (2005).
[3] M. Hippler, E. Miloglyadov, M. Quack, G. Seyfang, "Mass and Isotope Selective Infrared Spectroscopy, in "Handbook of High-Resolution Spectroscopy," Vol. 2, pp. 1069−1118, M. Quack and F. Merkt, eds, Wiley, Chichester (2011). ISBN-13:978-0-470-06653-9.
[4] J. E. Dickens, W. M. Irvine, M. Ohishi, M. Ikeda, S. Ishikawa, A. Nummelin, A. Hjalmarson, Astrophys. J. 489, 753 (1997).
[5] M. Quack, Adv. Chem. Phys. 157, 249−290 (2014).
[6] M. Quack, G. Seyfang and G. Wichmann, Chem. Sci. 13, 10598 (2022); M. Quack, G. Seyfang and G. Wichmann, ‘’Parity Violation in Chiral Molecules, from Theory towards Spectroscopic Experiment and the Evolution of Biomolecular Homochirality, in 'Chiral Matter' – Proceedings of the Nobel Symposium 167, Lidingö (Stockholm) 28 June−2 July 2021, pp. 209−268; Editors: E.Babaev, D.Kharzeev, M. Larsson, A.Molochkov, V.Zhaunerchyk, World Scientific Publishing Co. Singapore 2023.
[7] S. Albert, Z. Chen, K. Keppler, P. Lerch, M. Quack, V. Schurig and O. Trapp, Phys. Chem. Chem. Phys. 21, 3669 (2019).
[8] H. S. P. Müller, J. K. Jørgensen, J.-C. Guillemin, F. Lewen, S. Schlemmer, MNRAS 518(1), 185 (2023).
[9] H. S. P. Müller, J. K. Jørgensen, J.-C. Guillemin, F. Lewen, S. Schlemmer, J. Mol. Spectrosc. 394, 111777 (2023).
[10] Z. Chen, S. Albert, K. Keppler, G. Wichmann, M. Quack, V. Schurig and O. Trapp, Phys. Chem. Chem. Phys. (2025). doi.org/10.1039/D5CP03143e

[11] S. Albert, Z. Chen, K. Keppler, G. Wichmann, M. Quack, J. Stohner, V. Schurig and O. Trapp, Phys. Chem. Chem. Phys. 27, 14240 (2025).
[12] S. Albert, K. Keppler Albert, H. Hollenstein, C. Manca Tanner and M. Quack, “Fundamentals of Rotation-Vibration Spectra,” in Handbook of High-Resolution Spectroscopy, eds. M. Quack and F. Merkt, Wiley, Chichester, Vol. 1,117−173 (2011), S. Albert, K. Keppler Albert, M. Quack, ‘’High Resolution Fourier Transform Infrared Spectroscopy, ibid. Vol. 2, 965−1019.
[13] D. Luckhaus and M. Quack, Mol. Phys. 68(3), 745 (1989).
[14] I. E. Gordon, et al., “The HITRAN 2020 Molecular Database,” J. Quant. Spectrosc. Radiat. Transf. 277, 107949 (2022).
[15] C. Puzzarini, M. Biczysko, J. Bloino, V. Barone, Astrophys. J. 785, 107 (2014).

From Maths to Matter: An Experimental Realization of the Thomson Problem

Thomas Pohl, Jan Mayerhofer, Fabio Zappa, Paul Scheier
Department of Ion Physics and Applied Physics, University of Innsbruck

Hanqing Liu, Shengfu Yang, Andrew M. Ellis
School of Chemistry, University of Leicester

The Thomson problem, a century-old mathematical challenge of finding the minimum-energy configuration of identical charges on a sphere, has long served as a benchmark for global optimization on curved manifolds [1]. Its energy landscape, extensively explored theoretically in numerical studies of minimum-energy configurations [2], underpins concepts ranging from spherical crystallography to curvature-frustrated order [3].

We realize an experimental finite-N Thomson system using superfluid helium nanodroplets as isotropic, weakly screening spherical hosts for charged gold nanoparticles confined to the droplet surface. Upon impact with a transmission electron microscopy substrate, each droplet prints a two-dimensional orthographic projection of its three-dimensional charge configuration.

Quantitative comparison with orthographically projected numerical Thomson solutions [2] reveals excellent agreement for droplets with radii below 200 nm, indicating negligible rearrangement during deposition. For larger droplets, systematic deviations emerge from impact-induced splashing of particles situated at the rear hemisphere upon collision, providing insight into deposition dynamics on curved Coulomb crystals.

References

[1] Thomson, J. J., *Phil. Mag*., **7**, 1904
[2] Wales, D. J. et al., *Phys. Rev. B*, **74**, 2006
[3] Bowick, M. et al., *Phys. Rev. Lett*., **89**, 2002

Cryogenic hybrid trapping of Ca^+ ions and OH molecules for cold ion-molecule collision studies

Yaya Zhi[1], Yanning Yin[1], Christian Mangeng[1], Richard Karl[1], Pietro Vahramian[1] and Stefan Willitsch[1]
[1]Department of Chemistry, University of Basel, Klingelbergstrasse 80, 4056, Basel, Switzerland

Collisions between ions and molecules at very low temperatures are essential for understanding fundamental physical and chemical processes [1-2]. At low collision energies, only a few partial waves contribute, providing a clean regime for examining cold-collision mechanisms at the quantum level [3]. Such processes also play a key role in interstellar environments, where ion–molecule reactions govern molecular evolution [4].

In this work, we present a new experimental approach in which quantum-state–selected and phase-space–controlled OH radicals are produced with a Stark decelerator and confined in a magnetic trap and combined with cold Ca^+ ions prepared by laser cooling in a linear Paul trap [5-7]. Shuttling the Ca^+ ions brings them into spatial overlap with the trapped OH molecules, enabling the study of controlled cold collisions between Ca^+ and OH. The OH lifetime in the magnetic trap is measured by laser-induced fluorescence, and comparison of the measured lifetimes with and without Ca^+ ions reveal the effect of ion–molecule interactions. First results indicate that the Ca^+ ions reduce the trap lifetime of the OH radicals, indicating trap loss by either elastic or inelastic collisions.

References

[1] M. Deiß, et al *Nature Physics* **20**, 713-721 (2024).
[2] A. Voute, et al. *Physical Review Research* **5** (2023). [3] B. [3
[3] K. Stuhl, et al. *Annual review of physical chemistry* **65**, 501518 (2014).
[4] M. Larsson, *Reports on Progress in Physics* **75**, 066901 (2012).

[5] R. Karl, Y Yin, S. Willitsch, *Molecular Physics* **122**, 1-2 (2023).
[6] C. Mangeng, Y. Yin, R. Karl, and S. Willitsch. *Phys. Rev. Research* **5**, 043180 (2023)
[7] D. Haas, C. von Planta, T. Kierspel, D. Zhang & S. Willitsch, *Commun. Phys.* **2**, 101 (2019)

Effect of solvation in core-level excited states of propylamine

Karolína Fárníková, Eva Muchová
University of Chemistry and Technology, Prague, Czechia

Introduction

Biomolecular radiation damage is a natural process caused by high-energy photons. It is a complex process affected by the aqueous environment surrounding the biomolecule. Apart from altering the geometry of the molecule in the ground electronic state, the aqueous environment can also cause delocalization of the electron excited by high-energy radiation. The excited/emitted electron originates from core orbitals, making this a core-excitation/ionization process.

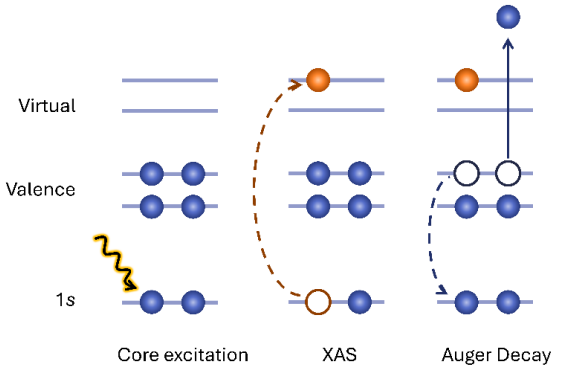

Figure 1: Scheme of XAS and RAES

Core-level excitation/ionization [1] is a process where an electron closest to the nucleus is excited or ejected from an atom (X-ray absorption spectra XAS, X-ray photoelectron spectra XPS). The X-ray spectroscopies are highly selective, both from element- and site perspective, allowing for an easier spectrum interpretation. Even more information can be extracted from resonant X-ray methods: resonant inelastic scattering (RIXS) or resonant Auger (RAES). These are multistep processes. First the excitation/ionization occurs,

followed by the core-hole relaxation. This results in the ejection of either an Auger electron in RAES or a photon in RIXS (Fig. 1).

The goal of our research was to describe the effect of the solvent on core-excitation and ionization. The study involves a set of small organic molecules which were selected to represent common biomolecules or structural motifs [2]. In addition, the kinetic energy of their Auger electrons has to be distinguishable from electrons emitted by water, they must have sufficient vapor pressure and water solubility to be studied in both gas and aqueous phases to observe the solvation effects. I have specifically investigated propylamine.

Methods

XAS spectra for the 1*s* orbitals of the nitrogen and carbon atoms were measured at the P04 beamline at DESY Hamburg by the experimental team of Prof. O. Björneholm. They were integrated from the 2D maps showing the kinetic energies of the emitted electrons.

For the theoretical modelling, classical molecular dynamics was used to sample both propylamine and propylammonium in solution to account for the organization of solvent by the solute. Various conformations with different solvation shells were sampled and used

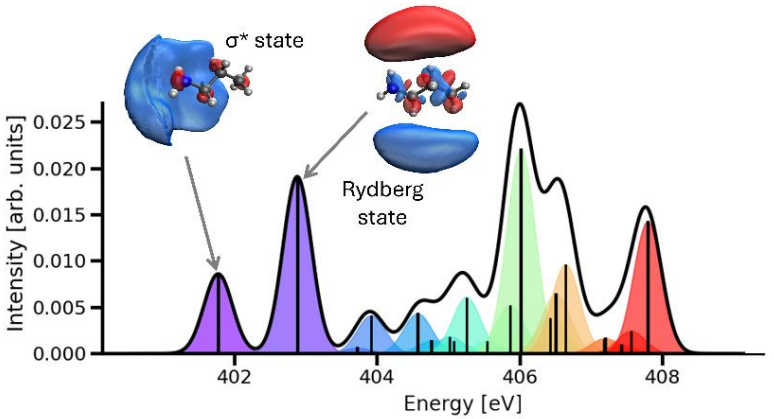

Figure 2: XAS for the 1s orbital of nitrogen calculated on the EOM-CCDS level.

for theoretical calculations of XAS with quantum mechanical methods.

Results

We successfully reproduced and interpreted the gas phase data for both the XAS for the 1*s* orbital of the nitrogen atom (Fig. 2) and the 1*s* orbital of the carbon atoms at the accurate EOM-CCSD level.

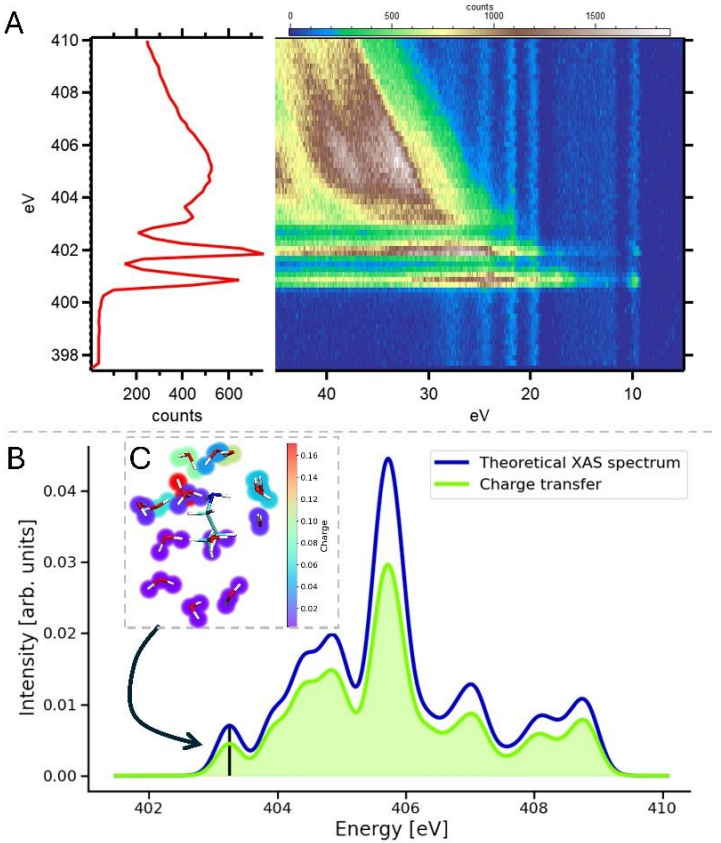

Figure 3: A – Experimental 2D map for the 1s orbital of nitrogen in gas phase. B – XAS (blue) for 1s nitrogen orbital for propylamine solvated by 15 water molecules with visualized charge transfer (green) and first state (black). C – Exciton distribution on the water molecules surrounding propylamine for the first excited state.

To include the effects of solvation and to perform calculations on a large set of sampled structures, a cheaper method had to be utilized. Therefore, we opted for TD-DFT, where a small solvation shell was simulated explicitly and long-range polarization effects were included using a polarizable continuum model. The results were comparable to the experimental spectra.

Focusing on the nitrogen 1*s* orbital, there are two main pre-edge peaks at around 401.5 and 403 eV, corresponding to the excitation into the σ* and Rydberg state respectively (Fig. 2). Introduction of the solvent (Fig. 3B) diminishes their intensity. The protonation of the NH_2 group seemingly shifts the pre-edge peaks to higher energies.

From the results of TD-DFT, exciton analysis was performed [3]. One of the results was its distribution within the system and how the electron density is distributed over the surrounding water molecules (Fig. 3C). For excitation from the 1*s* nitrogen orbital, the highest charge from the electron is distributed over the water molecules closest to the nitrogen atom.

4. Conclusion

Modelling the core-excitation of propylamine and its protonated form in both gas and aqueous phase allows us to gain a better understanding of the influence of solvation. The main effect of both solvation and protonation is observable in the nitrogen 1*s* XAS. This is due to the position of the proton, which also interacts with the solvent more favourably in comparison to the amine group.

References

[1] M. N. Piancastelli et al., *Rep. Prog. Phys* **83**. 016401 (2019)
[2] M. Ekimova, et al., *J. Phys. Chem. B* **122**, 31 (2018)
[3] J. M. Herbert et al., *Phys. Chem. Chem. Phys.* **26**. 5 (2024)

Low-energy Electron Collisions with Molecules of Biological Interest: Elucidating the Influence of Microhydration

G. Schöpfer, V. T. T. Nguyen, T. Lob, S. Denifl, M. Ončák
University of Innsbruck, Institute for Ion Physics and Applied Physics

Introduction

Radiotherapy is a common way of cancer treatment. However, one of the biggest issues associated with it is the fact that the radiation does not primarily damage cancer cells, but mainly healthy tissue. This is because cancer cells are hypoxic, i.e., they lack oxygen. The idea of one kind of radiosensitizers is to imitate the effect of oxygen, and therefore increase the effect of radiotherapy on cancer cells. One such radiosensitizer is nimorazole which has already been investigated in a clinical phase III study. It showed to significantly increase the survival rate of patients with supraglottic larynx and pharynx carcinoma, in comparison with patients receiving the radiotherapy without nimorazole as a radiosensitizer.[1] Therefore, it is advisable to investigate the underlying molecular processes in more detail to obtain generalizable results. 2-amino-5-nitrothiazole was shown to be an effective hypoxic radiosensitizer as well. However, *in vivo* it appeared not be a good choice due to its toxicity.[2] 2-bromo-5-nitrothiazole (BNT) is less toxic but might act similarly well as a radiosensitizer, clearly making it worth studying it further. One important molecular property of radiosensitizers is their behaviour upon attachment of low-energy electrons. While reactions upon low-energy electron attachment to isolated molecules have already been investigated,[3] the effects of microhydration are unknown, even though of high biological importance. Hence, in this work we investigate the behaviour of microhydrated nimorazole and BNT upon attachment of low-energy electrons.

Experiments

Experimentally, this was done using a crossed electron-molecular beam setup incorporating a time-of-flight mass spectrometer. The experiments show that nimorazole does form mixed clusters of nimorazole and water, both in its anionic and in its cationic form, i.e., [$Nimo^-(H_2O)_n$] and [$Nimo^+(H_2O)_n$]. In contrast, the BNT anion does not form any clusters with water molecules, and the BNT cation does so much less than nimorazole. This clearly shows the hydrophilic character of nimorazole and the hydrophobic character of BNT, along with the biological consequences when used as radiosensitizer. Interestingly, even though clusters of [$BNT^-(H_2O)_n$] are not observed, the water environment heavily influences the fragmentation behaviour.

Calculations

From the theoretical point of view, the results are supported using quantum chemical calculations. Using our molecular genetic algorithm,[4] which is combined with graph-based structure clustering,[5] we locate the lowest-lying structures of [$BNT^{+/-}(H_2O)_{0–10}$] and [$Nimo^{+/-}(H_2O)_{0–10}$]. Orbital analysis shows that the attached electron, and therefore the excess charge of –1*e*, is located at

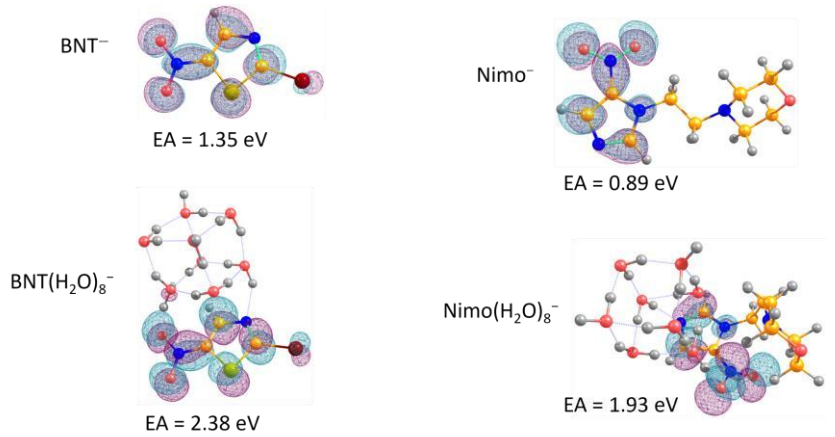

Figure 1: Anionic nimorazole and BNT, isolated and hydrated. Shown is the orbital of the attached electron as well as the electron affinity as calculated at the ωB97XD/def2-TZVP//PBEPBE/def2-SVP level of theory.

nimorazole or BNT, respectively, but not at the surrounding water molecules. In this regard, the water molecules barely influence this orbital, see Figure 1.

Furthermore, we calculated electron affinities and energies for competing reactions, explaining the experimentally observed clustering behaviour. Figure 2 shows this exemplary for the case of low-energy electron attachment to and ionization of Nimo$(H_2O)_8$. As can be seen, the energy of 1.47 eV available from electron attachment is enough to evaporate one water molecule, but is not enough to evaporate all water molecules in the form of a water cluster, explaining why mixed clusters of nimorazole and water could be observed experimentally. Similarly, in the case of the nimorazole cation, evaporation is energetically more favourable than evaporation of all water molecules at once.

Apart from these thermodynamic considerations, we model reaction pathways and transition states to account for kinetic effects. Furthermore, we increase the number of water molecule to up to 50 to obtain a more realistic model of microhydration.

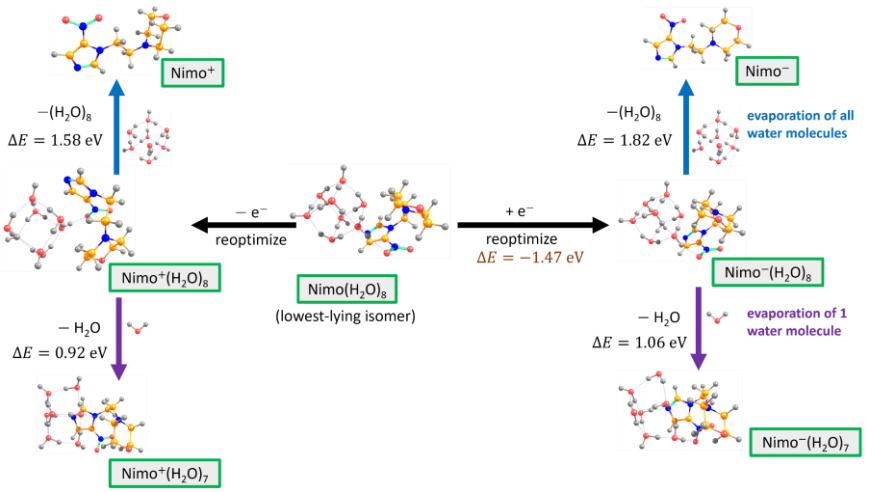

Figure 2: Reaction path ways upon ionizati on (left) and electron attachment (right) to Nimo(H 2O)8 as calculated at the PBE/def2 -SVP level of theory.

References

[1] J. Overgaard et al., *Radiother. Oncol.* **46**, 135–146 (1997).
[2] S. Rockwell et al., *Radiat. Res.* **90**, 575–585 (1982).
[3] J. Chen et al., *J. Chem. Phys.* **162**, 044304 (2025).
[4] G. Schöpfer et al., git.uibk.ac.at/c7441332/genetic-algorithms.
[5] M. Gatt et al., github.com/photophys/structure_clustering.

Posters (Group A)

Controlled Molecules for ultrafast-chemical-dynamics studies

A. Ayasli1, A. Pradhan1,3, I. Vinklarek1, W. Jin1, N. Vadassery1,3, H. Bromberger1, S. Trippel1,4, J. Küpper1,2,3,4
[1]Center for Free-Electron Laser Science (CFEL), Deutsches Elektronen-Synchrotron DESY, Hamburg, Germany
[2]Department of Physics, Universität Hamburg, Germany
[3]Department of Chemistry, Universität Hamburg, Germany
[4]The Hamburg Center for Ultrafast Imaging (CUI), Universität Hamburg, Germany

The combination of species selection and orientation control of small molecules in the gas phase by dc- and ac-electric fields has proven to be a powerful tool to study dynamics in the molecular frame [1,9]. Possible probing mechanisms include the investigation of molecular-frame photoelectron angular distributions [2] or the detection of structural changes via x-ray or electron diffraction [3-6].
Here, we present our work on the field-free 3D alignment and mixed-field orientation of indole, an asymmetric top molecule, by shaped laser pulses. The degree of alignment and orientation is quantified and analyzed by the comparison of the observed rotational revival structure with theoretical predictions. Furthermore, we will show our results on the alignment of small heterodimers, like indole-water [7], which are model systems to study the influence of the solvent environment on the photophysics and ultrafast chemical dynamics of biological chromophores. Furthermore, we show results on laser field-free alignment of complex molecules using pulse shaping [8].

References

[1] J. Hansen, H. Stapelfeldt et al., Phys. Rev. Lett., 106, 073001 (2011)
[2] L. Holmegaard, J. Hansen et al., Nature Physics, 6, 428 (2010); arXiv:1003.4634 [physics]
[3] F. Filsinger, G. Meijer, H. Stapelfeldt, H. Chapman, and J. Küpper, Phys. Chem. Chem. Phys., 13, 2076 (2011); arXiv:1009.0871 [physics]

[4] J. Yang, et int. (18 authors), X. Wang, Science, 368, 6493 (2020)
[5] C. J. Hensley, J. Yang, and M. Centurion, Phys. Rev. Lett., 109, 133202 (2012)
[6] J. Küpper, S. Stern, L. Holmegaard et al., Phys. Rev. Lett., 112, 083002 (2014); arXiv: 1307.4577 [physics]
[7] S. Trippel, J. Wiese, T. Mullins, & J. Küpper, J. Chem. Phys., 148, 101103 (2018)
[8] T. Mullins, et int. (8 authors), J. Küpper, Nat Comm., 13, 1431 (2022)
[9] J. Onvlee, S. Trippel, and J. Küpper,. Nat. Comm., 13, 7462 (2022); arXiv:2103.0717 [physics]

Unimolecular rate constants and master equation modeling of radiative processes with AWATAR

Magdalena Salzburger, Jessica C. Hartmann, Michael Hütter, Gabriel Schöpfer, Marc Reimann, Christian van der Linde, Milan Ončák and Martin K. Beyer
Universität Innsbruck, Institut für Ionenphysik und Angewandte Physik, Technikerstraße 25, 6020 Innsbruck, Austria

Unimolecular rate constants of gas-phase reactions are usually calculated with the RRKM methods, which describe a chemical reaction using the density of states of a local minimum and the sum of states of a transition structure. In many cases, however, isomerization to low-lying isomers faces much smaller barriers than the reaction of interest and is thus taking place at a much faster rate. However, isomerization reactions are not accounted for by RRKM theory. To address this problem, we recently introduced AWATAR – All Wells And Transition structures Are Relevant. For a typical dissociation reaction, the AWATAR rate constant can be calculated via eq. (1).

$$k_{\mathrm{AWATAR}}(E) = \frac{\sum_j N_j(E-E_{0,j})}{h\sum_i \rho_i(E)} \qquad (1)$$

Here $\rho_i(E)$ is the density of states of local minimum *i*, often called well in unimolecular rate theory. By summing over all energetically accessible wells *i*, we account for the additional quantum states that are accessible by isomerization between the different wells. Loose transition structures for dissociation consist of two fragments, and the sum of states $N_j(E-E_{0,j})$ of a loose transition structure *j* with zero-point corrected energy $E_{0,j}$ describes the quantum states that are accessible along the dissociation asymptote.

In this contribution, we will show some examples of AWATAR and discuss the differences to classical, single-well RRKM theory. We

also show some applications using AWATAR in master equation modeling of radiative processes, such as black-body infrared radiative dissociation (BIRD) [2,3] and infrared multiple photon dissociation (IRMPD).

References

[1] J. C. Hartmann *et al.*, *Physical Chemistry Chemical Physics* **26**, 10904-10918 (2024)
[2] M. Salzburger *et al.*, *Journal of Chemical Physics* **160**, 134304 (2024)
[3] M. Hütter *et al.*, *RSC Advances* **14**, 22185-22194 (2024)

Oxygen atom recombination on aluminium surfaces: effect of ion bombardment

Shu Zhang, Andrey Volynets, Garret Curley and Jean-Paul Booth
Laboratoire de Physique des Plasmas,
CNRS/Ecole Polytechnique, Palaiseau, France

We have studied the density and kinetics of oxygen atoms in radiofrequency (13.56 MHz) capacitively-coupled plasmas in pure O_2 using single-mode laser cavity ringdown spectroscopy of oxygen atoms at 630 nm. The absolute atom densities and translational temperatures were determined over a range of pressures (67-800 Pa) and RF power. At 267 Pa and above the mole-fraction increases with RF power and decreases with pressure, reaching a maximum of 15%. However, at 133 and below it passes through a distinct maximum with power before decreasing significantly. The atom recombination processes are probed by time-resolved measurements in the afterglow of pulse-modulated plasmas. At 133 and 67 Pa the atom loss is dominated by surface recombination, and we see clear evidence that this rate is increased by energetic ion bombardment. The effect lasts about 0.5 seconds, after which the recombination probability decreases to a constant value that is independent of the ion bombardment. This effect partially explains the observed decrease in dissociation at high RF power. The timeresolved results also allow the O^- negative ion density to be determined, and indicate the creation of ozone in the afterglow. At higher pressures gas phase recombination mechanisms become dominant, however gas convection driven by gas cooling in the afterglow makes it complex to analyse the time-resolved data.

References

[1] Booth et al., *Plasma Sources Science and Technology*, **32**, 095016 (2023)

Electronic spectroscopy of cationic fullerenes and carbon chains

Lisa Ganner[1], Florian Foitzik[1], Gabriel Schöpfer[1], Milan Ončák[1], Helgi R. Hrodmarsson[2], Paul Scheier[1], Serge Krasnokutski[3], and Elisabeth Gruber[1]

[1] *Institute for Ion Physics and Applied Physics, University of Innsbruck, Technikerstr. 25, 6020 Innsbruck, Austria*

[2] *CNRS, LISA UMR 7583, Univ Paris Est Créteil and Université Paris Cité, 61 avenue du Général de Gaulle, 94010 Créteil, France*

[3] *Laboratory Astrophysics and Cluster Physics Group of the Max Planck Institute for Astronomy at the Friedrich Schiller University Jena, Helmholtzweg 3, D-07743 Jena, Germany*

The diffuse interstellar bands (DIBs) are a set of absorption features in the UV to near IR spectra of stars. These absorption features are caused by the interstellar medium but despite many research efforts, the C_{60}^+ fullerene remains the only firmly identified carrier of any DIBs to date [1]. To enable the potential assignment of additional DIB carriers, laboratory electronic spectra are required for comparison with astronomical observations. In this contribution, we report the electronic spectra of several C_{60}^+ derivatives (C_{60}^+–water complexes, $C_{60}H^+$, $C_{60}D^+$, and $C_{60}Mg^+$) as well as of C_n^+ (n = 3–6) clusters, which were considered promising DIB carrier candidates [2, 3]. While most of the studied ions do not have absorption features that match any DIBs, C_4^+ exhibits two strong absorptions that match closely with a DIB at 504 nm [2, 3]. Furthermore, we remeasured the electronic spectra of C_{60}^+ and C_{70}^+, providing additional spectral detail [3, 4].

The spectra were obtained using a helium-tagging messenger spectroscopy setup [5]. In this setup, helium-tagged ions are generated by shrinking helium nanodroplets doped with the ionic species of interest. The tagged ions are then overlapped with a tunable laser beam. Upon excitation via photon absorption, the weakly bound helium atoms evaporate; by monitoring this process

with a mass spectrometer while scanning the laser wavelength, an absorption spectrum is recorded.

Acknowledgements

This research was funded in whole or in part by the Austrian Science Fund (FWF) [10.55776/V1035, 10.55776/P34563, 10.55776/P35013, 10.55776/W1259, 10.55776/I6221]. This publication is based upon work from COST Action CA21126 - Carbon molecular nanostructures in space (NanoSpace), supported by COST (European Cooperation in Science and Technology). S.A.K. is grateful to the DFG (grant No. 413610339).

References

[1] E. K. Campbell et al., *Nature*, **523** 322–323 (2015)
[2] S. A. Krasnokutski et al., *The Astrophysical Journal*, **982** 34 (2025)
[3] L. Ganner et al., *The Astrophysical Journal*, **993** 47 (2025)
[4] L. Ganner et al., *ACS Earth and Space Chemistry*, **9**, 11, 2694-2704 (2025)
[5] S. Bergmeister et al., *Review of Scientific Instruments*, **94** 055105 (2023)

Spectroscopic Studies of C_2^- in a Cryogenic Multipole Ion Trap

M. Hauck, S. Purushu Melath, Robert Wild, and Roland Wester
Institut für Ionenphysik und Angewandte Physik, Universität Innsbruck, Technikerstraße 25, 6020 Innsbruck, Austria

While laser cooling is a standard procedure for many atoms, molecules and cations, no negative ions have been laser cooled to date [1]. A laser-cooled anion would allow more precise chemical and spectroscopic studies of anions. Sympathetic cooling with a laser-cooled negative ion has been proposed as a method to prepare cold antiprotons [2].
The dicarbon anion C_2^- has been proposed as a candidate for laser-cooling because of favourable Franck-Condon factors and short lifetimes of the excited state [3].
Our group has measured the main laser cooling transitions between the vibrational groundstate of the X and B electronic states [4]. Decay to higher-lying vibrational states represent a challenge for optical pumping schemes. We use inelastic collisions with H_2 to close the optical cycle for inital studies using fluorescence measurements. Our group measured the quenching rate coefficient of the v = 1 level of the X state with H_2 [1].
Here we present additional spectroscopic measurements in our 16 pole cryogenic radiofrequency ion trap on the next relevant transitions for repumping the v = 1 and 2 levels, allowing us to extract a precise value for the vibrational energy difference. We also present improved fluorescence images.
Additionally we measured the near threshold photodetachment cross section for photodetachment to the ground and first excited state of C_2, showing clear p- and s-wave character respectively. The shape of these two threshold gives information on the internal state distribution of the anion and the neutral. By fitting a rotational transitions model we were able to extract a precise value for the electron affinity of C_2.

References

[1] M. Nötzold, et al., Phys. Rev. Lett. 131, 183002 (2023).
[2] A. Kellerbauer, J. Walz, New J. Phys., 45 (2006).
[3] P. Yzombard, et al., Phys. Rev. Lett. 114, 213001 (2015).
[4] M. Nötzold, et al., Phys. Rev. A 106, 23111 (2022).

Electronic Spectroscopy of Cationic Pyrene and its Derivatives

Franziska Hölzler*, Florian Foitzik, Gabriel Schöpfer, Milan Ončák and Elisabeth Gruber
Institute for Ion Physics and Applied Physics, University of Innsbruck, Technikerstr. 25, 6020 Innsbruck, Austria
**franziska.hoelzler@uibk.ac.at*

The diffuse interstellar bands are absorption bands in the visible and near infrared spectra of stars. The molecules or molecular ions, responsible for these bands are, despite a lot of efforts, widely unknown. One hypothesis is, that polycyclic aromatic hydrocarbons (PAHs) are responsible for a number of these DIBs [1].
One molecule, which has gained increased attention as a potential DIB carrier is the pyrene radical cation due to its photostability against UV-radiation, along with a strong absorption line in the close vicinity of the λ4430 band, as previously demonstrated in neon and argon matrices [2,3]. The recent detection of all isomers of cyano-substituted pyrene in space reinforces the hypothesis of pyrene, or a pyrene-derivative to be the carrier of one or more DIBs [4,5].
In this contribution we present the electronic spectra of cationic pyrene, protonated pyrene and cyanopyrene. These were obtained by tagging spectroscopy with helium or hydrogen. The tagged ions are produced through controlled shrinking of helium nanodroplets doped with the ionic species. Absorption spectra were obtained by irradiating the tagged ions with a tunable laser and detecting excitation-induced helium loss using mass spectrometry [6].

References

[1] Salama et al., *Proc. Int. Astron. Union*, **9**, 364-369 (2013)
[2] Salama et al., *Nature,* **358**, 42-43 (1992)
[3] Ghanta et al., *J. Mol. Struct.,* **1191**, 32-42 (2019)
[4] Wenzel et al., *Science*, **386**, 810-813 (2024)
[5] Wenzel et al., *Nature Atron*., **9**, 262-270 (2025)
[6] S. Bergmeister et al., *Rew. Sci. Instrum.*, **94**, 055105 (2023)

Competition between photoionization and predissociation in electronically excited states of He_2 using detection of metastable He fragments

Maxime Holdener, Josef-Anton Agner, Hansjürg Schmutz, Frédéric Merkt
Department of Chemistry and Applied Biosciences, Department of Physics, Quantum Center, ETH Zürich

He_2 has been called a Rydberg molecule because its ground electronic state is repulsive, whereas its electronically excited states are strongly bound and have Rydberg character [1-3]. These states lie more than 19 eV above the ground state and can predissociate. The electronic structure of the triplet Rydberg states of He_2 is presented in Fig. 1. The potential-energy functions depicted in the figure are adapted from Ref.[4].

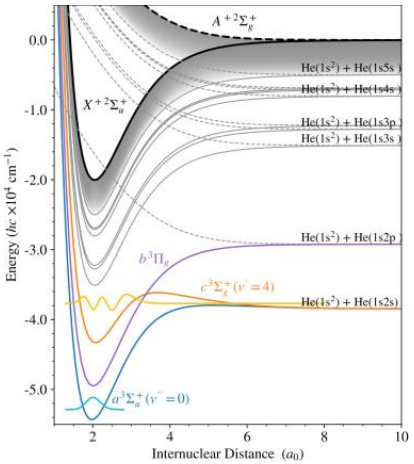

Figure 1: Potential-energy functions of the lowest three excited triplet electronic states of He_2 [3] and of the ground and first electronically excited states of the He_2^+ ion [4]. The gray (thin) solid and dashed lines represent Rydberg states converging to the He_2^+ $X\,^2\Sigma_u^+$ and $A\,^2\Sigma_g^+$ states, associated with the relevant dissociation limits given on the right.

Most studies of the electronic spectrum of He_2 were carried out by monitoring emission cascades in electric discharges of He (see, *e.g.,* Refs.[2,5] and references therein) or by studying the photoexcitation spectrum of the metastable a $^3\Sigma_u^+$ state. Only low vibrational levels ($v' \leq 3$) could be observed in these studies, and almost no information is available on vibrational levels with $v' \geq 4$, although it is known that the Rydberg states of He_2 must have approximately the same number of vibrational levels as the ground state of the He_2^+ ion, *i.e.,* 24 [6,7].

We have recently demonstrated that 1+1' two-photon excitation via the $v' = 3$ and 4 levels of the $c\ ^3\Sigma_g^+$ state provides access to very high vibrational levels of high-lying Rydberg states of He_2 [7]. In the present work, we present an experimental approach to systematically study the high vibrational levels of He_2 using 1+1' excitation via the $c\ ^3\Sigma_g^+$ state. This strategy relies on the simultaneous detection of photoionization and predissociation processes using the experimental setup depicted schematically in Fig. 2 and described in its caption.

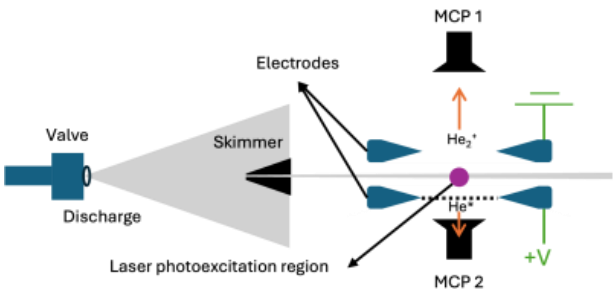

Figure 2: Schematic representation of the experimental setup consisting of (1) a supersonic-beam source connected to an electric discharge used to generate metastable He_2 molecules in the $a\ ^3\Sigma_u^+$ (v'' = 0-2, N'' =1, 3, …, 29) states, (2) a laser system with two tunable dye lasers used to photoexcite He_2 from the $a\ ^3\Sigma_u^+$ (v'', N'') states to selected intermediate $c\ ^3\Sigma_g^+$ (v', N') states and to higher-lying Rydberg states or to the ionization continua in multiply resonant photoexcitation processes, (3) a stack of parallel electrodes used to extract the He_2^+ ions generated by photoionization toward an MCP

detector (MCP 1), and (4) an MCP detector (MCP 2) used to detect the He*(1s2s) $^3S_1$ metastable fragments produced by predissociation.

To illustrate this approach, we first present a study of the tunneling predissociation of the *c* $^3\Sigma_g^+(v' = 4)$ state (see Fig. 3) and demonstrate the very efficient detection of predissociation in He_2 by monitoring the metastable He(1s2s $^3S_1$) fragments on a microchannel-plate (MCP) detector.

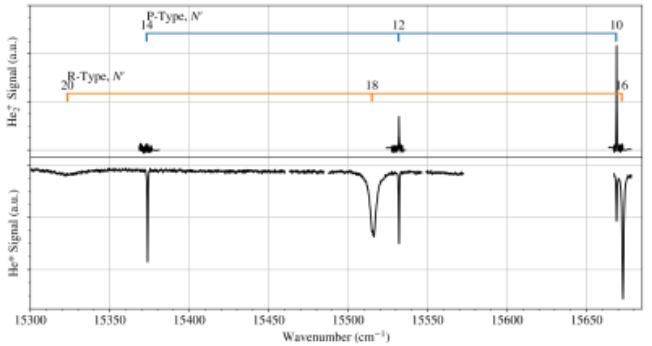

Figure 3: Spectra of the *P(11), P(13), P(15), R(15), R(17),* and *R(19)* and transitions of the *c* $^3\Sigma_g^+(v' = 4) \leftarrow a\ ^3\Sigma_u^+(v'' = 0)$ band, showing the tunneling predissociation of the *N* = 10, 12, 14, 16, 18, and 20 rotational levels of the *c* $^3\Sigma_g^+(v' = 4)$ state. Upper panel: (1 + 1') two-photon ionization spectrum recorded by monitoring the He_2^+ ionization signal. Lower panel: Spectrum recorded by monitoring the yield of He*(1s2s) $^3S_1$ metastable fragments generated by tunneling predissociation through the barrier of the *c* $^3\Sigma_g^+$-state potential.

We then explore the predissociation of He_2 in the vicinity of the He(1s^2) $^1S_0$ + He(1s2p) $^3P_{0,1,2}$ thresholds in a study of transitions to vibrationally excited levels of the *f* $^3\Sigma_u^+$, f'$^3\Pi_u$, and d$^3\Sigma_u^+$ states. This contribution presents the main results of this study. As an example, Fig. 4 displays the spectra of the *f'* $^3\Sigma_u^+(v = 3, N = 1, 2, 3) \leftarrow c\ ^3\Sigma_g^+(v' = 2, N = 0,2)$ transitions. These spectra reveal signals in both the predissociation and photoionization channels, indicating competition

between photoionization and predissociation. The He*-fragment signal detected after a short flight to MCP 2 reveals an asymmetric distribution reflecting the geometry of the photoexcitation and detection regions (see Fig. 4). The dashed lines indicate that the positions of the maxima in the distributions depend on the degree of rotational excitation of the predissociating molecules. The ability to detect dissociation products makes it possible to observe transitions to rapidly dissociating molecular states that cannot be observed by photoionization or laser-induced fluorescence, as illustrated in Fig. 3.

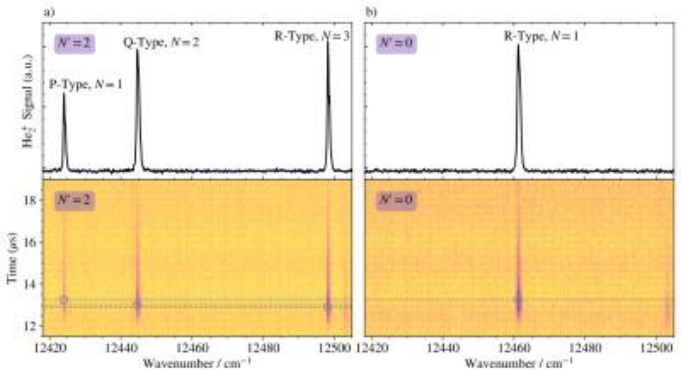

Figure 4: Simultaneously recorded spectra of competing photoionization and predissociation via the *f'* $^3\Sigma_u^+$(*v* =*3, N*) levels of He_2, obtained from the intermediate *c* $^3\Sigma_g^+$ (*v' = 2, N'*) states with (a) *N'* = 2 and (b) *N'* = 0. In each panel, the upper spectrum corresponds to the He_2^+ signal produced by (1 + 1' + 1) photoionization, and the lower spectrum corresponds to metastable He* atoms produced by predissociation of the *f'* state. The maxima in the time-of-flight distributions are marked by gray circles, and dashed gray lines indicate their arrival times.

This work is supported financially by the Swiss National Science Foundation (SNSF) under Grant No.00021-236716. We thank V.Wirth for discussions and for his initial contribution to this project.

References

[1] G. Herzberg, Ann. Rev. Phys. Chem. 38, 27 (1987).
[2] M. L. Ginter, and J. G. Eden, Can. J. Chem. 82, 6 (2004).
[3] D. R. Yarkony, J. Chem. Phys. 90, 12 (1989).
[4] J. Xie, B. Poirier, G. I. Gellene, J. Chem. Phys. 122, 18 (2005).
[5] M. Ginter, J. Chem. Phys. 45, 1 (1966).
[6] A. Carrington, Ch. H. Pyne, and P. J. Knowles, J. Chem. Phys. 102, 15 (1995).
[7] M. Holdener, V. Wirth, N. A. Shahin, M. Beyer, and F. Merkt, Phys. Rev. A, 112, 2 (2025).

UV-VIS photodissociation spectra of sodium and potassium nitrate cluster anions

Sarah J. Madlener, Claus Schwendinger, Jessica C. Hartmann, Christian van der Linde, Milan Ončák and Martin K. Beyer
Universität Innsbruck, Institut für Ionenphysik und Angewandte Physik, Innsbruck/AT

The uptake of nitric acid by sea salt aerosols is followed by release of HCl, leaving NO_3^- in the particle. Nitrate is an important trace species in the atmosphere, as well as the hydrosphere [1]. In the actinic region >290 nm it is photolyzed to NO_2^- as well as O^-. The latter reacts with water to form a hydroxyl radical $OH^\cdot$ together with OH^- [2]. Also in arctic ices, it was found that the photolysis of nitrate in snow/ice has a significant influence on the composition of ambient air and therefore affecting the overlying boundary layer [3]. A previous study on copper nitrate clusters showed a small quantum efficiency for the n - π* transition in the UV region, leading to the photolysis of nitrate. In this study the clusters mainly fragmented *via* the loss of neutral copper nitrate units [4].
The small quantum yield for the production of these fragments in aqueous solution is attributed to the cage effect, *i.e.* the solvent prevents the separation of the products. Studying NO_3^- in small anionic salt clusters reduces this cage effect, since the nitrate anion is predominantly located at the surface, which allows to study the photochemistry more directly.

In the work presented here, UV-VIS spectra of potassium nitrate $K_n(NO_3)_{n+1}^-$ and sodium nitrate $Na_n(NO_3)_{n+1}^-$ clusters were investigated using an Apex Qe 9.4 T FTICR mass spectrometer. The clusters were produced using an electrospray ionization source and the spectra were recorded in the wavelength range from 220 - 350 nm. The spectra show three main absorption features where one lies towards 220 nm and two were seen within the actinic region lying at 298 nm and 318 nm. Similar to the results of the previous study for copper nitrate, also the loss of neutral potassium and sodium

nitrate units was dominant in these experiments. Fragments containing O^- and NO_2^- were detected with partial photodissociation cross sections in the range of 10^{-21} cm^2.

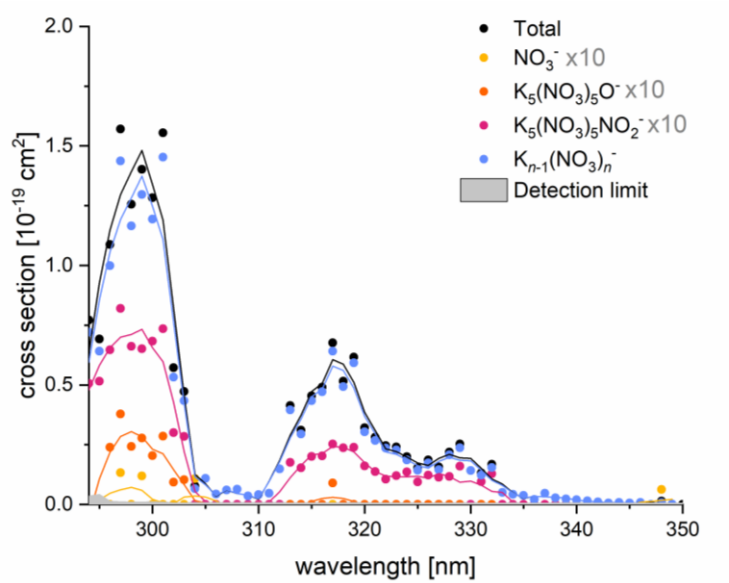

Figure 1: Fragment resolved UV photodissociation spectrum of $K_5(NO_3)_6^-$ with an irradiation time of 20s. Lines are a 6-point running average using the Savitzky-Golay method.

References

[1] D. J. Goebbert, et al., *J. Phys. Chem. A* **113**, 26 (2009)
[2] O. Svoboda, P. Slavíček, *J. Phys. Chem. Lett.* **5**, 11 (2014)
[3] A. M. Grammas, et al., *Atmos. Chem. Phys.* **7**, 16 (2007)
[4] T. F. Pascher, et al. *Phys. Chem. Chem. Phys.* **23**, 16 (2021)

Modelling Quantum-Controlled Molecular Collisions of N_2^+ ions with He atoms

Shimoni Patel, Markus Meuwly and Stefan Willitsch
Department of Chemistry, University of Basel, Switzerland

Octavio Roncero
Departamento de Astrof´ısica Molecular, Instituto de Fìsica Fundamental (IFF-CSIC), Spain

The molecular ion N_2^+ plays a central role in both atmospheric and cold ion–neutral chemistry. [1, 2] In the upper atmosphere, it is generated predominantly through ionization processes and strongly influences ionospheric composition and reactivity under high-energy radiation and cosmic particle impacts. In cold and ultracold environments, helium (He) acts as a buffer gas to cool N_2^+ via elastic and inelastic collisions, controlling both translational and internal quantum states. Motivating the present work, our group has recently demonstrated full quantum-state preparation and non-destructive quantum-logic spectroscopy of single trapped N_2^+ ions [3]. These advances open the door to probing molecular ion–neutral collisions at the single-particle level with exceptional sensitivity and state resolution. Leveraging this new experimental capability, we investigate the state-dependent collisional dynamics of N_2^+ with He under precisely controlled conditions.

At low collision energies, only non-reactive scattering is expected in the N_2^+ –He system, although rotational state-changing collisions may occur. To characterize these processes, we computed the N_2^+ potential energy surface (PES) at the UCCSD(T)/aug-cc-pVQZ level using MOLPRO, and subsequently constructed a three-dimensional N_2^+ –He PES via Reproducing Kernel Hilbert Space (RKHS) [4] interpolation. The potential well depth of this system is approximately 180 cm−1. All bound ro-vibrational levels of the complex were calculated, including detailed analyses of para- and ortho- N_2^+ states via wavefunction characterization.

Quasi-classical trajectory (QCT) and full quantum dynamical (QD) calculations were performed to obtain final rotational (j) distributions for ortho- and para- N_2^+, as well as the ratios of elastic to inelastic scattering events and the corresponding cross sections. In parallel, ongoing experiments are measuring the inelastic-to-elastic scattering ratio, providing key benchmarks for theoretical predictions.

Overall, this work provides a high-fidelity description of N_2^+ –He interactions and establishes a robust theoretical framework for understanding and ultimately controlling cold ion–neutral collisions, with implications quantum-controlled collision dynamics.

References

[1] D. M. Hunten et al. Planetary and Space Science, vol. 10, no. C, pp. 37–45, (1963)

[2] M. Beseda et al., Computational and Theoretical Chemistry, vol. 1215, p. 113809, (2022)

[3] M. Sinhal et al., Science 367, 1213–1218 (2020)

[4] O. T. Unke et al., J. Chem. Inf. Model. 57, 1923–1931 (2017)

Controlled laboratory astrochemistry: Ion-molecule chemistry of CO^+ with neutral H_2O

Aswin Ravindran[1], Lucille Kuster[2], Stefan Willitsch[1], Alexandre Faure[3], Astrid Bergeat[4] and Jutta Toscano[1]
[1] *Department of Chemistry, University of Basel, Switzerland*
[2] *Department of Chemistry, University of Quebec, Montreal, Canada*
[3] *Institut de Planétologie et d'Astrophysique de Grenoble (IPAG), Université Grenoble Alpes, CNRS, Grenoble, France*
[4] *Institut des Sciences Moléculaires, Université de Bordeaux, CNRS, UMR5255, Talence, France*

The reaction between CO^+ ions and H_2O is prevalent and important in the comae of outgassing comets, as well as in the carbon/oxygen chemistry of Photodissociation regions (PDRs) [1,2,3]. It proceeds via two competing pathways, charge-transfer and bimolecular reaction, that produce H_2O^+ and HCO^+, respectively. Both of these products may undergo further reactive collisions with neutral H_2O to form H_3O^+. To better understand the chemistry in cometary atmospheres, it is therefore essential to investigate the reaction rates and branching ratios of the $CO^+ + H_2O$ reaction under controlled laboratory conditions. In this work, we use a linear Paul trap to confine CO^+ ions in a Ca^+ Coulomb crystal and subsequently react them with neutral H_2O with control over the rotational temperature of the latter. Indeed, we compare the reaction rate and branching ratio for water with a thermal distribution of rotational states at 298 K and 5 K with that of rotational-state-selected water. We can separate para- and ortho-water in a molecular beam using an electrostatic deflector due to their different effective dipole moments [4]. We characterise the kinetics and branching ratio of this reaction by analyzing the reactants and products ion signals following the ejection of the ion crystals as a function of the reaction time using mass spectrometry.

References

[1] W. T. Huntress et al., Astrophys. J. Suppl. Ser. 44 (1980).
[2] S. A. Fuselier et al., A&A 583, A2 (2015).
[3] M. G. Wolfire et al., Annu. Rev. Astron. Astrophys. 60 (2022).
[4] D. Horke et al., Angew. Chem. Int. Ed. 53 (2014).

Low Temperature Ultraviolet Photodissociation Spectroscopy of $[dAMP-H]^-$

C. Sprenger, S. J. M. White, M. Westermeier, G. Schöpfer, F. Dahlmann*, E. S. Endres, R. Wester
University of Innsbruck, Department of Ion Physics and Applied Physics, Technikerstraße 25, 6020 Innsbruck

U. Namangalam, S. Mohandas, S. Kumar
Indian Institute of Science, Education and Research Tirupati, Department of Physics, Panguru, Andra Pradesh, India – 517619

**Current adress: Department of Chemical Engineering, KTH Royal Institute of Technology, 100 44 Stockholm, Sweden*

Ultraviolet radiation has sufficient energy to fragment DNA molecules, which can have a significant effect on the organism the DNA belongs to [1,2]. However, the underlying fragmentation mechanisms are not fully understood yet. To increase this understanding we performed a wavelength dependent photoabsorption study of the deprotonated nucleotide anion $[dAMP-H]^-$ [3]. Within the studied wavelength range, between 240 nm and 270 nm we observed several spectral features, which could not be resolved in a previous study [4]. We attribute the difference of these results to the fact that our experiment was performed in our cryogenic 16-pole radio frequency ion trap which achieves buffer gas temperatures as low as 3 K during operation. Moreover we measured and analysed the product ion yields of five ionic fragments of the photofragmentation process. Finally we were able to determine the absolute photofragmentation cross section of $[dAMP-H]^-$ through a comparative measurement of the photodetachment cross section of I^-. The results of our measurements, which were recently published [3], will be presented.

References

[1] M. Wei et al., *Cell Div.,* **19, 1** (2024)

[2] J. Cadet et al., *Mutat. Res./Fundam. Mol. Mech. Mutagen.,* **571, 3-17** (2005)
[3] C. Sprenger et al., *J. Phys. Chem. A,* **129, 50, 11571-11579** (2025)
[4] J. C. Marcum et al., *Phys. Chem. Chem. Phys.,* **11, 1740-1751** (2009)

Metrology of the b $^3\Pi_g$ (v = 3) − a $^3\Sigma_u^+$ (v = 0) Transition of the Helium Dimer with a Spectral Resolution of 3 ppb and a Precision of 60 ppt

V. Wirth, M. Cairns, J. A. Agner, H. Schmutz and F. Merkt
Institute of Molecular Physical Science, ETH Zurich, Zurich, Switzerland

The helium dimer (He_2), having only four electrons, no nuclear spin and being the prototypical example of a Rydberg molecule [1], serves as a benchmark system for testing ab initio calculations. Recently, highly accurate calculations from first principles including relativistic and quantum-electrodynamical effects have become feasible in this four-electron system [2-4]. Accurate experimental data on the low-lying triplet electronic states of He_2 are needed to validate the current theoretical advances. The fine structure of $^3\Pi$ states, arising from the spin-spin, spin-rotation, spin-orbit and Λ-doubling interactions are of special interest as a test of the calculation of nonadiabatic and relativistic corrections. The accurate description of these states represents a real challenge even to state-of-the-art theoretical treatments of molecular structure and requires a multitude of effects to be considered. The low-lying triplet states of He_2 include the metastable *a* $^3\Sigma_u^+$ state, formally a 2s Rydberg state with a He_2^+ *X* $^2\Sigma_u^+$ ground-state core, and the *c* $^3\Sigma_g^+$ and *b* $^3\Pi_g$ states, which have 3pσ and 2pπ character at short range. Whereas the *a* $^3\Sigma_u^+$ and *c* $^3\Sigma_g^+$ states are now well characterized experimentally [5–10], much less is known on the *b* $^3\Pi_g$ state. Spectra of the (0 − 0) and (1 − 1) vibrational bands of the *b*−*a* transition have been reported with linewidths of ∼1 GHz, insufficient for a satisfactory characterization of the fine structure of the *b* state. Consequently, large uncertainties persist concerning the Λ-doubling, spin-spin, spin-orbit and spin-rotation structure in this state.

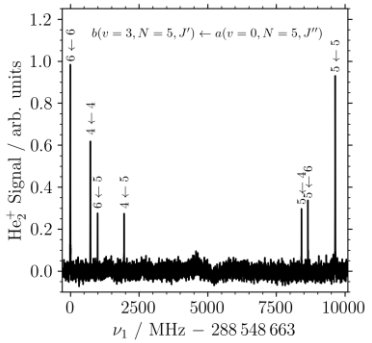

Figure 1: Overview spectrum of the Q(5) transition of the b(v=3)-a(v=0) band.

We report on a high-resolution spectroscopic study of the fine structure of the $b\ ^3\Pi_g$ (v = 3) − $a\ ^3\Sigma_u^+$ (v = 0) transition of He_2 in the near IR around 1040 nm. The measurements employed the recently developed Doppler-free method of imaging-assisted single-photon (IASS) [11] technique and applied it for the first time to a molecule. A narrowband continuous-wave (cw) laser locked to a frequency comb referenced to a SI-traceable frequency standard [12] was used to drive transitions from the fine-structure levels of the $a\ ^3\Sigma_u^+$ (v = 0) to those of the $b\ ^3\Pi_g$ (v = 3) state. The b-state levels were then photoionized with a pulsed dye laser. The spectrum displaying the fine structure of the $b(v = 3, N = 5, J' = 6) \leftarrow a(v = 0, N = 5, J'' = 6)$ rotational line is presented in Figure 1.

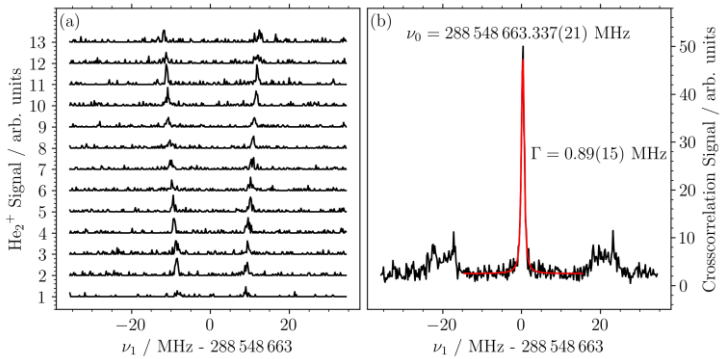

Figure 2: (a): Raw spectra of each slice of the camera.
(b): Summed cross-correlation spectrum of all slices shown in (a).

To eliminate systematic uncertainties from residual Doppler shifts arising from an imperfect orthogonal alignment of the laser beam and the supersonic beam of metastable He_2, a small deviation angle α from 90° was intentionally introduced and the laser beam was retroreflected at a mirror located beyond the photoexcitation region. An interferometric alignment of the retroreflection featuring a Michelson-type interferometer, a corner cube and a quadrant photodiode was used to reduce possible misalignment angles from exact retroreflection to below 20 µrad, as described in Ref. [13]. With this arrangement, each line was split into a red-shifted (ν_r) and a blue-shifted (ν_b) component by the Doppler effect and the first-order-Doppler-free line center was determined as $\nu_c = (\nu_r + \nu_b)/2$.

To optimize the spectral resolution, each Doppler component was further split into sub-Doppler components by imaging the photoexcited molecules in the direction perpendicular to both the laser and the molecular beams. The imaging was achieved by photoionizing the excited molecules and extracting the He_2^+ ions towards an MCP detector connected to a phosphor screen and a CCD camera. Typical spectra recorded with this arrangement are presented in Figure 2(a), where the different traces correspond to the He_2^+ ions detected in neighbouring slices of the images. A cross-correlation analysis of these data allows the combination of the information contained in all spectra and the obtaining of a Doppler-free line with a high signal-to-noise ratio. The profile of the *b(v=3, N=5, J=6) − a(v=0, N=5, J=6)* transition is depicted on an enlarged scale in Figure 2(b) and reveals a Voigt profile with a full width at half maximum Γ_{FWHM} of ~0.9 MHz and Lorentzian and Gaussian contributions of 0.49(15) and 0.61(10), respectively, three orders of magnitude narrower than in the previous measurement of the *b* $^3\Pi_g$ state [5]. The line center could be determined with a statistical uncertainty of only 21 kHz from a single spectrum. Table 1 lists the corrections and systematic
uncertainties considered from 15 individual measurements to obtain the energy difference between the two states involved in the transition, i.e., 288 548 663.339(6)$_{stat}$(10)$_{sys}$ MHz.

This work is supported financially by the Swiss National Science Foundation under the project No. 200021-236716.

Source	$\Delta\nu$	σ_{stat}	σ_{sys}
First-order Doppler shift	0	6	0
Photon-recoil shift	23.1	0	0
Second-order Doppler shift	-0.7	0	0
Zeeman shift	0	0	<1
ac-Stark shift	0	0	<10
Sum	22.4	6	10

Table 1: Systematic shifts and uncertainties for the b(v=3,N=5,J=6) - a(v=0,N=5,J=6) transition. All values are in kHz. The statistical uncertainty was determined from the analysis of 15 independent measurements.

References

[1] G. Herzberg, *Annu. Rev. Phys. Chem.* **38**, 27-56 (1987)
[2] Á. Margócsy, B. Rácsai, P. Jeszenszki, E. Mátyus, arXiv:2506.19116 v1 [physics.chem-ph]
[3] B. Rácsai, P. Jeszenszki, Á. Margócsy, E. Mátyus, *J. Chem. Phys.* **163**, 081102 (2025).
[4] P. Jeszenszki, P. Hollósy, Á. Margócsy, E. Mátyus, arXiv:2506.19131 v1 [physics.chem-ph].
[5] S. A. Rogers, C. R. Brazier, P. F. Bernath, *Mol. Phys.*, **63**, 901-908 (1988)
[6] W. Lichten, M. V. McCusker, T. L. Vierima, *J. Chem. Phys.*, **61**, 2200-2212 (1974)
[7] M. Kristensen, N. Bjerre, *J. Chem. Phys.*, **93**, 983-990 (1990).
[8] I. Hazell, A. Norregaard, N. Bjerre, *J. Mol. Spectrosc.*, **172**, 135-152 (1995)
[9] L. Semeria, P. Jansen, G. Clausen, Josef A. Agner, H. Schmutz, F. Merkt, *Phys. Rev. A*, **98**, 062518 (2018)
[10] V. Wirth, M. Holdener F. Merkt, *Phys. Rev. A*, **98**, 062518 (2018)

[11] G. Clausen, S. Scheidegger, J. A. Agner, H. Schmutz, F. Merkt, *Phys. Rev. Lett.,* **131**, 103001 (2023)
[12] D. Husmann et al., *Opt. Express*, **29**, 24592 (2021)
[13] G. Clausen, K. Gamlin, J. A. Agner, H. Schmutz, F. Merkt, *Phys. Rev. A.,* **111**, 012817 (2025)

Posters (Group B)

Toward understanding of the ultrafast dynamics of uracil-water clusters

A. Ayasli[1], A. Pradhan[1,3], I. Vinklarek[1], W. Jin[1], N. Vadassery[1,3], H. Bromberger[1], S. Trippel[1,4], J. Küpper[1,2,3,4]
[1]Center for Free-Electron Laser Science (CFEL), Deutsches Elektronen-Synchrotron DESY, Hamburg, Germany
[2]Department of Physics, Universität Hamburg, Germany
[3]Department of Chemistry, Universität Hamburg, Germany
[4]The Hamburg Center for Ultrafast Imaging (CUI), Universität Hamburg, Germany

The microsolvation of biomolecules enables a bottom-up approach for investigating solvation effects on the ultrafast dynamics of “isolated” molecules. For instance, the properties of ultraviolet-absorbing chromophores are sensitive to their local solvation environment [1]. Mass discrimination, i.e., size selecting a particulate cluster of choice, of such neutral solvent-solute aggregates can be challenging. Our group specializes in the preparation of rotationally cold and pure neutral molecular-beam samples [4] to investigate the dynamics of size selected clusters at ultrafast femtosecond timescales.
We developed a versatile and transportable endstation for controlled-molecule experiments (eCOMO) [2], where we purify sample beams using the electric deflector [3] based on the molecules’ rotational temperatures, rotational constants, and effective dipole moments. These purified samples are then probed in the ultrafast regime using a double-sided velocity-map-imaging spectrometer to record photoions and photoelectrons in coincidence. Here, we present our current progress on the ultrafast dynamics of uracil and its modification through microsolvation in uracil-water cluster aggregates.

References

[1] G.A. Olah et al., *J. Am. Chem. Soc.* **133**, 33 (2011)
[2] W.H. Brune et al*. Science* **372**, 6543 (2021)

[3] M. Ceppelli et al. *Plasma Sources Sci. Technol*. **30**, 115010 (2021)
[4] L.M. Martini et al. *Plasma Phys. Control. Fusion* **60**, 014016 (2018)
[5] M. Ceppelli et al. *Plasma Sources Sci. Technol*. **29**, 065019 (2020)
[6] C. Montesano et al. *J. Phys. Chem. C* **127**, 10045 (2023)
[7] V. Guerra et al. *78 Annual Gaseous Electronics Conference 2025,* Seoul, Republic of Korea.

Towards the photodetachment spectroscopy of BN^-

Emilia Jovcic, Katrin Dulitz
Universität Innsbruck, Institut für Ionenphysik und Angewandte Physik, Innsbruck, Austria

1. Introduction

Despite their importance in numerous research fields, including fundamental physics and astrochemistry, the properties of negative ions are much less characterized than those of their positive counterparts. Cold negative ions would allow for more accurate determinations of the structure and interactions of negative ions. However, no negative ion has been cooled to the Doppler limit to date. Developing techniques for cooling anions to such low temperatures requires a detailed knowledge of their fundamental molecular constants and interactions.

Beyond ongoing work on the laser cooling of C_2^-, including efforts here in Innsbruck [1], BN^- has recently been considered as a possible candidate ion for optical cycling and Doppler laser cooling. A brief discussion of results from the recent investigation into a proposed optical cycling scheme for cooling cold, trapped $^{11}B^{14}N^-$ ions using excitation from the $X^2\Sigma^+$ ground state to the $B^2\Sigma^+$ excited state will be presented [2]. The findings indicate that slow population decay via the first excited electronic state, $A^2\Pi$, cannot be neglected. The presentation will also discuss progress towards the characterization of the molecular structure of BN^- using one- and two-photon photodetachment spectroscopy in an ion beam and in a cryogenically cooled radiofrequency ion trap, respectively. In the future, our efficient ion source will allow us to study a wide range of boron-containing species whose molecular structure is still not well-known.

References

[1] M. Nötzold, R. Wild, C. Lochmann, T. Rahim, S. Purushu Melath, K. Dulitz, B. Mant, J. Franz, F. A. Gianturco and R. Wester,

Phys. Rev. Lett. **131**, 183002 (2023). DOI: 10.1103/PhysRevLett.131.183002
[2] K. Dulitz, S. V. Jerosimić, P. del Mazo-Sevillano, J. Alonso de la Fuente, C. Sanz-Sanz, L. González-Sánchez, F. A. Gianturco, *Phys. Scr.* **100**, 055411 (2025). DOI: 10.1088/1402-4896/adce43

Reaction Dynamics of N^+ Ions with CO_2 Molecules

Jerin Judy, Dasarath Swaraj, Fabio Zappa and Roland Wester
Institut für Ionenphysik und Angewandte Physik, Universität Innsbruck, Technikerstraße 25, Innsbruck, Austria

Crossed molecular beam techniques are a powerful approach for investigating the dynamics of elementary reactions in the gas phase [1], while velocity map imaging (VMI) enables the determination of energy- and angle-resolved differential cross sections [2]. In earlier work, we examined the reactive scattering of N^+ ions with O_2 molecules and identified two distinct product pathways [3]. In the present work, we report the first measurements of energy- and angularly resolved differential cross sections for reactions between N^+ ions and CO_2 over a collision energy range of 0.16 to 1.52 eV. The reaction proceeds through two dominant channels, corresponding to charge transfer and atom transfer processes. Branching ratios for these channels are determined, and velocity map images are analyzed to extract angular distributions and internal energy partitioning of the products. Our findings underscore the importance of complementary theoretical studies to advance the fundamental understanding of ion–molecule reaction dynamics.

References

[1] N. Balucani, G. Capozza, F. Leonari, E. Segoloni and P. Casavecchia, *Int.Rev. Phys. Chem.* **25**, 109 (2006)
[2] R. Wester, *Phys. Chem. Chem. Phys.* **16**, 396 (2014)
[3] D. Swaraj, J. Judy, F. Zappa and R. Wester, *Phys. Scr.* **100**, 025408 (2025)

Mutual neutralization reactions in a cryogenic ion trap

Maximilian Märk, Michael Hauck, Robert Wild and Roland Wester
Institut für Ionenphysik und Angewandte Physik, Universität Innsbruck, Austria

While there are many studies on ion-neutral reactions at low temperatures, mutual neutralization (MN) reactions are still experimentally poorly understood. However, these anion-cation reactions play a crucial role in the astrochemical models of interstellar clouds [1]. In the literature the majority of these reactions are assigned the same rate coefficient, which is an approximation [2]. We will address this gap by measuring MN reactions for abundant ions in interstellar space. To achieve this, we will utilize our cryogenic 16-pole wire trap, which is designed to create a relatively flat potential with steep walls [3]. The wires of the trap are driven with an RF voltage to contain the ions radially. A DC voltage is usually applied to endcap electrodes for axial confinement, but this only works for one charge polarity at a time. To perform MN reactions, we will also drive the axial confinement using an RF voltage. The large expected cross section due to the attractive Coulomb potential will be offset by the low densities in the ion trap. Therefore, long storage times are essential. Our group has already demonstrated long trapping lifetimes for three-body reaction studies [4]. Our measurements will constrain MN kinetics at low temperatures and provide much-needed data for astrochemical models.

References

[1] T. J. Millar, *Chem. Rev.* **117**, (2017).
[2] N. S. Shuman et al., *J. Phys.:* **Conf. Ser. 300** (2011).
[3] M. Nötzold et al., *Phys. Rev. A*, **106** (2022).
[4] C. Lochmann et al., *J. Phys. Chem. A*, **127** (2023).

A quantum dynamical study of the cis-trans isomerisation in Rhodospin

E. Gindensperger[1], M. Haldar[1], S. Mandal[1], R. Marquardt[1]
[1]*Laboratoire de Chimie Quantique,*
Institut de Chimie, UMR 7177 CNRS/Université de Strasbourg

The photoisomerisation around a CC double bond is investigated quantum dynamically on the basis of a three mode two state model of the protonated Schiff base (PSB) in rhodopsin [1,2].

The original model is slightly changed and the cis to trans isomerisation is studied in terms of time evolving wave packets and reaction probabilities.

Time dependent stimulated emission and photoproduct absorption spectra are calculated. The generic results from the model are used to rationalise signatures of «vibrational coherence» evoked in experimental data [3,4].

Keywords: Rhodopsin isomerisation, quantum dynamics, vibrational coherence.

References

[1] E. Marsili, M. H. Farag, X. Yang, L. De Vico, M. Olivucci, J. Phys.Chem. A, **123**, 1710 (2019), doi: 10.1021/acs.jpca.8b10010
[2] E. Marsili, M. Olivucci, D. Lauvergnat, F. Agostini, J. Chem. Theory Comp., **16**, 6032 (2020), doi: 10.1021/acs.jctc.0c00679
[3] J. Léonard, I. Schapiro, J. Briand, S. Fusi, R. R. Paccani, M. Olivucci, S. Haacke, Chem. Eur. J., **18**, 15296 (2012), doi : 10.1002/chem.201201430
[4] M. Gueye, M. Paolino, E. Gindensperger, S. Haacke, M. Olivucci, J. Léonard, Far. Disc., **221**, 299 (2020), doi : 10.1039/c9fd00062c

Splashing of Multiply Charged Helium Nanodroplets upon Impact with Solid Surfaces

Jan Mayerhofer, Thomas Pohl, Fabio Zappa, Elisabeth Gruber, Paul Scheier
University of Innbruck -Institute for Ion Physics and Applied Physics, Technikerstraße 25, 6020 Innsbruck, Austria

In recent years, helium nanodroplets (HNDs) have emerged as highly versatile cryogenic matrices for the synthesis of clusters and nanoparticles (NPs) [1,2] as well as for ltheir subsequent deposition onto designated substrates. Deposition is typically achieved by colliding the droplets with a respective surface, where the droplets act as a kinetic-energy buffer, thereby enabling exceptionally gentle deposition of tailor-made NPs with minimal structural deformation. This approach provides a powerful platform for the fabrication of novel materials and coatings that are otherwise inaccessible by conventional methods.

Our research group has recently demonstrated that doping multiply charged HNDs results in the formation of uniformly sized clusters localized at charge centers that are regularly arranged close to the surface of the droplets [3]. In the present communication, we utilize an advanced experimental setup which employs a high-intensity molecular beam of multiply charged HNDs to generate large quantities of size-uniform gold NPs via gas-phase pickup. The NPs are deposited onto transmission electron microscopy (TEM) grids and subsequently characterized. Although the present results were obtained using gold as the dopant material, the method is broadly applicable to virtually any substance that can be introduced into the gas phase.

Most recently, we achieved direct imaging of NPs synthesized within individual HNDs by reducing the droplet size through collisions with room-temperature helium atoms prior to surface impact. For small HNDs, we observed that nearly all NPs are deposited on the droplet surface, resulting in a two-dimensional projection corresponding to the minimum-energy configuration of points on a sphere, as described by the Thomson problem. In contrast, larger HNDs exhibit

an apparent absence of NPs originating from the hemisphere oriented away from the substrate at the moment of impact, suggesting the existence of a critical droplet size above which NPs begin to disappear from the deposited distribution. Martini et al. [4] reported that HNDs undergo splashing upon surface impact, leading to the backscattering of a substantial fraction of the embedded NPs. However, the precise conditions under which HNDs splash efficiently enough to eject NPs remain undetermined. Imaging NPs from individual HNDs offers a novel experimental approach to identify this apparent critical droplet size and to elucidate the fundamental mechanisms governing this process. To further investigate and ultimately gain control over this behavior, we have initiated experiments employing two complementary strategies: (i) deceleration of HNDs to velocities below the Landau critical velocity prior to impact, and (ii) implementation of a two-target configuration, where a primary target serves as the impact surface and a secondary target collects the backscattered NPs.

References

[1] R. Messner, et al., *J. Phys. Chem. Lett.* (2021) 12, 145–150.
[2] P. Thaler, et al., *Phys. Rev. B* (2014) 90, 155442.
[3] L. Tiefenthaler et al., *Rev. Sci. Instrum.* (2020) 91, 033315.
[4] P. Martini et al., *Phys. Rev. Lett.* (2021) 127, 263401

Cold chemistry of single trapped H_2O^+ ions with neutral HD molecules in a cryogenic ion trap

Nanditha Sunil Kumar, Prerna Paliwal, Mikhail Popov, and Stefan Willitsch
Department of Chemistry, University of Basel, Klingelbergstrasse 80, 4056 Basel, Switzerland.

Anyang Li
Key Laboratory of Synthetic and Natural Functional Molecule of the Ministry of Education, College of Chemistry and Materials Science, Northwest University, 710127 Xi'an, P. R. China.

Hua Guo
Department of Chemistry and Chemical Biology, Center for Computational Chemistry, University of New Mexico, Albuquerque, New Mexico 87131, United States.

Precise quantum control of trapped molecules has emerged as a key technology in a wide range of applications such as precision spectroscopy, quantum computing, tests of fundamental physics, and state-to-state chemistry [1, 2, 3]. Trapped ions can also serve as an excellent platform for probing cold ion–neutral reactions, facilitating investigation at the low-temperature, low-density conditions characteristic of the interstellar medium (ISM). In our recently developed cryogenic ion trap setup, we explore cold collisions between a single trapped H_2O^+ ion with cold HD molecules at a collision energy of 6 K. Isotope effects in this reaction were investigated by analyzing the products. The experiments reveal a pronounced isotopic effect at a low collision energy of 6 K.
The current experimental setup is being developed with the primary goal of extending complex quantum logic spectroscopy (QLS) schemes to polar and polyatomic ions, specifically H_2O^+. With the advancement in experimental techniques for the preparation, cooling, and coherent manipulation of molecular ions [4,5], precise quantum control of polyatomic molecular ions is feasible. Such

quantum control can open new prospects and allow state-selected chemistry studies in the future.

References

[1] M. Sinhal et al. *Science* 367, 6483 (2020)
[2] M. Sinhal et al. p. 305 ff. in "*Photonic Quantum Technologies: Science and Applications"*, ed. M. Benyoucef, Wiley-VCH (2023)
[3] G. D. Scholes et al. *J. Phys. Chem. Lett*. 16, 1376-1396 (2025)
[4] C.W. Chou et al. *Nature* 545, 7653 (2017)
[5] F. Wolf et al. *Nature* 530, 7591 (2015)

The exposure of serine clusters to soft X-rays and atomic hydrogen

T.J. ten Napel[1], B. M. Szihalmi[1], O. Kavatsyuk[2], V. Zamudio-Bayer[4], J.C. Poully[3], M. Salverda[1], T. Schlathölter[1,2],
[1]ZIAM, University of Groningen
[2]UCG, University of Groningen
[3]GANIL, Caen
[4]Helmholz-Zentrum Berlin (HZB) BESSY II Berlin

Serine and its clusters have been a topic of interest in the last three decades since the discovery of its octamer cluster [1]. The octamer cluster is remarkably stable and its preference for homochirality and magic numbers suggests that serine could have played an important role in homochiralgenesis, the emergence of homochirality in most amino acids of all lifeforms. This potential role of serine has been the motivation for a range of studies on photo-interactions and electron interactions [2], [3], [4].
Additionally, serine clusters exhibit a preference for even numbered clusters (magic numbers), suggesting that they are built from dimers [1].

Soft X-ray spectroscopy is a particularly powerful technique to study photo-physics of clusters, as it allows for site sensitive probing of the system. In this contribution we present an experiment where we perform Near Edge X-ray Absorption Mass Spectrometry (NEXAMS [5]) measurements on serine clusters of various sizes. The K-edges of carbon (284 – 304 eV), nitrogen (397 – 412 eV) and oxygen (529 – 545 eV) are studied at the Ion Trap end station of the BESSY II synchrotron (HZB Berlin, Germany) [6].

Using electrospray ionisation (ESI), protonated serine clusters are brought into the gas phase and transported by radiofrequency ion guides. The protonated clusters are then trapped in a cryogenic ion trap where they are irradiated by the X-ray beam. The fragments that

are formed by this process are extracted into a time-of-flight (TOF) mass spectrometer.
We observe that the dimer undergoes violent fragmentation into a number of small fragments (m/z < 50). For larger clusters (tetramer, hexamer and octamer), larger fragments such as m/z = 106 Da/q and 211 Da/q are observed, which correspond to the protonated monomer and dimer respectively. This suggests an underlying scenario, where the dimer that contains the photoabsorbing site always undergoes fragmentation whereas other dimers in the cluster remain internally cold enough to survive the process intact, or only dissociate into two monomer units. For a detailed understanding of the interplay between covalent and non-covalent bonds in energy dissipation and charge redistribution, quantum chemical calculations will be required.

In the second experiment we have stored mass-selected protonated serine dimers in an ion trap and exposed them to a thermal beam of atomic hydrogen. After trapping, we use a quadrupole mass spectrometer to analyze the fragments that are created.

Hydrogen exposure to the protonated serine dimer leads to the appearance of multiple fragments in the mass range between the monomer and the dimer. Clearly, hydrogen attachment leads to intra-cluster reactions in which molecules are formed that are substantially more complex than a simple serine unit. Surprisingly, hydrogen attachment does not appear to cause mere dimer fragmentation into monomers.

There are large regions of the interstellar medium where atomic hydrogen is abundant. The hydrogen attachment to small biomolecular clusters (such as serine dimers) that are formed in these regions could contribute to an increase of molecular complexity.

References

[1] R. Graham Cooks, D. Zhang, K. J. Koch, F. C. Gozzo, M. N. Eberlin, *Analytical Chemistry* **73**, 15 (2001)

[2] V. Scutelnic, M. A. S. Perez, M. Marianski, et al. *Journal of the American Chemical Society,* **140**, 24 (2018)
[3] F. Da Silva, S. Denifl, T. D. Märk, A. M. Ellis, and P. Scheier. The Journal of Chemical Physics **132,** 21 (2010)
[4] O. Licht, D. Barreiro-Lage, P. Rousseau, et al. *Angewandte Chemie* **135**, 15, (2023)
[5] O. González-Magaña, G. Reitsma, M. Tiemens, L. Boschman, R. Hoekstra, and T. Schlathölter. *The Journal of Physical Chemistry A* **116**, 44, (2012)
[6] Helmholtz-Zentrum Berlin für Materialien und Energie. *Journal* of large-scale research facilities, **2**, A96 (2016)

ESPECDAS – A Database of *Ab Initio* Electronic Spectra of Small Molecules for Identification of Potential DIB Carriers

Milan Ončák, Michael Gatt, Marc Reimann, Gabriel Schöpfer
Department of Ion Physics and Applied Physics, Universität Innsbruck, Austria

Alexander Ebenbichler
Department of Physics & Astronomy, University of Western Ontario, Canada

Norbert Przybilla
Department of Astro- and Particle Physics, Universität Innsbruck, Austria

Despite a considerable effort, only one carrier of Diffuse Interstellar Bands (DIBs) has been confirmed up to this point, namely C_{60}^+ [1]. Chemical composition of the remaining carriers stays unclear, and spectra of various carbon-based compound are being intensely investigated in this context. However, there is also a possibility that some DIB carriers are small molecules [2]. Many such candidate molecules are exotic species for which no experimental spectroscopic information is available.
The Electronic Spectroscopy Database for Astrochemical Studies (ESPECDAS) will provide *ab initio* calculated spectra of small molecules in various electronic states. We primarily focus on diatomic species, in particular on transition metal oxides, carbides, nitrides, and hydrides, as well as a selection of triatomic molecules such as SiO_2 and TiO_2, employing automated Multireference Configuration Interaction (MRCI) calculations.

References

[1] E. K. Campbell, M. Holz, D. Gerlich, J. P. Maier. *Nature* **523** 322–323 (2015).
[2] A. Ebenbichler, M. Ončák, N. Przybilla, H. R. Hróðmarsson, J. V. Smoker, R. Lallement, A. Farhang, C. Bhatt, J. Cami, M. Cordiner,

P. Ehrenfreund, N. L. J. Cox, J. Th. van Loon, B. Foing. *Astronomy and Astrophysics* **695**, A212 (2025).

Towards quantum-state–selected ion-neutral collisions

Viviane C. Schmidt, Jerin Judy, Dasarat Swaraj, Fabio Zappa and Roland Wester

Institut für Ionenphysik und Angewandte Physik, Universität Innsbruck, Technikerstraße 25, 6020 Innsbruck, Austria

The interactions of neutral and charged molecules are ultimately governed by the laws of quantum mechanics. These processes can be studied in detail by colliding different species under very well defined initial conditions and measuring the parameters of the resulting reactions precisely. An optimal set-up to do this is a crossed-beam experiment with velocity map imaging (VMI) capabilities. Here, reaction parameters, for example scattering angles and internal excitations of the resulting products, can be measured [1,2]. One such set-up is located at the University of Innsbruck. It includes an additional octupole trap prior to the reaction chamber, where the charged reactants can be buffer gas cooled to liquid nitrogen temperatures [1]. In the project presented here, we are planning to upgrade this octupole trap with a cryostat. This will enable buffer gas temperatures down to about 20K. At this temperature range, the internal state distribution of molecules is dominated by a few, often even a single ro-vibronic excitation of the system. The upgraded set-up will be used to investigate the effect rotational excitation of the charged reactant has on the fundamental reaction of HeH^+ with H_2 [3].

References

[1] R. Wester, Phys. Chem. Chem. Phys. **16**, 396-405 (2014)
[2] B. Bastian *et al.*, J. Phys. Chem. A **124**, 10, 1929-1939 (2020)
[3] N. G. Adams *et al.*, J. Chem. Phys. **52**, 5101-5105 (1970)

Resolving rotational states in the ion-molecule charge transfer reaction of Ar^+ with H_2

Dasarath Swaraj, Jerin Judy, Fabio Zappa, Tim Michelsen, Arnab Khan and Roland Wester*
Institut für Ionenphysik und Angewandte Physik, Universität Innsbruck, Technikerstraße 25, 6020 Innsbruck, Austria

Guodong Zhang, Hong Gao
Beijing National Laboratory for Molecular Sciences (BNLMS), Institute of Chemistry, Chinese Academy of Sciences, Beijing 100190, China, University of Chinese Academy of Sciences, Beijing 100049, China

Siting Hou, Changjian Xie
Institute of Modern Physics, Shaanxi Key Laboratory for Theoretical Physics Frontiers, Northwest University, Xi'an, Shaanxi 710127, China

Dandan Lu
State Key Laboratory of High Temperature Gas Dynamics, Institute of Mechanics, Chinese Academy of Sciences, 100190 Beijing, China

Hua Guo
Department of Chemistry and Chemical Biology, Center for Computational Chemistry, University of New Mexico, Albuquerque, New Mexico 87131, USA

Detailed insight into the dynamics of elementary reactions in the gas phase can be obtained from crossed-beam reactive scattering experiments. Angle and energy differential cross-section can be obtained by combining the velocity map imaging (VMI) with crossed-beam scattering [1][2]. In this contribution, we present the differential cross-section measurement of an ion-molecule charge transfer reaction of argon ions with neutral hydrogen molecules, imaged

using VMI with rotationally resolved product distribution significantly improved over our previous study.
$Ar^+ (^2P_{3/2}) + H_2 (v=0, j=0,1) \rightarrow H_2 + (v' , j') + Ar(^1S_0) + 0.333$ eV

The ions were created in the spin-orbit ground state of Ar^+ by Resonance Enhanced Multiphoton ionization (REMPI) [3]. The ions were produced with high energy resolution with our new experimental configuration of electrostatic lenses [4]. Chemical reactions are initiated by the beam of ions intersecting with the beam of neutral molecules generated in a supersonic expansion. The reaction products are collected by the new VMI spectrometer and then detected and imaged. The results show that high product rotational excitation is found, in contrast to reactions of spin-orbit excited Ar^+ ($^2P_{1/2}$). Quantum scattering calculations were performed and results were compared with experimental observations.

References

[1] R.Wester *Phys. Chem. Chem. Phys*., **vol. 16**, pp. 396–405, (2014)
[2] T. Michaelsen, *J. Chem. Phys*., **vol. 147**, no. 1, (2017).
[3] G. Zhang, *Nat.Chem,* **vol. 15,** no. 9, pp. 1255–1261, (2023).
[4] D. Swaraj, *Mol.Phys*, **vol. 122**, no. 1-2, p. e2194455

Electrostatic Trapping of Multiply Charged Helium Nanodroplets on the Minute-Scale

Matthias Veternik[1], Lutz Schweikhard[2], Paul Scheier[1], Elisabeth Gruber[1]
[1]University of Innsbruck, Institute of Ion Physics and Applied Physics
[2]University of Greifswald, Institute of Physics

A multi-reflection time-of-flight (MR-ToF) device, developed and produced in a collaboration between the TU Darmstadt and the University of Greifswald [1], is used to trap highly charged helium nanodroplets (HNDs) for several tens of seconds up to the minute range, thereby extending the possible observation time by a factor of more than four orders of magnitude. Initial proof-of-principle measurements demonstrate efficient storage with several thousand revolutions of the droplets inside the instrument. The residual pressure inside the machine (~10^{-8} mbar) was identified as the main limiting factor for longer storage times.

Recent measurements include the observation of blackbody infrared radiative decay (BIRD) of water-doped HNDs. The embedded water clusters absorb the infrared radiation emitted by the vacuum chamber at room temperature and subsequent thermalization leads to enhanced helium evaporation from the HNDs. This can be monitored by a decrease of the droplet-signal intensity as a function of time, when they are released to the external ion detector by a partial reduction of the trapping potential [2].

Future plans include the implementation of a so-called pick-up electrode in order to study changes in the charge, mass, and energy of the droplets over time. This method provides a new approach for nano-calorimetry, opening up entirely new approaches for thermodynamic studies at the nanoscale. The development of image-charge detection for multiply charged HNDs is motivated by the pioneering measurements of Hanozin et al. [3], in which

significant charge loss and Rayleigh decay of aqueous droplets were observed.

This research was funded in whole or in part by the Austrian Science Fund (FWF) [10.55776/I6221, 10.55776/V1035].

References

[1] Schlaich et al., Int. *J. Mass Spectrom.* **495**, 117166 (2024)
[2] M. Veternik et al., *Phys. Rev. Lett.*, **136**, 013201 (2026)
[3] Hanozin et al., *ACS Cent. Sci.,* **9 (8)**, 1611–1622 (2023)

Author Index